

ANALYZING QUALITY-LATENCY-RESOURCE TRADE-OFFS IN A TECHNICAL DOCUMENTATION RAG ASSISTANT USING LORA ADAPTATION

Evgenii Palnikov¹, Elizaveta Gavrilova¹

¹HSE University

ABSTRACT

We study quality–latency–resource trade-offs in a documentation-grounded retrieval-augmented generation (RAG) system that uses Low-Rank Adaptation (LoRA) of the generator. We build a manually verified benchmark of 5,144 question–answer pairs over the official Kubernetes documentation and combine it with a fixed hybrid-retrieval pipeline (BGE-M3 dense, BGE-M3 native sparse, Reciprocal Rank Fusion, cross-encoder reranking). Over this benchmark we ablate 20 LoRA configurations on Llama-3.2-3B-Instruct and Llama-3.1-8B-Instruct across rank and target-module choices, and evaluate each on token-level F1, LLM-judged groundedness and correctness (pass@4), inference latency, inference memory, and training cost, all reported with bootstrap 95% confidence intervals. Pareto analysis shows that LoRA adapters acting only on the q and v attention projections consistently dominate the front, while the 3B/8B choice mainly defines operating regime. A param-matched control comparison further indicates that the q/v advantage is structural rather than purely parametric. The benchmark, selected adapters, and code are available at <https://github.com/EugPal/rag-lora-tradeoffs>.

1 INTRODUCTION

Retrieval-augmented generation (RAG) has become a standard way to ground large language models (LLMs) in external corpora when their parametric memory is insufficient or stale (Lewis et al., 2020; Gao et al., 2023; Wu et al., 2024). For *documentation-oriented* assistants – where users expect answers backed by specific configuration flags, API versions, or feature gates – the bar is even higher: a deployable system must combine factual accuracy and visible support from the retrieved context with acceptable latency, inference memory, and training cost. In practice these objectives are in direct tension. Larger generators improve answer quality but increase inference memory and latency; richer retrieval and reranking add overhead; more expressive LoRA (Hu et al., 2022) adapters change the cost of training. Picking a working point therefore requires reasoning about a *multi-objective* trade-off rather than a single quality metric.

Existing work largely studies these dimensions in isolation. RAG surveys focus on retrieval/fusion/reranking design choices (Gao et al., 2023; Yu et al., 2024); parameter-efficient fine-tuning surveys focus on the LoRA family in general purpose tasks (Han et al., 2024; Wang et al., 2025); RAG-evaluation work focuses on quality and groundedness on standard QA sets (Es et al., 2024; Yu et al., 2024). A few recent papers combine RAG with LoRA, but they typically treat LoRA as a single technique – a single rank, a single target-module set – and compare it against alternatives like DoRA or full fine-tuning (Tahir et al., 2024; Zhao et al., 2024a; Baqar & Khanda, 2025). This leaves an open question: *how does the choice of LoRA configuration – rank, target modules, base-model size – interact with retrieval quality, latency, and training cost when the rest of the RAG pipeline is held fixed?*

We address this question by constructing a documentation-grounded RAG benchmark and analysing a structured space of LoRA configurations on it. Our benchmark consists of 5,144 manually verified question–answer pairs over the official Kubernetes documentation, paired with a fixed hybrid retrieval pipeline (BGE-M3 (Chen et al., 2024) dense + BGE-M3 native sparse + Reciprocal Rank

Fusion (Cormack et al., 2009) + a cross-encoder reranker). Over this pipeline we ablate 20 LoRA configurations on Llama-3.2-3B-Instruct and Llama-3.1-8B-Instruct (5 ranks \times 2 target-module sets per base model) against the corresponding non-adapted baselines. Each configuration is evaluated on (i) token-level F1, (ii) LLM-as-a-judge groundedness and correctness (pass@4), (iii) inference latency, (iv) inference VRAM, and (v) training time and VRAM, with bootstrap 95% confidence intervals on all point estimates and paired bootstrap on key ΔF_1 comparisons. To probe robustness, we re-run the full grid under 10 retrieval/prompting ablation regimes.

Three findings emerge. First, on every Pareto front we examine – F1-vs-latency, F1-vs-inference-memory, and F1-vs-training-cost – non-dominated points are dominated by LoRA adapters that act only on the q and v attention projections. `full_attention` adapters (q, k, v, o) never appear on the training Pareto front and win at most 2/10 ablation regimes on groundedness. Second, the 3B/8B choice mainly determines the operating regime rather than the achievable quality: the strongest LoRA-adapted 3B configuration is statistically indistinguishable from the unadapted 8B baseline on F_1 ($\Delta F_1 \in [-0.021, +0.026]$), while costing roughly 9 GB less inference VRAM. Third, a *param-matched* control comparison – in which the total number of trainable LoRA parameters is held constant across the q/v and full-attention schemes – shows that the q/v advantage is structural and not a consequence of having more parameters.

Our contributions are: (i) a manually verified, license-clean RAG benchmark over Kubernetes documentation, designed for multi-criteria evaluation; (ii) a systematic LoRA-configuration study within a fixed hybrid-retrieval pipeline, with statistical inference on all reported trade-offs; (iii) a param-matched control comparison that isolates the structural effect of the target-module choice from the effect of parameter count; (iv) the released benchmark and selected adapters, intended as a reproducible starting point for follow-up work on retrieval-augmented fine-tuning of documentation assistants.

2 RELATED WORK

RAG and retrieval components. Retrieval-augmented generation (Lewis et al., 2020) has been thoroughly surveyed in recent years (Gao et al., 2023; Wu et al., 2024): modern RAG is not a single architecture but a family of designs that differ in how retrieval, fusion, reranking, and context use are organised. On the retrieval side, dense passage retrieval was canonicalised by Karpukhin et al. (2020), classical sparse retrieval by BM25 (Robertson & Walker, 1994; Robertson et al., 1995; Robertson & Zaragoza, 2009), and training-aware extensions such as RocketQA (Qu et al., 2021) and ColBERTv2 (Santhanam et al., 2022) show that retrieval quality depends as much on the training scheme as on the index type. Recent multi-functional embedders – in particular BGE-M3 (Chen et al., 2024) – are widely adopted in hybrid pipelines combined with cross-encoder reranking (Nogueira & Cho, 2019; Yoon et al., 2024) and rank-level fusion (Cormack et al., 2009). For documentation-grounded assistants the overall quality is therefore a property of the whole pipeline, not of the generator alone.

Parameter-efficient fine-tuning. Full fine-tuning of instruction-tuned LLMs is expensive in both compute and memory; PEFT surveys (Han et al., 2024; Wang et al., 2025) document a large literature of methods that change model behaviour while keeping the backbone frozen. Among these, LoRA (Hu et al., 2022) introduces low-rank adapters on linear projections and has spawned a family of follow-ups, including QLoRA (Dettmers et al., 2023) and LoRA+ (Hayou et al., 2024), plus throughput-focused training infrastructure such as ASPEN (Ye et al., 2023). Collectively, this line shows that LoRA can deliver domain adaptation without full fine-tuning. It does not, however, answer the question of which LoRA *configuration* – rank, target modules, base-model size – to pick when the adapter is plugged into a retrieval-augmented system.

RAG evaluation, groundedness, and quality–cost trade-offs. The evaluation literature (Yu et al., 2024; Es et al., 2024) stresses that RAG quality must be measured not only on the final answer but on retrieval quality, groundedness of the answer in retrieved evidence, and generation properties. Closer to the trade-off framing of this paper, Baek et al. (2026) treat LoRA-configuration selection itself as a non-trivial optimisation problem inside the LoRA hyperparameter space, and Baqar & Khanda (2025) compare RAG, LoRA, and DoRA jointly from an accuracy-and-faithfulness viewpoint.

Combining RAG and LoRA. A small but growing body of work studies RAG and LoRA together. JORA (Tahir et al., 2024) contributes infrastructure for retrieval-augmented LoRA fine-tuning; RAMoLE (Zhao et al., 2024a) uses retrieval to select between multiple LoRA experts at inference time. Among empirical studies, Baqar & Khanda (2025) is closest in spirit to this work – it contrasts RAG, LoRA, and DoRA on question answering – but, like other work in this group, treats LoRA as a single technique to be plugged in rather than as a configuration space to be searched over.

Research gap. Across the four sub-areas above, work on RAG focuses on retrieval and pipeline design; work on LoRA/PEFT focuses on efficient adaptation in the abstract; work on RAG evaluation establishes that groundedness and multi-criteria analysis are necessary. What remains underexplored is the *systematic empirical analysis of how different LoRA configurations inside a fixed RAG architecture for technical documentation interact with answer quality, latency, inference memory, and training cost*. This is the gap addressed by the present paper.

3 TASK AND BENCHMARK

3.1 TASK FORMULATION

We consider documentation-grounded question answering over a fixed corpus $D = \{d_1, \dots, d_n\}$ of text chunks. A fixed retrieval-and-reranking module R maps every question q to a context $c = R(q, D)$. The research variable is the generator configuration $x \in \mathcal{X}$, characterised by the base model, the LoRA rank, and the set of target modules. For each configuration x the system produces an answer $a_x(q, c)$. We associate with x a quality score $Q(x) = F_1(x)$ and a cost vector $C(x) = (L_{\text{inf}}(x), M_{\text{inf}}(x), T_{\text{train}}(x), M_{\text{train}}(x))$, where L_{inf} is mean inference latency, M_{inf} is peak inference VRAM, T_{train} is total training time, and M_{train} is peak training VRAM. The goal is not a single $x^* = \arg \max Q(x)$ but the Pareto-optimal set (Lewis et al., 2020; Yu et al., 2024).

3.2 CORPUS AND QA CONSTRUCTION

The corpus is the official Kubernetes documentation, cleaned and segmented into semantically coherent chunks suitable for retrieval and answer attribution. The QA set was built in two stages. We hand-wrote 500 QA pairs directly from the documentation, then drafted further candidates one-by-one with an LLM agent based on GPT-5.4 – not via bulk synthetic augmentation. All candidates went through manual verification by the author: pairs were discarded on ambiguous questions, missing supporting evidence, duplicates, or factual errors in the reference answer. Of 5,467 candidates, 323 ($\approx 5.9\%$) were rejected and $\approx 20\%$ of the remaining pairs were edited; the rest were accepted as-is. The final benchmark contains 5,144 verified pairs (500 hand-written + 4,644 LLM-drafted and manually verified), partitioned into train/eval/test as in Table 1.

Split	Rows	Exact	Normal
Train	3,614	1,449	2,165
Eval	745	361	384
Test	785	475	310

Table 1: Split sizes and distribution of answer types (EXACT vs. NORMAL).

Same-family risk. The QA-generation model (GPT-5.4) and the LLM judge used in §6 (gpt-5.4-mini) belong to the same model family, which raises a same-family-bias concern. There is no direct train/test leak: the judge is not trained on the gold answers, and all gold answers were manually verified. We discuss this residual risk explicitly as a limitation (§9).

3.3 ANSWER TYPES

We annotate each QA pair as either EXACT or NORMAL. EXACT pairs require near-literal answers – flags, paths, field names, API versions, feature gates – while NORMAL pairs are factual answers that tolerate paraphrasing as long as the meaning is preserved. This typology was designed for this

benchmark; it is used as a supervision signal at training time and as a stratification axis at evaluation time, but it is *not* passed to the generator at inference, which receives only the question and the retrieved context. This separation of training- and test-time conditioning follows the evaluation protocols in prior RAG work (Yu et al., 2024; Es et al., 2024).

4 RAG PIPELINE

The pipeline follows the standard three-step structure – retrieval, reranking, generation – consistent with modern RAG surveys (Lewis et al., 2020; Gao et al., 2023; Wu et al., 2024).

Retrieval. The main configuration uses a hybrid retrieval contour. Dense retrieval runs over a FAISS (Douze et al., 2024; Johnson et al., 2019) index of BGE-M3 (Chen et al., 2024) embeddings; sparse retrieval uses the native sparse channel of BGE-M3. Dense and sparse candidate lists are merged via Reciprocal Rank Fusion (Cormack et al., 2009). Classical BM25 (Robertson & Zaragoza, 2009) is used only as the sparse component in a separate ablation regime (§7.4), not in the main pipeline.

Reranking. The fused candidate list passes through a pretrained cross-encoder reranker, BAAI/bge-reranker-v2-m3, building on the standard cross-encoder and listwise reranking literature (Nogueira & Cho, 2019; Yoon et al., 2024) and on retrieval extensions of large language models (Li et al., 2023).

Generator and prompting. The generator is one of two instruction-tuned models from the Llama 3 family (Dubey et al., 2024): Llama-3.2-3B-Instruct and Llama-3.1-8B-Instruct. Both are decoder-only transformers with RoPE positional encoding, grouped-query attention, and SwiGLU MLP blocks. At inference we use a *neutral* prompting mode, with no explicit instruction to “answer only from the context” – the role of strict grounding is left to LoRA fine-tuning and to retrieval quality rather than to prompt engineering. This separates the contribution of adaptation from that of prompt-side anchoring and keeps the comparison between adapters honest. At training time the model retains the option to condition on the answer-type label (EXACT/NORMAL, §3.3), but the inference prompt does not carry that label. This split between training and test-time conditioning follows established practice in RAG evaluation (Yu et al., 2024; Es et al., 2024).

Inference context. The main inference regime uses `eval_top_k=2` retrieved chunks, matching `embed_top_k=2` at training time. For sensitivity analysis we additionally run the full grid with `eval_top_k` ∈ {1, 4} (§7.5).

5 LORA CONFIGURATIONS AND EXPERIMENTAL DESIGN

5.1 CONFIGURATION SPACE

Full fine-tuning of the chosen Llama-3 models is too expensive for the configuration search we want to run. We therefore use Low-Rank Adaptation (Hu et al., 2022), which is well-suited for ablations because it changes the generator’s behaviour while keeping the backbone frozen (Dettmers et al., 2023; Han et al., 2024).

We train 20 LoRA adapters on top of two base models. For each base model we vary two factors: the LoRA rank $r \in \{4, 8, 16, 32, 64\}$ and the set of adapted modules. The latter takes two values: `qv_only` adapts the q and v attention projections only; `full_attention` adapts all four major attention projections (q, k, v, o). The two unadapted base models, 3B baseline and 8B baseline, serve as controls evaluated under the same inference protocol.

5.2 FIXED TRAINING HYPERPARAMETERS

All training runs use a common optimisation setup: `num_train_epochs=8`, `learning_rate=2 × 10-5`, AdamW (Kingma & Ba, 2015; Loshchilov & Hutter, 2019) with cosine schedule (Loshchilov & Hutter, 2017) and a linear warm-up over $\approx 3\%$ of the total steps, in `bf16` mixed

precision. We use `embed_top_k= 2` retrieved chunks per training example. LoRA-side hyperparameters are also fixed across runs: `bias=none`, `task_type=CAUSAL_LM`, and `lora_dropout= 0.05`. We tie `lora_alpha` to rank via the rule $\alpha = 2r$. With these constraints, the comparison isolates three sources of variation: the base-model size, the rank, and the target-module choice.

The training prompt uses a mixed-context strategy. When supporting chunks are pre-annotated for an example they are used directly; otherwise the context is materialised from the retrieval contour (§4). This is methodologically close to retrieval-augmented fine-tuning setups such as JORA (Tahir et al., 2024), and narrows the gap between idealised training and the actual inference regime.

5.3 HARDWARE AND INFERENCE STACK

All runtime cost metrics (*latency*, *inference VRAM*, *training time*, *training VRAM*) are measured on a *single* hardware configuration, to remove device-related variance from the comparison. The compute node runs in Yandex DataSphere: one NVIDIA A100 (40 GB), 28 vCPU, and 114 GB of host RAM. The same node is used both for LoRA training and for inference, so training and inference metrics are directly comparable across configurations.

The inference stack is Hugging Face Transformers with PEFT: the base model is loaded in its native precision without quantisation (`-no-quant-generator` and `-no-quant-judge` are set), the LoRA adapter is attached separately via `PeftModel.from_pretrained`, and the mixed-precision setting matches training (`bf16`). The retrieval contour uses BAAI/bge-m3 for dense embeddings and BAAI/bge-reranker-v2-m3 for reranking (`reranker_batch_size= 16`, `retrieve_top_n= 20`). Generation is greedy (no sampling) with a fixed maximum answer length shared across configurations.

Latency is measured per-sample (effective generator batch size of 1) as the mean wall-clock time per test example over the full test split ($n = 785$), counting all pipeline stages: query embedding, dense and sparse retrieval, reranking, prompt construction, and generation. Inference VRAM is logged as peak device memory via `torch.cuda.max_memory_allocated()` at the end of each run.

5.4 HYPOTHESES

The experimental design tests four working hypotheses: (i) scaling the base model improves quality but raises both latency and inference memory; (ii) increasing rank expands adaptation capacity, but with diminishing returns at high r ; (iii) broader target-module coverage (`full_attention`) is not necessarily preferable once training and inference costs are factored in; and (iv) among the resulting configurations, the practically useful working points are not the per-metric maxima but the Pareto-optimal set.

6 EVALUATION METHODOLOGY

6.1 QUALITY METRICS

The primary quality metric is *token-level* F_1 between the generated and the gold answer (Yu et al., 2024). All headline results and per-regime tables and plots in §7 and Appendix I are computed on the held-out test split ($n = 785$); the eval split ($n = 745$) is used for configuration selection during the experimental loop. Along with the point estimate of F_1 we report a non-parametric bootstrap 95% confidence interval (1,000 resamples on the test split). For paired comparisons of ΔF_1 between configurations we use the paired bootstrap on the same test split, which is appropriate for ranking close configurations on a shared sample.

We do not report embedding-based semantic metrics such as BERTScore (Zhang et al., 2020). For documentation-grounded question answering with a high share of EXACT questions, token F_1 is the most directly interpretable similarity metric; the semantic side of quality is instead captured by the judge-based scores described next.

6.2 JUDGE-BASED GROUNDEDNESS AND CORRECTNESS

We add two judge-based quality axes computed by an external LLM judge, `gpt-5.4-mini`. The judge receives only the triple (*question*, *context*, *answer*) and is blind to the generator identity – no `model_id` or configuration name is provided – so that scores are not contaminated by adapter or model branding. It assigns two independent ratings: *correctness*, the content-level accuracy of the answer with respect to the provided context, and *groundedness*, the degree to which the answer is supported by the context with no unsupported additions (Yu et al., 2024; Es et al., 2024; Baqar & Khanda, 2025).

We aggregate these into two pass-at- k scores, *correctness_pass@4* and *groundedness_pass@4*: the fraction of answers that the judge rates ≥ 4 on the corresponding scale. These judge-based scores are used as a *second* axis of quality alongside F_1 , not as a replacement. As §7.3 shows, the configuration that maximises F_1 is often not the configuration that maximises grounding, which is itself an informative finding.

6.3 COST METRICS

We measure four cost quantities. The two inference-side metrics are mean latency L_{inf} and peak inference VRAM M_{inf} (§5.3). The two training-side metrics are total training time T_{train} and peak training VRAM M_{train} . The four together form the cost vector used in the Pareto analysis (§3.1). This setup follows the quality–cost framing used in RAG and LoRA evaluation literature (Es et al., 2024; Baek et al., 2026; Baqar & Khanda, 2025).

6.4 PARETO ANALYSIS

Comparison across the resulting configuration set is done with a multi-objective Pareto analysis. A configuration x is Pareto-optimal if there is no other configuration x' that is at least as good on quality and at least as good on every cost dimension, and strictly better on at least one of them (§3.1). In the two-dimensional fronts of §7 the quality coordinate is F_1 and the cost coordinate alternates between mean inference latency, peak inference VRAM, training time, and training VRAM. This protocol focuses the discussion on the non-dominated set rather than on a single “best” configuration; the latter view is incompatible with the actual practical question of choosing a working point under a cost budget.

7 RESULTS

All results below are computed on the held-out test split ($n = 785$) with the fixed hybrid-retrieval pipeline described in §4 and the fixed training and inference setup described in §5. Unless noted otherwise, F_1 denotes token-level F1 and *grnd@4* (resp. *corr@4*) denotes the LLM-judge groundedness (resp. correctness) pass@4 score (§6). 95% bootstrap confidence intervals (CIs) are computed with 1,000 resamples; for paired comparisons of ΔF_1 between configurations we use the paired bootstrap on the same test split.

7.1 QUALITY VS. INFERENCE COST

On the F_1 -vs-latency front the non-dominated configurations are 3B `r64 qv_only` ($F_1 = 0.597$ [0.574, 0.622]) and 8B `r64 qv_only` ($F_1 = 0.617$ [0.593, 0.639]); see Table 2. The 8B point gains $\Delta F_1 = +0.020$ over the 3B point with paired-bootstrap 95% CI [+0.0005, +0.0410] – a small but statistically supported margin – at the cost of an additional ~ 9 GB of inference memory and a 0.057 s latency increase. Notably, 3B `r64 qv_only` is statistically indistinguishable from the unadapted 8B `baseline` (0.595 [0.572, 0.620]): $\Delta F_1 \in [-0.021, +0.026]$. The runtime-front choice is therefore not between two qualities but between two operating regimes.

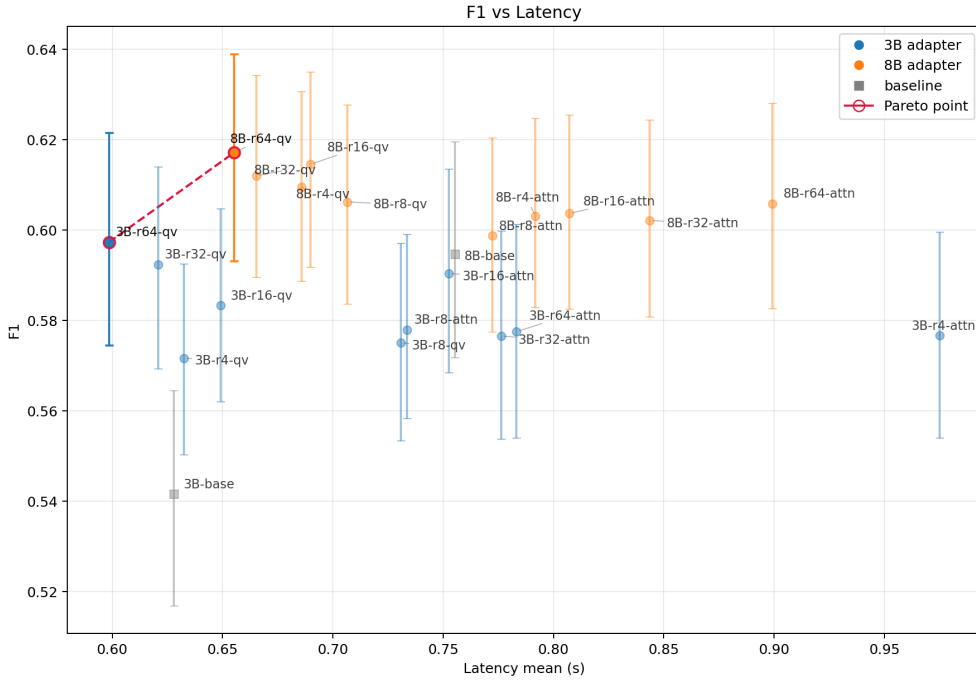


Figure 1: Token-level F_1 vs. end-to-end inference latency (per query) in the base regime. Error bars are 95% bootstrap CIs on F_1 . The Pareto front (red dashed) connects the two non-dominated configurations, 3B r64 qv_only and 8B r64 qv_only; all full_attention adapters lie strictly inside the front.

Config.	F_1 [95% CI]	Lat. (s)	VRAM (GB)
3B r64 qv_only	0.597 [0.574, 0.622]	0.598	12.76
8B r64 qv_only	0.617 [0.593, 0.639]	0.655	21.93

Table 2: Non-dominated points on the F_1 -vs-latency front in the base regime.

The F_1 -vs-inference-VRAM view cleanly separates the 3B and 8B families (VRAM difference ~ 9 GB), whereas within each family the VRAM spread is only 0.3–0.4 GB – well below the 95% CI width of F_1 . Inference memory therefore acts as a discrete family selector rather than a continuous trade-off knob.

7.2 TRAINING COST

The cheapest training point is 3B r4 qv_only (52.95 min, 19.07 GB). Stronger training-side trade-offs cluster around qv_only configurations at $r=32$ and $r=64$ for the 3B family and $r=16$ and $r=64$ for the 8B family. No full_attention configuration appears on the training Pareto front (Table 3). Within the 8B family the upper qv_only points ($r=16$ and $r=64$) have largely overlapping F_1 CIs, so the choice between them is driven by secondary criteria, not by a robust quality gap.

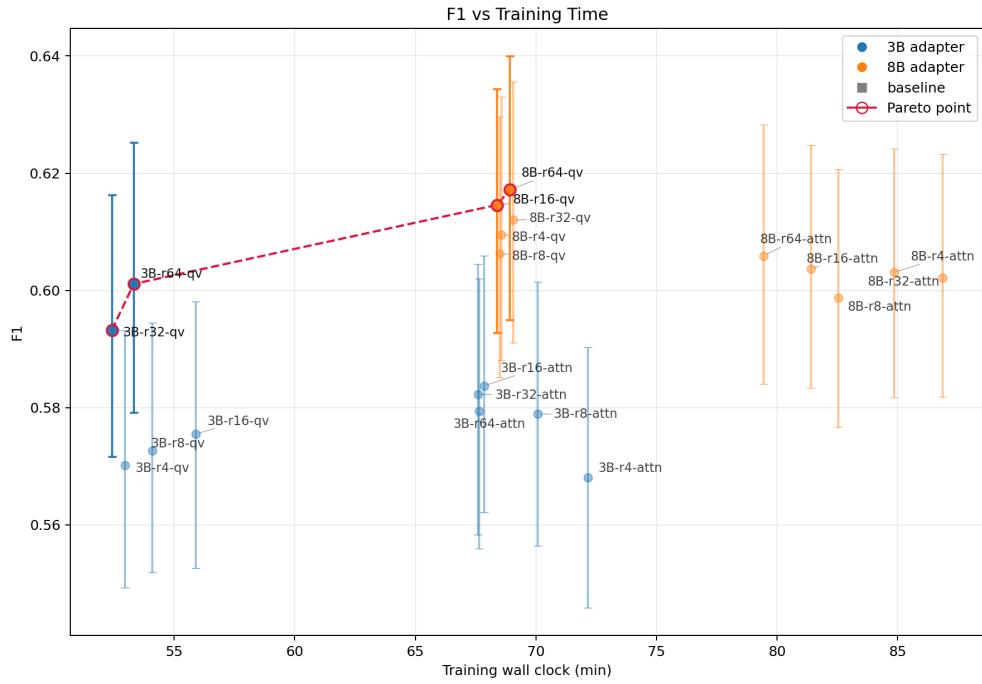


Figure 2: F_1 vs. training wall-clock time (minutes) over all 20 LoRA configurations. The Pareto front (red dashed) is dominated by `qv_only` adapters; no `full_attention` configuration appears on it. Error bars are 95% bootstrap CIs on F_1 .

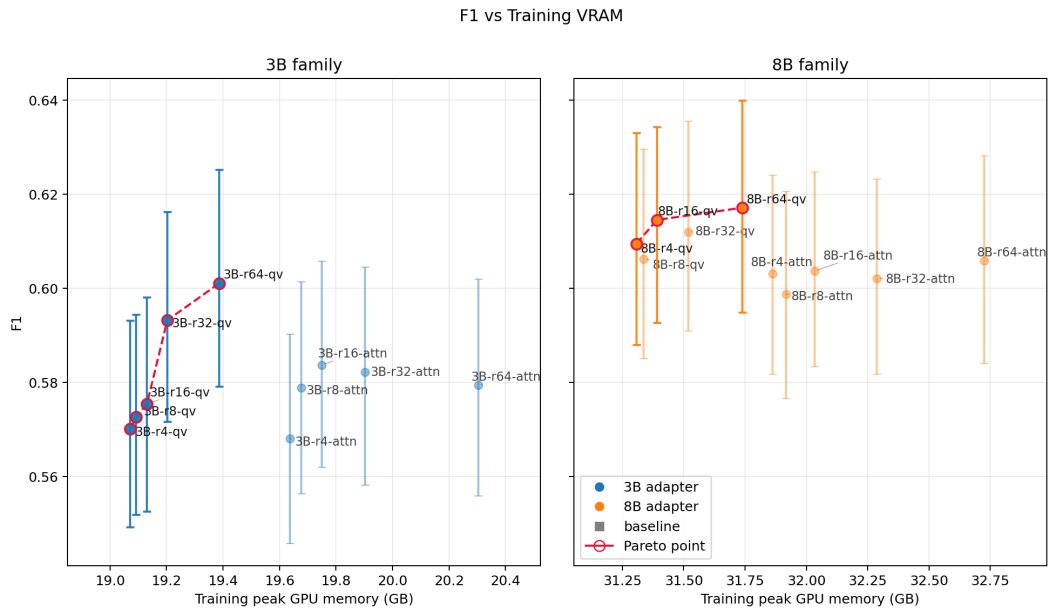


Figure 3: F_1 vs. peak training GPU memory, split by base-model family (3B / 8B). Within each family, the training Pareto front is again populated entirely by `qv_only` adapters. Error bars are 95% bootstrap CIs on F_1 .

Config.	F_1 [95% CI]	Train (min)	VRAM (GB)
3B r4 qv_only	0.572 [0.550, 0.592]	52.95	19.07
3B r8 qv_only	0.573 [0.552, 0.594]	54.08	19.09
3B r16 qv_only	0.583 [0.562, 0.605]	55.90	19.13
3B r32 qv_only	0.592 [0.569, 0.614]	52.41	19.20
3B r64 qv_only	0.597 [0.574, 0.622]	53.32	19.39
8B r4 qv_only	0.610 [0.588, 0.633]	68.57	31.31
8B r16 qv_only	0.615 [0.593, 0.634]	68.38	31.39
8B r64 qv_only	0.617 [0.595, 0.640]	68.93	31.74

Table 3: Non-dominated points on the training Pareto front (time and VRAM). All training-front points use the qv_only adaptation scheme.

7.3 GROUNDEDNESS AS A SECOND QUALITY AXIS

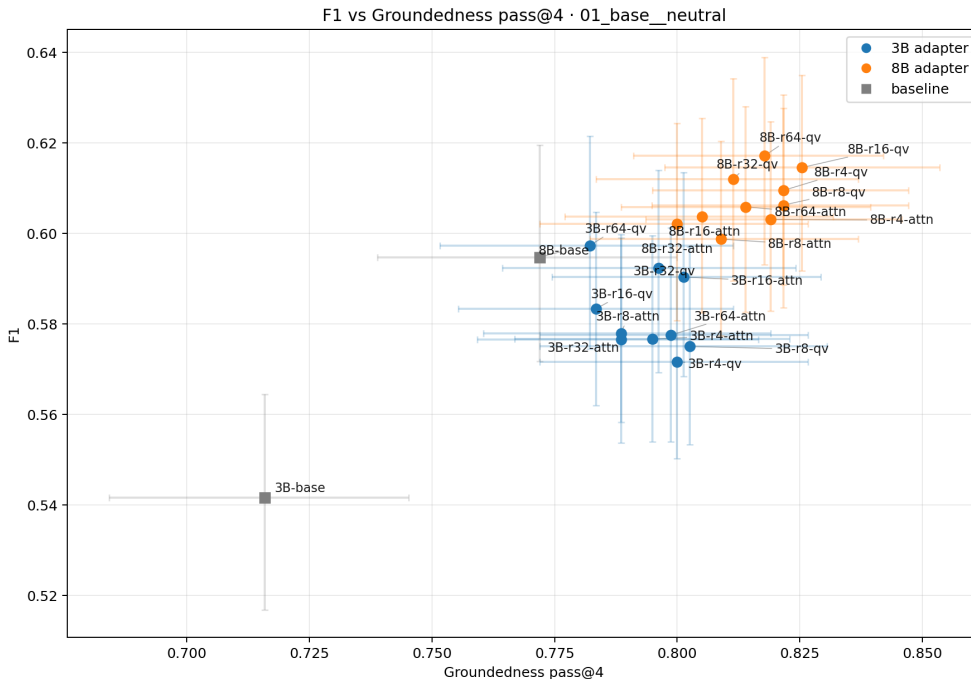


Figure 4: F_1 vs. LLM-judge groundedness pass@4 in the base regime. Error bars are 95% bootstrap CIs on both axes. Adapted configurations cluster tightly in the upper right, while the unadapted baselines are clearly separated on $grnd@4$.

The configuration with the highest point F_1 , 8B r64 qv_only ($F_1 = 0.617$, $grnd@4 = 0.818$), does *not* maximise groundedness. The $grnd@4$ maximum (0.825) is reached by 8B r16 qv_only ($F_1 = 0.615$); the two are statistically indistinguishable on F_1 ($\Delta F_1 \in [-0.011, +0.016]$). LoRA-adapted configurations also shift $grnd@4$ upward by 0.05–0.08 over the unadapted baselines at comparable latency – a margin that exceeds the typical CI width (≈ 0.03). Within already-adapted configurations, $grnd@4$ spread mostly falls inside the CIs and separation is driven by the 3B/8B choice. Task quality and grounding are therefore not interchangeable: for documentation QA, the choice of optimal configuration depends on whether the deployment prioritises exact-match agreement, supportedness, or a compromise between them.

7.4 ROBUSTNESS ACROSS RETRIEVAL AND PROMPTING

To test whether the LoRA conclusions are an artefact of one pipeline choice, we re-run the full grid under 10 retrieval/prompting regimes: five retrieval variants (base, reranker_off, dense_only,

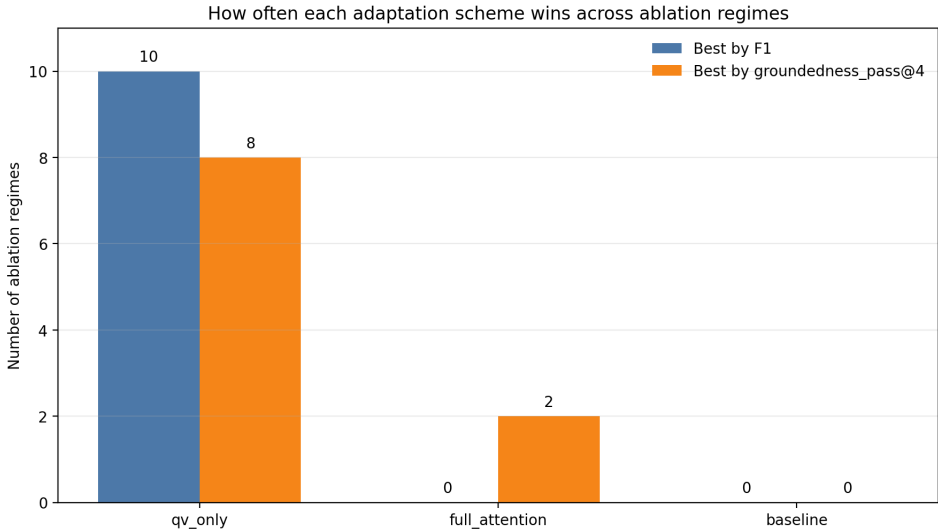


Figure 5: Frequency with which each adaptation scheme yields the best configuration across the 10 retrieval/prompting ablation regimes, separately for F_1 (blue) and $grnd@4$ (orange).

sparse_only, hybrid_bm25) crossed with two prompting modes (neutral, explicit_ grounded). Two main observations hold across all 10 modes (Table 4, full per-regime tables in Appendix I). First, the best- F_1 configuration is 8B r64 qv_only in *all* 10 modes, and the best- $grnd@4$ configuration concentrates on qv_only adapters in 8 of 10 modes (full_attention appears only in two sparse-based modes). Second, the F_1 -optimal and $grnd@4$ -optimal points never coincide (same_point=no in 10/10 modes). The choice of working configuration is therefore a function of the retrieval-prompting setup *and* the quality criterion, not of LoRA alone.

Criterion	qv_only wins	full_attention wins
Best F_1	10/10	0/10
Best $grnd@4$	8/10	2/10

Table 4: Frequency with which each adaptation scheme yields the best configuration across the 10 retrieval/prompting ablation regimes.

7.5 STATISTICAL ROBUSTNESS OF ΔF_1

Table 5 reports paired-bootstrap CIs for six key comparisons. The reliably supported effects are (i) 3B r64 qv_only over 3B baseline, (ii) 3B r64 qv_only over the param-matched 3B r64 full_attention adapter, and (iii) the family-level ΔF_1 of qv_only over full_attention averaged over the eight param-matched pairs analysed in §8. In contrast, the gaps between 3B r64 qv_only and the 8B baseline, and between the top two 8B qv_only points, are not distinguishable from sampling noise at $n = 785$. The headline of this work is therefore not any single local maximum on F_1 , but the structural advantage of the qv_only adaptation scheme.

Comparison	ΔF_1	95% CI
3B r64 qv_only - 3B baseline	+0.056	[+0.033, +0.078]
3B r64 qv_only - 8B baseline	+0.003	[-0.021, +0.026]
8B r64 qv_only - 3B r64 qv_only	+0.020	[+0.0005, +0.0410]
8B r64 qv_only - 8B r16 qv_only	+0.003	[-0.011, +0.016]
3B r64 qv_only - 3B r64 full_attention	+0.020	[+0.004, +0.036]
qv_only - full_attention*	+0.007	[+0.001, +0.012]

* mean ΔF_1 over the 8 param-matched pairs (Table 6).

Table 5: Paired-bootstrap 95% CIs on ΔF_1 ($n = 785, 1,000$ resamples).

8 PARAM-MATCHED CONTROL COMPARISON

Up to this point, the F_1 advantage of `qv_only` adapters (§7.1–§7.4) could have two natural explanations. The first is *structural*: adapting exactly the two projections that select and re-weight the retrieved context is sufficient inside this RAG architecture, while extending adaptation to k and o projections grows the adapter without buying proportional quality. The second is *parametric*: with the same rank r , `full_attention` adapts twice as many projections as `qv_only` and thus splits a fixed-shape low-rank budget more thinly across attention sub-spaces, so the per-projection capacity may simply be too small.

To distinguish the two, we run a param-matched control. Because `full_attention` adapts four projections instead of two, equal total LoRA parameter counts are achieved by halving the rank for `full_attention`. We therefore pair each `qv_only` configuration at rank r with the `full_attention` configuration at rank $r/2$, computing $\Delta F_1 = F_1(\text{QV_ONLY}) - F_1(\text{FULL_ATTENTION})$ on the test split with paired bootstrap 95% confidence intervals. Results are reported in Table 6.

Family	Param budget	qv_only	full_attention	ΔF_1	95% CI
3B	256d	$r=64$	$r=32$	+0.021	[+0.005, +0.037]
3B	128d	$r=32$	$r=16$	+0.002	[-0.013, +0.017]
3B	64d	$r=16$	$r=8$	+0.005	[-0.008, +0.020]
3B	32d	$r=8$	$r=4$	-0.002	[-0.014, +0.011]
8B	256d	$r=64$	$r=32$	+0.015	[-0.001, +0.030]
8B	128d	$r=32$	$r=16$	+0.008	[-0.006, +0.023]
8B	64d	$r=16$	$r=8$	+0.016	[+0.003, +0.027]
8B	32d	$r=8$	$r=4$	+0.003	[-0.009, +0.017]

Table 6: Param-matched comparison between `qv_only` and `full_attention` at equal total LoRA parameter count. d is the per-projection rank dimensionality budget. Paired-bootstrap 95% CIs on ΔF_1 .

Two observations follow. First, at equal parameter budget, `qv_only` is significantly better in 2 of 8 pairs (one in each family), statistically indistinguishable from `full_attention` in the remaining 6, and significantly worse in none. The advantage therefore survives the parameter-count control: it is not the case that `full_attention` would dominate once you give it the same budget as `qv_only`. Second, the only family-budget combination at which `full_attention` comes close is 3B at the smallest budget (32d, $r=8$ vs. $r=4$), where the CI of ΔF_1 straddles zero on the negative side. This is consistent with the interpretation that at very low rank `qv_only` is itself capacity-constrained, and `full_attention` can match it by spreading the same budget over more projections; once rank grows beyond $r=8$ for either scheme, the structural advantage of `qv_only` re-emerges.

9 DISCUSSION

9.1 WHY QV_ONLY WINS ON THE PARETO FRONT

Across every Pareto front in §7 the non-dominated points concentrate around `qv_only` adapters, and the paired-bootstrap test against the param-matched `full_attention` alternative gives a

mean $\Delta F_1 = +0.007 [+0.001, +0.012]$ (§7.5, §8). The most plausible explanation is that, inside a fixed retrieval contour, the adapter’s job is not to globally restructure attention but to refine how the generator *selects from* and *re-weights* the already-supplied context. The q and v projections are precisely the two attention projections that control these two operations; adapting also k and o increases the adapter size and the training cost faster than it buys robust gain on the front.

9.2 BACKBONE SIZE SETS THE REGIME, NOT THE VERDICT

The 3B/8B split looks structural but should not be read as the headline. A larger 8B backbone does set the upper F_1 ceiling, but it almost automatically commits the system to a more expensive operating regime – roughly 9 GB of additional inference VRAM and ~ 15 extra training minutes per adapter. Crucially, the strongest adapted 3B configuration is statistically indistinguishable from the unadapted 8B baseline ($\Delta F_1 \in [-0.021, +0.026]$). So scaling the backbone is not the only way to recover that level of quality: targeted LoRA adaptation closes the gap at a fraction of the cost. The backbone choice is therefore best understood as selecting an operating regime (small vs. large inference budget), with the within-regime quality controlled mainly by the adapter scheme.

9.3 RANK EFFECT IS SUB-LINEAR BUT PRACTICALLY USEFUL

Increasing r helps F_1 more than it hurts inference cost in this pipeline. For 3B `qv_only`, going from $r=4$ to $r=64$ moves F_1 from 0.572 to 0.597, while latency stays in 0.60–0.63 s and inference VRAM moves only from 12.67 to 12.76 GB – well inside the noise of measurement. The dominant inference cost in this pipeline is the base model and the retrieval contour, not the LoRA adapter itself. The same monotone-but-saturating pattern holds for the 8B family, but the upper rungs ($r=16$ vs. $r=64$) are within paired-bootstrap noise, so within the top 8B configurations the rank should be picked by secondary criteria (e.g., groundedness, or training cost), not by point F_1 .

9.4 RETRIEVAL AND PROMPTING SHIFT THE OPTIMUM BUT NOT THE FAMILY

The 10-mode ablation shows that switching off the reranker, going dense- or sparse-only, or replacing the native sparse channel with BM25, together with the choice of neutral vs. explicit-grounded prompting, *does* move the per-mode optimum point inside the same configuration grid. What it does *not* do is overturn the qualitative pattern: 8B `r64 qv_only` is the best- F_1 configuration in 10/10 modes, and `qv_only` adapters win on `grnd@4` in 8 of 10. Retrieval and prompting therefore decide how favourable the operating environment is, not which adaptation scheme should be used in it.

9.5 SENSITIVITY TO CONTEXT BUDGET (top_k)

A separate generalisation run varies the number of retrieved chunks at inference time, holding all adapters fixed. Increasing `eval_top_k` from 1 to 4 raises the best F_1 from 0.600 to 0.632 but adds ~ 0.12 s of latency (Figure 6, Table 7). The best- F_1 configuration is 8B `r64 qv_only` for all three values of `top_k`; the runtime Pareto front collapses to a single point at `top_k=1` and gains 3B `r64 qv_only` as a second non-dominated point at `top_k` $\in \{2, 4\}$. The conclusion is that broadening retrieval is not a free quality lever, but the structural ranking of LoRA configurations survives the change.

<code>top_k</code>	Best- F_1 config	F_1 [95% CI]	Lat. (s)	Runtime front
1	8B <code>r64 qv_only</code>	0.600 [0.577, 0.623]	0.604	{8B <code>r64 qv_only</code> }
2	8B <code>r64 qv_only</code>	0.617 [0.593, 0.639]	0.655	{3B <code>r64 qv_only</code> , 8B <code>r64 qv_only</code> }
4	8B <code>r64 qv_only</code>	0.632 [0.612, 0.654]	0.719	{3B <code>r64 qv_only</code> , 8B <code>r64 qv_only</code> }

Table 7: Sensitivity to retrieval context budget at inference time, in the base regime. All adapters held fixed.

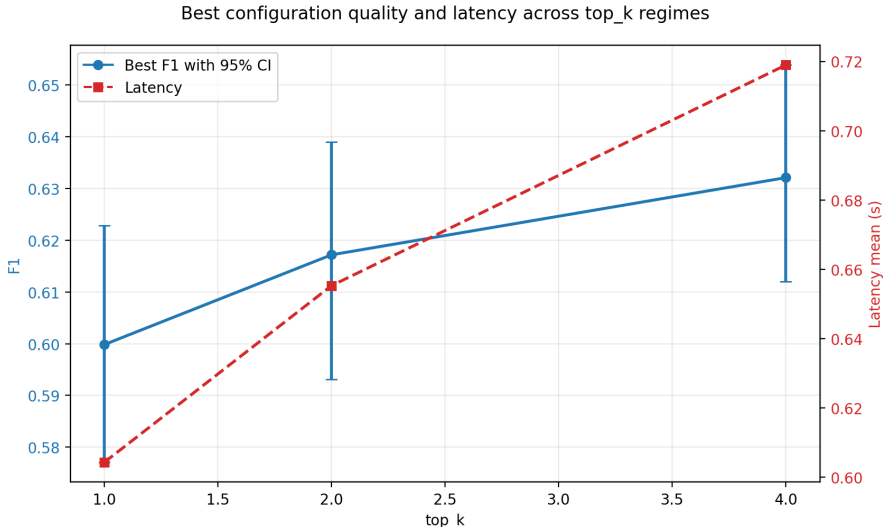


Figure 6: Effect of the retrieval cutoff k on the best F_1 (left axis, blue; with 95% bootstrap CI) and on mean end-to-end inference latency (right axis, red). The chosen working point $k=2$ corresponds to the “knee” of the curve, beyond which marginal F_1 gains are dominated by marginal latency cost.

9.6 ERROR ANALYSIS

To make the discussion of residual errors quantitative, we sampled 100 mis-predictions on the test split (50 each from 3B r64 qv_only and 8B r64 qv_only, $F_1 < 1$, seed= 42) and labelled them into four operational classes: *retrieval miss*, *overclaiming*, *incomplete answer*, and *exact/precision failure* (Table 8). *Exact/precision* errors dominate (53% overall, 66% for the 8B adapter): a substantial share of the remaining gap is not about missing knowledge but about reproducing a literal command, flag, version, or field name verbatim. Incomplete answers (24%) and retrieval misses (19%) follow; pure overclaiming is rare in this sample (4%). This taxonomy suggests two natural follow-up directions: post-hoc constrained decoding for the exact-class sub-distribution, and groundedness-aware re-training for the incomplete-answer class.

Error type	3B r64 qv_only	8B r64 qv_only	Total
retrieval miss	11 (22%)	8 (16%)	19 (19%)
overclaiming	2 (4%)	2 (4%)	4 (4%)
incomplete answer	17 (34%)	7 (14%)	24 (24%)
exact/precision failure	20 (40%)	33 (66%)	53 (53%)

Table 8: Manual error-type taxonomy on a balanced 100-sample subset of mis-predictions ($F_1 < 1$, fixed random seed).

10 CONCLUSION

We presented a systematic study of LoRA configurations inside a fixed documentation-grounded RAG pipeline. Three findings stand out. First, on every Pareto front we examined – F_1 against latency, inference VRAM, training time, and training VRAM – the non-dominated points concentrate around adapters that act on the q and v attention projections only; full-attention adapters do not appear on the training Pareto front in this study, and the param-matched control comparison confirms that the advantage of qv_only is structural rather than just a parameter-count artefact. Second, the 3B/8B choice determines the operating regime (small vs. large inference budget), but a strong LoRA-adapted 3B configuration reaches statistically comparable F_1 to the unadapted 8B baseline at roughly 9 GB less inference VRAM, so backbone size and adaptation interact as *complements*, not substitutes. Third, judge-based groundedness is not interchangeable with F_1 : the configuration

that maximises F_1 is not the configuration that maximises grounding, and at fixed F_1 the difference between them is robust across the 10 retrieval/prompting ablation regimes.

Practically, the paper produces three recommended working points: a lightweight one (3B r64 qv_only) when the deployment is inference-cost-constrained but expects high quality; the F1-maximising one (8B r64 qv_only) when an 8B budget is available; and a grounding-maximising 8B alternative (8B r16 qv_only) when supportedness is the priority.

To support reproducible follow-up work, we will release the manually verified Kubernetes QA benchmark and the selected LoRA adapters together with this paper. The most natural extensions of this study are multi-seed validation for the close-CI comparisons, a human-agreement study for the LLM judge, a port of the ablation protocol to a second documentation domain, and a re-measurement of the runtime axis on alternative inference stacks.

REFERENCES

- Sang-Eon Baek, Joon-Min Lee, Sung-Bae Kim, and Tae-Hyun Oh. Efficient hyper-parameter search for LoRA via language-aided Bayesian optimization, 2026.
- Mohammad Baqar and Rajat Khanda. Hallucinations and truth: A comprehensive accuracy evaluation of RAG, LoRA and DoRA, 2025.
- Jianlv Chen, Shitao Xiao, Peitian Zhang, Kun Luo, Defu Lian, and Zheng Liu. M3-Embedding: Multi-linguality, multi-functionality, multi-granularity text embeddings through self-knowledge distillation. In *Findings of the Association for Computational Linguistics: ACL 2024*, 2024.
- Gordon V. Cormack, Charles L. A. Clarke, and Stefan Büttcher. Reciprocal rank fusion outperforms Condorcet and individual rank learning methods. In *Proceedings of the 32nd International ACM SIGIR Conference on Research and Development in Information Retrieval*, pp. 758–759, 2009.
- Tim Dettmers, Artidoro Pagnoni, Ari Holtzman, and Luke Zettlemoyer. QLoRA: Efficient finetuning of quantized LLMs. In *Advances in Neural Information Processing Systems*, 2023.
- Matthijs Douze, Alexandr Guzhva, Chengqi Deng, Jeff Johnson, Gergely Szilvassy, Pierre-Emmanuel Mazaré, Maria Lomeli, Lucas Hosseini, and Hervé Jégou. The Faiss library, 2024.
- Abhimanyu Dubey, Abhinav Jauhri, Abhinav Pandey, Abhishek Kadian, Ahmad Al-Dahle, Aiesha Letman, Akhil Mathur, Alan Schelten, Amy Yang, Angela Fan, et al. The Llama 3 herd of models, 2024.
- Shahul Es, Jithin James, Luis Espinosa-Anke, and Steven Schockaert. RAGAs: Automated evaluation of retrieval augmented generation. In *Proceedings of the 18th Conference of the European Chapter of the Association for Computational Linguistics: System Demonstrations*, 2024.
- Yunfan Gao, Yun Xiong, Xinyu Gao, Kangxiang Jia, Jinliu Pan, Yuxi Bi, Yi Dai, Jiawei Sun, Meng Wang, and Haofen Wang. Retrieval-augmented generation for large language models: A survey, 2023.
- Zeyu Han, Chao Gao, Jinyang Liu, Jeff Zhang, and Sai Qian Zhang. Parameter-efficient fine-tuning for large models: A comprehensive survey, 2024.
- Soufiane Hayou, Nikhil Ghosh, and Bin Yu. LoRA+: Efficient low rank adaptation of large models. In *Proceedings of the 41st International Conference on Machine Learning*, 2024.
- Edward J. Hu, Yelong Shen, Phillip Wallis, Zeyuan Allen-Zhu, Yuanzhi Li, Shean Wang, Lu Wang, and Weizhu Chen. LoRA: Low-rank adaptation of large language models. In *International Conference on Learning Representations (ICLR)*, 2022.
- Jeff Johnson, Matthijs Douze, and Hervé Jégou. Billion-scale similarity search with GPUs. *IEEE Transactions on Big Data*, 7(3):535–547, 2019.
- Vladimir Karpukhin, Barlas Oğuz, Sewon Min, Patrick Lewis, Ledell Wu, Sergey Edunov, Danqi Chen, and Wen-tau Yih. Dense passage retrieval for open-domain question answering. In *Proceedings of the 2020 Conference on Empirical Methods in Natural Language Processing (EMNLP)*, 2020.

- Diederik P. Kingma and Jimmy Ba. Adam: A method for stochastic optimization. In *International Conference on Learning Representations*, 2015.
- Patrick Lewis, Ethan Perez, Aleksandra Piktus, Fabio Petroni, Vladimir Karpukhin, Naman Goyal, Heinrich Küttler, Mike Lewis, Wen-tau Yih, Tim Rocktäschel, Sebastian Riedel, and Douwe Kiela. Retrieval-augmented generation for knowledge-intensive NLP tasks. In *Advances in Neural Information Processing Systems*, volume 33, pp. 9459–9474, 2020.
- Chaofan Li, Zheng Liu, Shitao Xiao, and Yingxia Shao. Making large language models a better foundation for dense retrieval, 2023.
- Ilya Loshchilov and Frank Hutter. SGDR: Stochastic gradient descent with warm restarts. In *International Conference on Learning Representations*, 2017.
- Ilya Loshchilov and Frank Hutter. Decoupled weight decay regularization. In *International Conference on Learning Representations*, 2019.
- Rodrigo Nogueira and Kyunghyun Cho. Passage re-ranking with BERT, 2019.
- Yingqi Qu, Yuchen Ding, Jing Liu, Kai Liu, Ruiyang Ren, Wayne Xin Zhao, Daxiang Dong, Hua Wu, and Haifeng Wang. RocketQA: An optimized training approach to dense passage retrieval for open-domain question answering. In *Proceedings of the 2021 Conference of the North American Chapter of the Association for Computational Linguistics: Human Language Technologies*, 2021.
- Stephen Robertson and Hugo Zaragoza. The probabilistic relevance framework: BM25 and beyond. *Foundations and Trends in Information Retrieval*, 3(4):333–389, 2009.
- Stephen E. Robertson and Steve Walker. Some simple effective approximations to the 2-Poisson model for probabilistic weighted retrieval. In *Proceedings of the 17th Annual International ACM SIGIR Conference on Research and Development in Information Retrieval*, 1994.
- Stephen E. Robertson, Steve Walker, Susan Jones, Micheline Hancock-Beaulieu, and Mike Gatford. Okapi at TREC-3. In *Proceedings of the Third Text REtrieval Conference (TREC-3)*, 1995.
- Keshav Santhanam, Omar Khattab, Jon Saad-Falcon, Christopher Potts, and Matei Zaharia. ColBERTv2: Effective and efficient retrieval via lightweight late interaction. In *Proceedings of the 2022 Conference of the North American Chapter of the Association for Computational Linguistics: Human Language Technologies*, 2022.
- Anique Tahir, Bryan Cheng, Ian Price, et al. JORA: JAX tensor-parallel LoRA library for retrieval augmented fine-tuning. In *Proceedings of the 62nd Annual Meeting of the Association for Computational Linguistics: System Demonstrations*, 2024.
- Luping Wang, Sheng Chen, Linnan Jiang, Shu Pan, Runze Cai, Sen Yang, and Fei Yang. Parameter-efficient fine-tuning in large models: A survey of methodologies. *Artificial Intelligence Review*, 2025.
- Shangyu Wu, Ying Xiong, Yufei Cui, Haolun Wu, Can Chen, Ye Yuan, Lianming Huang, Xue Liu, Tei-Wei Kuo, Nan Guan, and Chun Jason Xue. Retrieval-augmented generation for natural language processing: A survey, 2024.
- Zhengmao Ye, Dengchun Li, Jingqi Tian, Tingfeng Lan, Yanbo Liang, Yexi Jiang, Jianjun Wang, Jiamu Xie, Kaichen Lu, and Yujie Bian. ASPEN: High-throughput LoRA fine-tuning of large language models with a single GPU, 2023.
- Soyoung Yoon, Eunbi Choi, Jiyeon Kim, Hyeongu Yun, Yireun Kim, and Seung-won Hwang. ListT5: Listwise reranking with fusion-in-decoder improves zero-shot retrieval. In *Proceedings of the 62nd Annual Meeting of the Association for Computational Linguistics*, 2024.
- Hao Yu, Aoran Gan, Kai Zhang, Shiwei Tong, Qi Liu, and Zhaofeng Liu. Evaluation of retrieval-augmented generation: A survey, 2024.
- Tianyi Zhang, Varsha Kishore, Felix Wu, Kilian Q. Weinberger, and Yoav Artzi. BERTScore: Evaluating text generation with BERT. In *International Conference on Learning Representations*, 2020.

Hao Zhao, Wensheng Gan, Yutao Song, et al. Retrieval-augmented mixture of LoRA experts for uploadable machine learning, 2024a.

Wayne Xin Zhao, Jing Liu, Ruiyang Ren, and Ji-Rong Wen. Dense text retrieval based on pretrained language models: A survey. *ACM Transactions on Information Systems*, 42(4):89:1–89:60, 2024b.

CONTENTS

1	Introduction	1
2	Related Work	2
3	Task and Benchmark	3
3.1	Task formulation	3
3.2	Corpus and QA construction	3
3.3	Answer types	3
4	RAG Pipeline	4
5	LoRA Configurations and Experimental Design	4
5.1	Configuration space	4
5.2	Fixed training hyperparameters	4
5.3	Hardware and inference stack	5
5.4	Hypotheses	5
6	Evaluation Methodology	5
6.1	Quality metrics	5
6.2	Judge-based groundedness and correctness	6
6.3	Cost metrics	6
6.4	Pareto analysis	6
7	Results	6
7.1	Quality vs. inference cost	6
7.2	Training cost	7
7.3	Groundedness as a second quality axis	9
7.4	Robustness across retrieval and prompting	9
7.5	Statistical robustness of ΔF_1	10
8	Param-Matched Control Comparison	11
9	Discussion	11
9.1	Why <code>qv_only</code> wins on the Pareto front	11
9.2	Backbone size sets the regime, not the verdict	12
9.3	Rank effect is sub-linear but practically useful	12
9.4	Retrieval and prompting shift the optimum but not the family	12
9.5	Sensitivity to context budget (top_k)	12
9.6	Error analysis	13

10 Conclusion	13
A Limitations	20
B Domain and Problem Statement	20
B.1 Domain	20
B.2 Problem statement	21
B.3 Task specifics	21
C Data and Corpus	22
C.1 Data source	22
C.2 Construction of the QA sets	22
C.3 Answer types	22
C.4 Dataset characteristics	23
D RAG System Architecture	23
D.1 Overall solution scheme	23
D.2 Retrieval component	23
D.3 Ranking and reranking	23
D.4 Generator and prompting	23
E LoRA Adaptation and Experimental Design	24
E.1 Motivation for using LoRA	24
E.2 Trained configurations	24
E.2.1 Baseline evaluation protocol	24
E.3 Fixed training hyperparameters	25
E.4 LoRA adaptation parameters	25
E.5 Training-context formation regime	25
E.6 Hardware configuration and inference stack	26
E.7 Experimental hypotheses	26
F Evaluation Methodology	26
F.1 Quality metrics	26
F.2 Judge-based groundedness and correctness	27
F.3 Cost metrics	27
F.4 Pareto analysis	27
G Experimental Results	27
G.1 Quality and latency	28
G.2 Quality and inference memory	29
G.3 Training cost	29

G.4	Judge-based groundedness as a second quality axis	31
G.5	Ablation experiments on retrieval and prompting	32
G.6	Statistical robustness of F1 differences	34
H	Discussion	34
H.1	Why <code>qv_only</code> adapters dominate	34
H.1.1	Param-matched comparison of <code>qv_only</code> vs <code>full_attention</code>	35
H.2	Why the backbone size sets the operating regime but does not cancel the LoRA effect	35
H.3	Why the effect of rank growth is non-linear	35
H.4	Why retrieval and prompting shift the optimum point but do not cancel the conclusions about LoRA	36
H.5	Generalization analysis by <code>top_k</code>	36
H.6	Practical recommendations	37
H.7	Error analysis	38
I	Per-Regime Detailed Tables	39
J	Per-Regime Plots	49

A LIMITATIONS

Single training seed. All LoRA adapters were trained with a single fixed seed (`seed=42`), which controls adapter initialisation, batch order, and dropout masks. The bootstrap CIs of §7 capture sampling variance over the test set (fixed model, varying test) but *not* training-time variance from re-running the same configuration with a different seed. In the LLM fine-tuning literature, seed-to-seed dispersion on task metrics can reach a few F_1 points (Baek et al., 2026), which is particularly relevant for the 0.002–0.005 F_1 gaps reported here. We therefore phrase claims about close configurations (e.g., 8B r64 qv_only vs. 8B r16 qv_only) as “statistically comparable” rather than as one strictly dominating the other.

Single LLM judge, no human-agreement calibration. The $grnd@4$ and $corr@4$ scores are produced by a single judge (`gpt-5.4-mini`) under a fixed protocol. The judge is blind to the generator (`no_model_id`), which removes the most direct form of generator-side bias, but we did not run a formal human-agreement study (e.g., Cohen’s κ on an expert-annotated sample) and we did not cross-validate the judge against an alternative judge model. The judge-based metrics should therefore be read as indicative scores from one automatic system rather than as final values of correctness or groundedness. Importantly, all main conclusions of the paper rely on the judge-free metric F_1 ; the judge-based scores are used only as a secondary axis to differentiate configurations that are close on F_1 . A residual concern is that the judge model (`gpt-5.4-mini`) and the model used in QA-candidate drafting (GPT-5.4, §3.2) come from the same family, which may introduce same-family bias against Llama-style answers. By construction this bias is uniform across all compared LoRA configurations, so the relative ordering on the Pareto front is preserved, but the absolute judge scores should be interpreted with this caveat.

Single domain. The empirical results, including absolute metric values and the shape of the Pareto fronts, are tied to the Kubernetes-documentation corpus and the curated QA set built on it. The domain has characteristic properties – many EXACT questions, technical terms, commands, flags, API versions – that affect both retrieval behaviour and the distribution of error types (§9.6). Absolute numbers should not be transported to other documentation domains (medical regulations, legal corpora, internal company docs) without re-running the protocol. The *qualitative* findings – qv_only advantage, sub-linear rank effect, and the family-as-regime split – are conjecturally transferable, but confirming this requires an equivalent ablation in a different domain.

Single retriever and reranker. The retrieval stack (BGE-M3 dense + BGE-M3 native sparse, merged via RRF, followed by the `bge-reranker-v2-m3` cross-encoder) is held fixed across all experiments. Replacing the embedder or reranker, or moving to a late-interaction architecture such as ColBERTv2 (Santhanam et al., 2022), can shift both absolute metrics and the position of the per-regime optimum. §7 is therefore best read as a statement about LoRA under this specific retrieval stack, not as a universal claim about RAG systems.

Single inference hardware and stack. Latency, inference VRAM, training time, and training VRAM are all measured on a single hardware setup (§5.3). Different batching, alternative inference engines (vLLM, TensorRT-LLM), different precisions (`fp16`, `int8`, `int4`), or different parallelism schemes can shift absolute values and possibly the relative ordering on the runtime axis. The shape of the quality-versus-cost curves is robust, but absolute numbers should be re-measured before transferring to a production deployment.

B DOMAIN AND PROBLEM STATEMENT

B.1 DOMAIN

The domain of the work is question answering over technical documentation. Unlike open-domain conversational systems, here the user expects not a generally plausible answer, but accurate and verifiable information grounded in the documentation. Such a setting fits the logic of Retrieval-Augmented Generation (RAG), in which the answer must rely on an external corpus rather than only on the parametric memory of the model Lewis et al. (2020); Gao et al. (2023); Wu et al. (2024); Yu et al. (2024).

A particular feature of this domain is its high sensitivity to the wording of the answer. For some questions a brief factual restatement is acceptable, while for others an almost literal form of the answer is essential: an exact flag, path, field name, API version, or specific parameter value. The system must therefore be able to handle both ordinary documentation-grounded answers and cases that require near-literal reproduction; for documentation question answering this is directly tied to the requirements of factual accuracy and degree of support by the retrieved context Yu et al. (2024); Es et al. (2024).

B.2 PROBLEM STATEMENT

We consider the task of building a RAG system that, given a user question about the Kubernetes documentation, must retrieve the relevant fragments of the corpus and generate an answer based only on the retrieved context. Such a formulation is in line with Retrieval-Augmented Generation for tasks that require access to an external knowledge base and with documentation question-answering systems Lewis et al. (2020); Gao et al. (2023); Wu et al. (2024); Yu et al. (2024).

Let $D = \{d_1, \dots, d_n\}$ denote the documentation corpus, represented as a set of text chunks, and let R be the fixed retrieval-and-reranking pipeline that for a question q selects the context $c = R(q, D)$. Let $x \in X$ denote the generator configuration inside this fixed retrieval pipeline, that is, the choice of base model, LoRA rank, and the scope of adapted modules. For each configuration x , the system maps a question q to an answer $a_x(q, c)$, where c is determined solely by the retrieval and reranking procedures, and the main research focus shifts to the generator adaptation and to comparing several adapter configurations Karpukhin et al. (2020); Robertson & Walker (1994); Robertson et al. (1995); Robertson & Zaragoza (2009); Zhao et al. (2024b); Qu et al. (2021); Santhanam et al. (2022); Chen et al. (2024); Nogueira & Cho (2019); Yoon et al. (2024); Hu et al. (2022); Dettmers et al. (2023); Hayou et al. (2024); Han et al. (2024); Wang et al. (2025); Ye et al. (2023).

For each configuration we introduce a quality function $Q(x) = F1(x)$ and a cost vector $C(x) = (L_{\text{inf}}(x), M_{\text{inf}}(x), T_{\text{train}}(x), M_{\text{train}}(x))$, where L_{inf} is the mean inference latency, M_{inf} is the peak inference memory consumption, T_{train} is the total training time, and M_{train} is the peak training memory consumption. For a specific deployment scenario the choice of configuration can be written as a constrained optimization problem of the form $x^* = \arg \max Q(x)$ subject to constraints on one or several components of $C(x)$.

However, the main interest of this work is not in a single solution x^* , but in the set of Pareto-optimal configurations:

$$P = \{x \in X \mid \nexists x' \in X : Q(x') \geq Q(x), \\ C_j(x') \leq C_j(x) \text{ for all } j, \text{ and at least one inequality is strict}\}.$$

This formulation matches the practical logic of the task, because the applied value of a documentation-oriented RAG assistant is determined not only by the maximum answer quality, but also by conflicting constraints on latency, memory, and training cost; this logic is consistent with works on multi-criteria evaluation of RAG and LoRA Yu et al. (2024); Es et al. (2024); Baek et al. (2026); Baqar & Khanda (2025).

B.3 TASK SPECIFICS

The task under study has a number of features that make it non-trivial compared with ordinary generative question answering. First, answers are heterogeneous in nature: some questions require literal reproduction of a value, while others demand a concise but complete and correct description of a fact. Second, generation quality strongly depends on the quality of retrieval and reranking, because the generator is restricted to the provided context. An error at the retrieval stage directly affects the final answer even with a strong generator.

Third, for a practical system computational constraints are critical. Even if a more complex configuration improves quality, it may be unsuitable in real conditions due to increased latency or memory consumption. Fourth, tuning LoRA inside a RAG system does not reduce to standard fine-tuning of a language model: one must account for the interaction between the retrieval stage, the prompt-formation mode, and the generator adaptation scheme. This is precisely why the work

uses a Pareto-based approach, which makes it possible to analyse not a single best point but a set of non-dominated configurations.

C DATA AND CORPUS

C.1 DATA SOURCE

The data source is the Kubernetes documentation. The corpus was pre-cleaned and converted into a set of text fragments suitable for retrieval and for grounding the answer in the supporting context. During corpus preparation, the documentation pages were brought into a structured textual representation and then segmented into semantically meaningful chunks. This segmentation follows the general logic of building corpora suitable for retrieval in RAG systems Gao et al. (2023); Wu et al. (2024); Yu et al. (2024); Karpukhin et al. (2020); Chen et al. (2024).

C.2 CONSTRUCTION OF THE QA SETS

The question-answer set was assembled in a combined way: 500 QA pairs were written by the author manually, while the remaining part was prepared using an AI agent based on the GPT-5.4 model (through the agent interface in the Cursor environment). Generation was performed one pair at a time: each question-answer pair was created individually from the Kubernetes documentation rather than obtained through bulk automated augmentation. The resulting set then underwent a full manual verification pass by the author, including verification of question correctness, reference answers, and their correspondence to the source fragments of the documentation. During verification, successive cleanup passes were applied to the whole set; a pair was discarded if the question was malformed or ambiguous, if no answer was present in the documentation corpus, if it was a duplicate of another pair, or if the reference answer contained a factual error. As a result of the cleanup passes, 323 pairs out of an initial pool of 5467 QA candidates were rejected (about 5.9%), and approximately 20% of the remaining pairs required editing of the wording or rephrasing of the reference answer to match the format of short documentation answers; the remaining pairs were accepted without changes. This logic is consistent with modern approaches to evaluating RAG systems, where both the quality of the answer and its support by the retrieved context matter Yu et al. (2024); Es et al. (2024). The final verified set of 5144 pairs (500 written manually from scratch and 4644 automatically generated and manually verified) was split into training, validation, and test parts. In the current configuration of the work we use the train, eval, and test splits, intended respectively for training adapters, selecting and comparing configurations, and the final evaluation.

In addition, it is worth recording the relationship between the model used to generate QA candidates (GPT-5.4) and the model used as the judge in §6 (gpt-5.4-mini). Although both models belong to the same family, no direct train/test leak arises between them: the judge was not trained on the gold answers, and the reference answers themselves underwent a full manual verification by the author. The residual risk of a same-family bias is discussed separately in Appendix A as a limitation of the judge-based metrics.

Thus the work produces not only a question-answer set, but an integrated evaluation benchmark: the documentation corpus, the QA set, the train/eval/test split, the metric system, and a unified protocol for ablation and Pareto experiments. This makes the resulting set usable not only for training and testing individual adapters, but also for the reproducible comparison of retrieval and LoRA configurations within a common experimental setting.

C.3 ANSWER TYPES

In the QA set two answer types are distinguished: `exact` and `normal`. The `exact` class covers cases in which the almost-literal form of the answer matters, for example flags, paths, field names, API version, feature gates, and other short literal values. The `normal` class covers ordinary factual answers, grounded in the documentation and admitting careful rephrasing while preserving meaning. This distinction is introduced in the present work as part of our own methodology for annotating and analysing answers.

This annotation was used both for manual analysis of the QA set and during adapter training. It is important to emphasize that in the current main inference regime the generator does not receive the answer-type label (`exact` or `normal`) as an input signal and operates in a neutral prompt-formation mode. The answer-type annotation is therefore used in the work primarily as a supervision signal during training and as a source of stratified quality metrics, but not as an explicit condition at test-time inference; this scheme methodologically aligns with the separation of training and testing regimes in RAG-evaluation works Yu et al. (2024); Es et al. (2024).

C.4 DATASET CHARACTERISTICS

The final sizes of the splits are given in Table 9.

Split	Rows	Exact	Normal
Train	3614	1449	2165
Eval	745	361	384
Test	785	475	310

Table 9: Sizes of the training, validation, and test parts of the QA set

Table 9 records the sizes of the training, validation, and test parts of the set, as well as the distribution of answer types within each part. These characteristics are used further as a description of the experimental base on which adapter training and final configuration evaluation are performed.

D RAG SYSTEM ARCHITECTURE

D.1 OVERALL SOLUTION SCHEME

The system under study is a Retrieval-Augmented Generation pipeline for question answering over technical documentation. Given a user question, the system first retrieves a set of candidates from the documentation corpus, then reranks the retrieved fragments, and finally passes the selected context to the generator. This three-step scheme of retrieval, reranking, and generation matches modern views on RAG systems Lewis et al. (2020); Gao et al. (2023); Wu et al. (2024); Yu et al. (2024).

D.2 RETRIEVAL COMPONENT

In the current main configuration we use a hybrid retrieval pipeline: dense retrieval based on a FAISS index is combined with native sparse retrieval based on BGE-M3, and the results are merged using Reciprocal Rank Fusion. This scheme draws on works on dense retrieval, BM25, hybrid retrieval, and result fusion Karpukhin et al. (2020); Robertson & Walker (1994); Robertson et al. (1995); Robertson & Zaragoza (2009); Zhao et al. (2024b); Qu et al. (2021); Santhanam et al. (2022); Chen et al. (2024); Douze et al. (2024); Johnson et al. (2019); Cormack et al. (2009); Li et al. (2023).

D.3 RANKING AND RERANKING

After the initial retrieval step the candidates additionally pass through reranking. In the system under study we use the pretrained reranker `BAAI/bge-reranker-v2-m3`. The very idea of reranking goes back to classical works on cross-encoder and listwise reranking Nogueira & Cho (2019); Yoon et al. (2024); for the BGE family the work on dense retrieval based on large language models Li et al. (2023) is also relevant.

D.4 GENERATOR AND PROMPTING

We consider two instruction-tuned models of the Llama 3 family as generators: `meta-llama/Llama-3.2-3B-Instruct` and `meta-llama/Llama-3.1-8B-Instruct`. Both models belong to successive releases of the Llama 3 family Dubey et al. (2024) – versions 3.2 and 3.1, respectively; they share the common architectural line of decoder-only transformers with RoPE,

GQA attention, and SwiGLU blocks described in Dubey et al. (2024). In the main inference regime we use a neutral prompt-formation mode that minimizes explicit control over answer style.

This prompt-formation mode allows adapters to be evaluated in a single inference regime and thus compared on a fairer basis. At training time, the option to condition on the answer type is preserved, which is important for handling both literal and ordinary factual answers; such a separation of training and testing regimes methodologically aligns with works on RAG evaluation Yu et al. (2024); Es et al. (2024).

E LORA ADAPTATION AND EXPERIMENTAL DESIGN

E.1 MOTIVATION FOR USING LORA

Full fine-tuning of modern instruction-tuned language models is costly both in memory and in time. We therefore use parameter-efficient fine-tuning, namely LoRA. This choice rests directly on works on LoRA, QLoRA, and general PEFT surveys Hu et al. (2022); Dettmers et al. (2023); Hayou et al. (2024); Han et al. (2024); Wang et al. (2025). For our research task, in which several adaptation configurations have to be compared, this approach is particularly convenient.

E.2 TRAINED CONFIGURATIONS

The current set of training artefacts comprises two baseline models and 20 trained LoRA configurations. For each base model we considered LoRA configurations with several rank values and two attention-module coverage schemes: adaptation of the query and value projections only (`q_proj`, `v_proj`) and adaptation of all main projections in the attention block (`q_proj`, `k_proj`, `v_proj`, `o_proj`).

Base model	Ranks	Adaptation schemes	Number of LoRA configs
3B	4, 8, 16, 32, 64	<code>qv_only</code> , <code>full_attention</code>	10
8B	4, 8, 16, 32, 64	<code>qv_only</code> , <code>full_attention</code>	10

Table 10: Composition of the trained LoRA configurations: base models, rank options, and adaptation schemes

The baseline configurations `3B baseline` and `8B baseline` were used as LoRA-free reference points and were compared against the trained adapters on the same evaluation metrics.

E.2.1 BASELINE EVALUATION PROTOCOL

For the baseline configurations we used the same inference protocol as for the main LoRA-adapter comparisons. The evaluation was performed in the neutral prompting mode, without any additional explicit requirement of a grounded-answer style in the prompt. On the retrieval side we used the same base pipeline as in the main `01_base_neutral` regime: dense retrieval, native sparse retrieval, candidate fusion via reciprocal rank fusion, and subsequent reranking with the pretrained reranker.

The number of context fragments at inference time was also kept fixed and matched the main comparison regime: `top_k = 2`. Thanks to this, the comparison of `3B baseline / 8B baseline` with the LoRA configurations was performed in the same retrieval and prompting pipeline in which the main results of §7 are interpreted, rather than in a separate special regime. This is important for the correctness of the subsequent comparisons, including the discussion of the closeness between `3B r64 qv_only` and `8B baseline` on F1.

E.3 FIXED TRAINING HYPERPARAMETERS

Parameter	Value	Comment
embed_top_k	2	Number of context fragments in a training example
num_train_epochs	8	Total number of epochs
learning_rate	2e-5	Single value used for all runs

Table 11: Fixed training hyperparameters shared across all LoRA configurations

In the current set of training runs a single scheme was used to form the training context. Across all configurations the number of retrieved context fragments was fixed as `embed_top_k = 2`, that is, every training example was built on top of two context fragments.

All runs in the current set used `num_train_epochs = 8` and `learning_rate = 2e-5`. The base optimization scheme follows the standard PEFT setup: the AdamW optimizer Kingma & Ba (2015); Loshchilov & Hutter (2019) with a cosine schedule on the learning rate Loshchilov & Hutter (2017) and a linear warm-up over approximately $\sim 3\%$ of the total training steps; mixed precision is set to `bf16`. Compared configurations were therefore trained in a comparable regime, and any differences in quality and cost can be attributed primarily to the adapter parameters rather than to changes in the optimization regime.

E.4 LoRA ADAPTATION PARAMETERS

For all runs we used `bias = none`, `task_type = CAUSAL_LM`, and `lora_dropout = 0.05`. The `lora_alpha` coefficient was chosen proportional to the rank via the rule `alpha = 2r`. As a result, when comparing configurations we varied primarily the model scale, the rank, and the scope of adapted modules, while the remaining LoRA parameters stayed fixed.

Configuration aspect	Value
r = 4	lora_alpha = 8
r = 8	lora_alpha = 16
r = 16	lora_alpha = 32
r = 32	lora_alpha = 64
r = 64	lora_alpha = 128
lora_dropout	0.05
qv_only	q_proj, v_proj
full_attention	q_proj, k_proj, v_proj, o_proj

Table 12: LoRA adaptation parameters: correspondence of rank to `lora_alpha`, dropout, and the attention-module coverage for the two compared schemes

In terms of the scope of adapted modules, two main schemes were used in the current experimental set. The `qv_only` configuration adapts only the `q_proj` and `v_proj` projections. The `full_attention` configuration extends adaptation to all main attention projections: `q_proj`, `k_proj`, `v_proj`, and `o_proj`. This comparison makes it possible to assess whether wider attention-block coverage justifies the additional training and inference cost inside the same RAG architecture.

E.5 TRAINING-CONTEXT FORMATION REGIME

Adapter training does not rely on a single context regime. We use a mixed scheme for forming the training example. If the example has pre-labelled supporting chunks, exactly those are fed as the supporting context. If no such labelling exists, the context is formed by the retrieval procedure. This scheme is methodologically close to the retrieval-augmented fine-tuning settings described in JORA Tahir et al. (2024) and helps reduce the gap between idealized training and the actual inference regime.

E.6 HARDWARE CONFIGURATION AND INFERENCE STACK

All runtime cost metrics (Latency, Inference VRAM, Training Time, Training VRAM) were measured in a single compute environment, so as to remove any contribution of hardware to the relative differences between configurations. The measurements were performed in Yandex DataSphere on a single compute node with the following characteristics: 1× NVIDIA A100 40 GB, 28 vCPU, and 114 GB of RAM. The same node was used both for training the LoRA adapters and for subsequent inference; thanks to this Training Time, Training VRAM, Latency, and Inference VRAM remain comparable across the entire set of experiments.

The inference stack is based on Hugging Face Transformers and PEFT Dettmers et al. (2023); Hayou et al. (2024): the base model (meta-llama/Llama-3.2-3B-Instruct or meta-llama/Llama-3.1-8B-Instruct) is loaded in the original precision without quantization (the flags `--no-quant-generator` and `--no-quant-judge`), and the LoRA adapter is loaded separately on top of the base model via `PeftModel.from_pretrained`; the mixed-precision setting matches `bf16`, as during training (see §E.5). The retrieval pipeline uses BAAI/bge-m3 for dense embeddings and BAAI/bge-reranker-v2-m3 for final reranking (`reranker_batch_size = 16`, `retrieve_top_n = 20`); in the main comparison regime the generator operates with a fixed `eval_top_k = 2` retrieved fragments, which matches the training-context formation scheme (`embed_top_k = 2`, see §E.5); additionally, for sensitivity control to the parameter, runs were performed with `eval_top_k ∈ {1, 4}`. Generation is performed in greedy decoding (no sampling) with the maximum answer length fixed in the code and identical across all configurations.

Latency is measured per sample (the effective generator batch size equals one), as the mean time of the complete processing of a single test example – from receiving the query to returning the generated answer – over the entire test split $n = 785$, and includes all pipeline stages: building the query embedding, dense and sparse retrieval, reranking, prompt formation, and answer generation. Inference VRAM is recorded as the peak GPU memory consumption on the device, obtained via `torch.cuda.max_memory_allocated` at the end of the run.

E.7 EXPERIMENTAL HYPOTHESES

The work tests the following hypotheses:

- scaling the model up improves quality but raises latency and memory consumption;
- increasing the rank expands the adaptation capacity, but does not always yield a proportional gain in quality;
- a wider coverage of adapted modules is not necessarily preferable once training and inference cost are accounted for;
- among the set of configurations there exist practical working points that do not maximize quality but offer the best balance between quality and cost.

F EVALUATION METHODOLOGY

F.1 QUALITY METRICS

The main quality metric in the work is token-level F1, used to compare configurations by the degree of agreement between the answer and the reference Yu et al. (2024). The final F1 values, the judge-based metrics, the summary tables of §7 and the corresponding plots are computed on the final test split ($n = 785$). The eval split ($n = 745$) is used for selection and intermediate comparison of configurations during the experimental cycle. In addition to point estimates we also compute 95% bootstrap confidence intervals on the test set (1000 resamples). For key configuration comparisons we use the paired bootstrap for the difference $\Delta F1$, which separates stable differences from narrow gaps lying within sampling noise. Semantic embedding-based metrics such as BERTScore Zhang et al. (2020) are not used in the main setting of the work: for documentation-oriented question answering with a high share of exact questions, token-level F1 provides a more direct and interpretable comparison with the reference, while the semantic dimension of quality is covered separately by the judge-based correctness and groundedness scores (see Section 5.2).

F.2 JUDGE-BASED GROUNDEDNESS AND CORRECTNESS

In addition, we use judge-based evaluation of groundedness and correctness. In this scheme an external judge language model `gpt-5.4-mini` receives the question, the retrieved context, and the generated answer, after which it assigns two independent scores: correctness as the degree of semantic correctness of the answer relative to the provided context, and groundedness as the degree to which the answer is supported by the retrieved fragments without unsupported additions. Evaluation is performed in a blind regime: the judge receives only the triple (`question`, `context`, `answer`) and does not receive the `model_id`, the configuration name, or any other generator metadata. This evaluation is used not as a replacement for the main F1 metric, but as an additional axis of quality that supports the analysis of supportedness of the answer by the retrieved context and of its faithfulness to that context Yu et al. (2024); Es et al. (2024); Baqar & Khanda (2025).

The main aggregates of the judge-based evaluation are `correctness_pass@4` and `groundedness_pass@4`, that is, the fraction of answers that received a score of at least 4 on the corresponding scale. These metrics are especially useful when several configurations have similar F1 values but differ in the degree of context support. In particular, the subsequent ablation experiments show that the configuration optimal in F1 does not necessarily coincide with the configuration optimal in groundedness, which indicates a stable trade-off between task quality and supportedness.

F.3 COST METRICS

To analyse computational cost we use both deployment and training metrics. The former include the mean answer latency and the peak GPU memory consumption at inference. The latter include the total training time and the peak GPU memory consumption at training. Such a set reflects the idea of jointly analysing quality and cost, emphasized in works on the efficiency evaluation of RAG and LoRA Es et al. (2024); Baek et al. (2026); Baqar & Khanda (2025).

F.4 PARETO ANALYSIS

To compare configurations in a multi-criteria setting we use Pareto analysis. A configuration is considered non-dominated if no other configuration is no worse in quality and at the same time no worse in cost, while being strictly better in at least one dimension. In two-dimensional fronts the role of the quality function is played by F1, while the role of cost is taken in turn by the mean inference latency, inference memory, training time, and training memory. This approach makes it possible to identify practical working points and to avoid simplistic model selection based on a single metric; the multi-criteria logic of such a comparison is consistent with works in which quality and cost are analysed jointly Baek et al. (2026); Baqar & Khanda (2025).

G EXPERIMENTAL RESULTS

In this appendix the results of comparing baseline systems and LoRA adapters are interpreted as multi-criteria trade-offs between quality, latency, memory, and training cost. All summary results in Tables 13, 14, 15 and 16, and in the corresponding plots, are computed on the final test split ($n = 785$).

G.1 QUALITY AND LATENCY

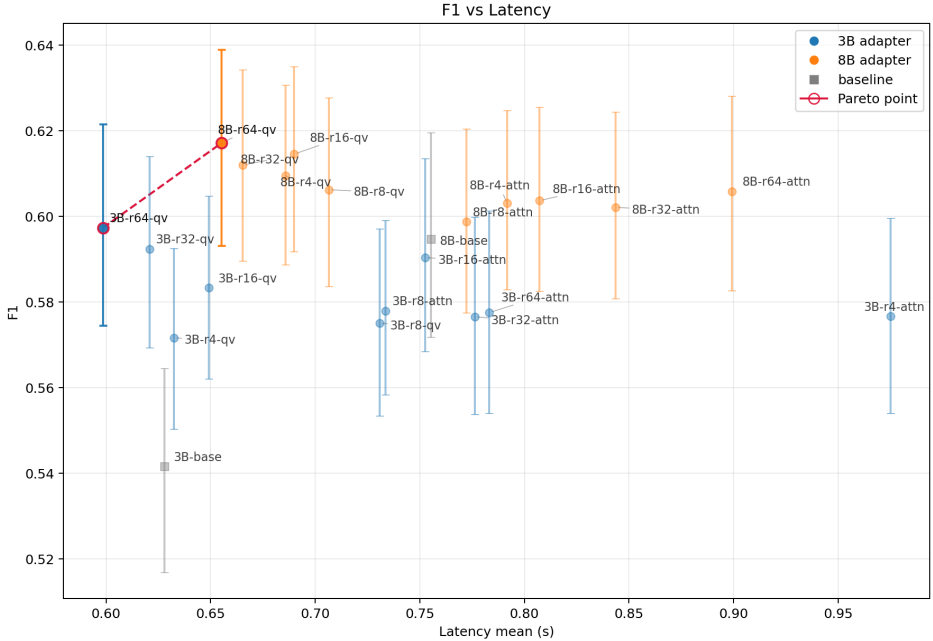


Figure 7: F1 vs Latency

On the main response-time front the non-dominated configurations are 3B r64 qv_only and 8B r64 qv_only. The first represents the strongest lightweight point, and the second yields the highest quality in the current set of experiments. These points are listed in Table 13.

Configuration	F1 [95% CI]	EM	Latency, s	Inference VRAM, GB
3B r64 qv_only	0.597 [0.574, 0.622]	0.250	0.598	12.760
8B r64 qv_only	0.617 [0.593, 0.639]	0.250	0.655	21.926

Table 13: Non-dominated points on the quality–latency front

Table 13 shows that the main response-time front (the runtime front) in the base regime consists of two points, between which the main practical trade-off lies. The transition from 3B r64 qv_only to 8B r64 qv_only brings approximately a 0.020 gain in F1, and the paired bootstrap for $\Delta F1$ gives a 95% CI of $[+0.0005, +0.0410]$. This indicates a small but test-set-supported advantage of the 8B configuration in F1, which at the same time comes with a transition to a substantially more expensive inference-memory regime and a latency increase of approximately 0.057 s. Importantly, 3B r64 qv_only with F1 = 0.597 [0.574, 0.622] turns out to be statistically comparable to the unadapted 8B baseline configuration (0.595 [0.572, 0.620]): for $\Delta F1$ the 95% CI is $[-0.021, +0.026]$. The choice between these points is therefore determined not only by quality, but also by whether the system needs a lightweight 3B regime or a more expensive 8B regime with the highest point quality.

G.2 QUALITY AND INFERENCE MEMORY

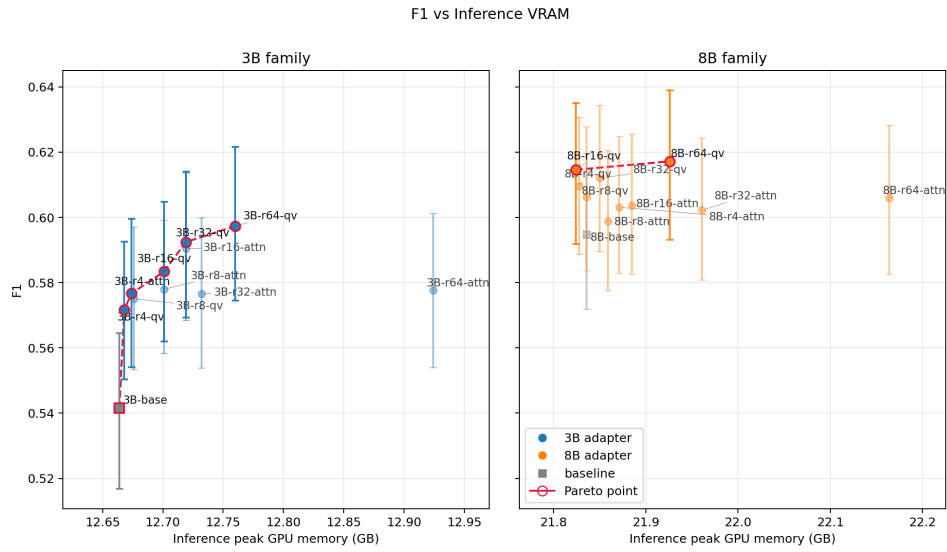


Figure 8: F1 vs Inference VRAM

The inference-memory plot shows a clear separation between the 3B and 8B families. The 3B configurations occupy a more compact area in memory and therefore remain most attractive for constrained hardware.

G.3 TRAINING COST

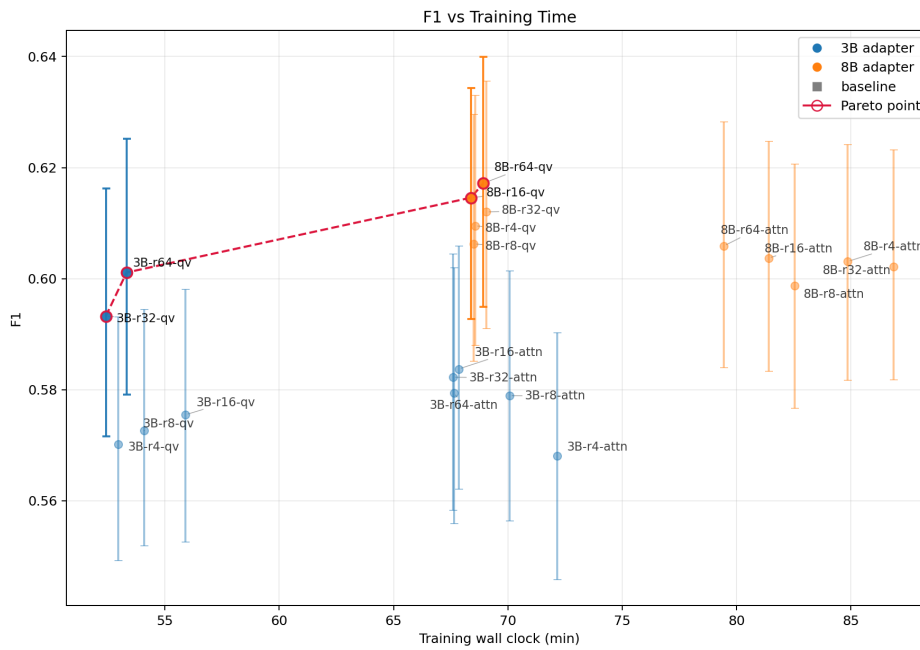


Figure 9: F1 vs Training Time

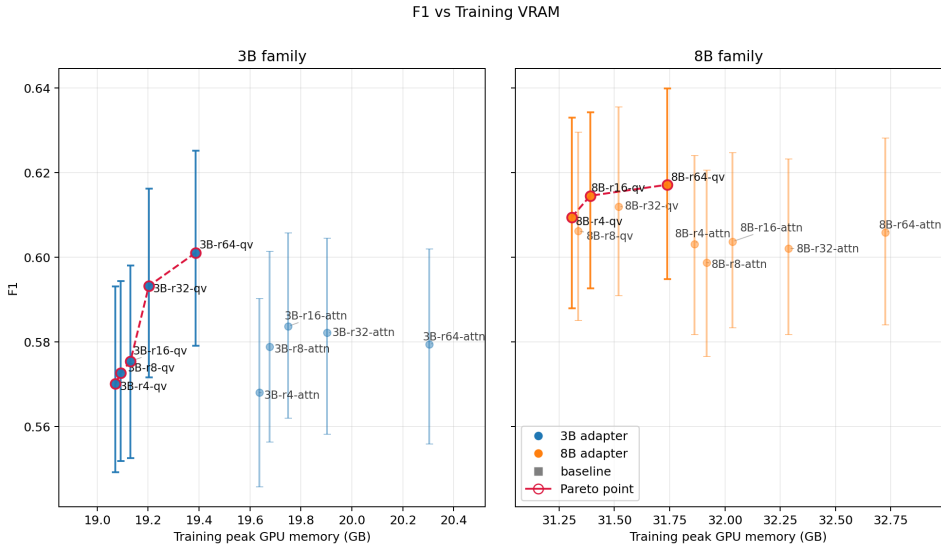


Figure 10: F1 vs Training VRAM

In terms of training time and training memory the cheapest point remains 3B r4 qv_only, however the current training Pareto fronts are no longer limited to the lowest ranks. The strongest training-side trade-offs form around qv_only configurations with ranks $r = 32$ and $r = 64$ in the 3B family and $r = 16/r = 64$ in the 8B family. The composition of the non-dominated training-front points is given in Table 14.

Configuration	F1 [95% CI]	Training time, min	Train VRAM, GB	Front
3B r4 qv_only	0.572 [0.550, 0.592]	52.95	19.072	vram
3B r8 qv_only	0.573 [0.552, 0.594]	54.08	19.092	vram
3B r16 qv_only	0.583 [0.562, 0.605]	55.90	19.131	vram
3B r32 qv_only	0.592 [0.569, 0.614]	52.41	19.203	time, vram
3B r64 qv_only	0.597 [0.574, 0.622]	53.32	19.387	time, vram
8B r4 qv_only	0.610 [0.588, 0.633]	68.57	31.307	vram
8B r16 qv_only	0.615 [0.593, 0.634]	68.38	31.391	time, vram
8B r64 qv_only	0.617 [0.595, 0.640]	68.93	31.740	time, vram

Table 14: Non-dominated points by training criteria

Table 14 shows that inside the 3B family the move to $r = 32$ and $r = 64$ is accompanied by a noticeable improvement in F1, while training time and memory grow only moderately compared to the lower ranks. At the same time, full_attention configurations do not appear at all on the current training Pareto fronts, which further emphasizes the structural advantage of qv_only. For the 8B family the differences in training time between qv_only configurations are also small relative to the overall backbone cost, while the upper points $r = 16$ and $r = 64$ have almost fully overlapping F1 intervals, so the choice between them is driven more by additional criteria than by a stable quality gap.

G.4 JUDGE-BASED GROUNDEDNESS AS A SECOND QUALITY AXIS

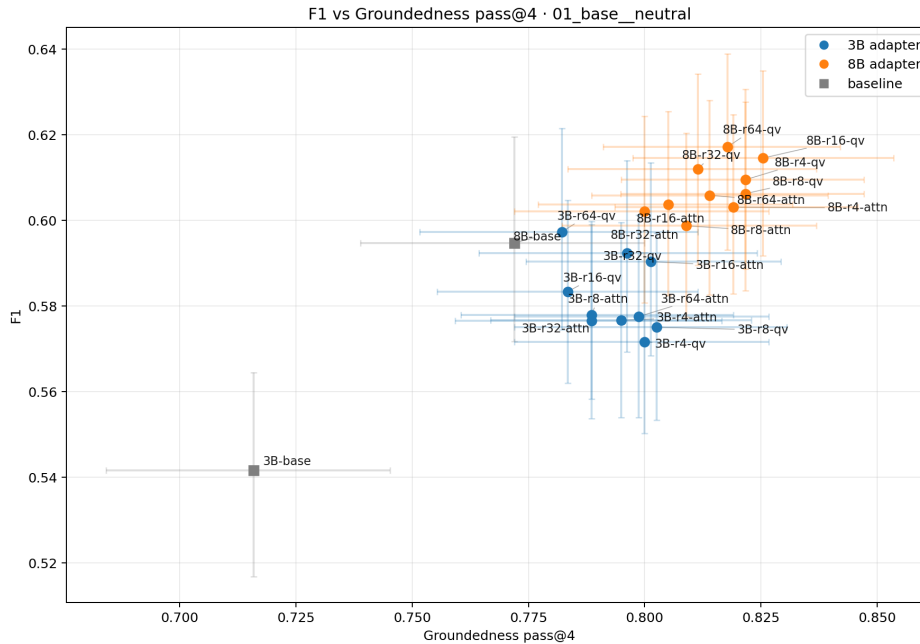


Figure 11: F1 vs Groundedness pass@4

Alongside the main task metric $F1$, the work additionally considered a judge-based groundedness evaluation, aggregated as `groundedness_pass@4`. This metric measures how often the model produces answers that are sufficiently grounded in the retrieved context and contain no unsupported additions. Unlike $F1$, it captures not just agreement with the reference answer but also the degree of supportedness of the result inside the retrieval-augmented pipeline.

The plot shows that configurations with the best point $F1$ do not necessarily coincide with configurations optimal in `groundedness_pass@4`. In the base regime the best- $F1$ configuration 8B r64 qv_only attains $F1 = 0.617$ [0.593, 0.639], while the groundedness maximum (0.825) is achieved by 8B r16 qv_only at $F1 = 0.615$ [0.592, 0.635]. For the paired difference $\Delta F1$ between them the 95% CI is [-0.011, +0.016], that is, on $F1$ these two points are statistically indistinguishable on the current test set. This means that a gain in task quality is not equivalent to a gain in the factual support of the answer by the context. Consequently, for documentation-oriented question answering the quality of the system cannot be fully described by $F1$ alone: some configurations reach higher groundedness at a statistically comparable level of the main metric.

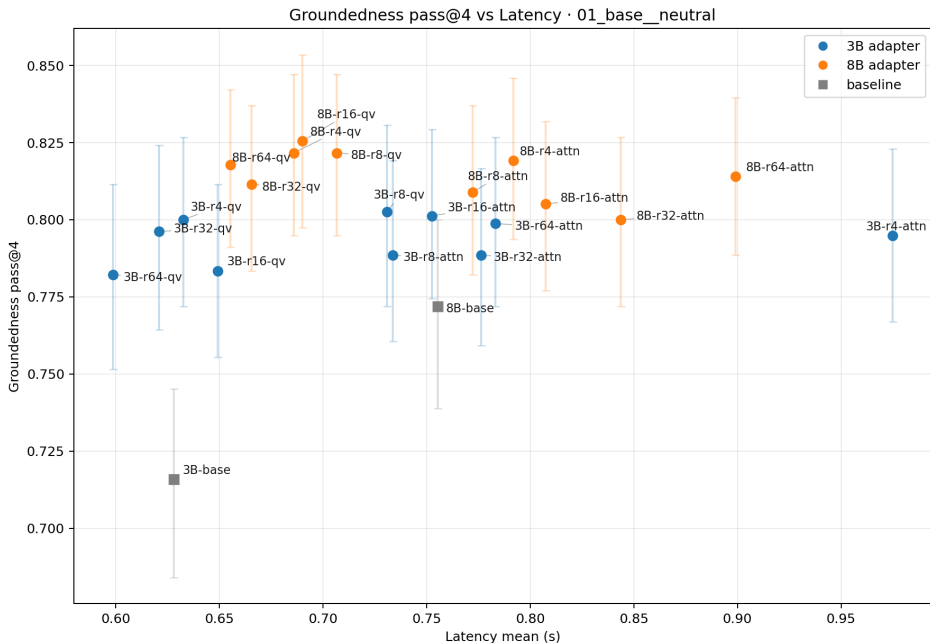


Figure 12: Groundedness pass@4 vs Latency

The comparison of `groundedness_pass@4` against latency further shows that the LoRA-free baseline configurations (3B-base, 8B-base) systematically lie below all adapted points: at comparable latency, LoRA fine-tuning shifts `groundedness_pass@4` upward by 0.05–0.08, and in absolute value this shift exceeds the width of the 95% CI (≈ 0.03). Within already-adapted configurations the `groundedness_pass@4` spread mostly falls inside the CI band, and the separation is driven mainly by the 3B/8B split. Latency and groundedness therefore do not form a non-trivial front beyond the one already visible on F1, but fine-tuning remains a necessary condition for a high level of supportedness. The resource view by inference VRAM carries no additional information either: within each family the VRAM spread does not exceed 0.3–0.4 GB, while the corresponding `groundedness` spread fully lies within the 95% CI band, so the corresponding projection is not shown.

Thus the judge-based analysis confirms the overall multi-criteria logic of the work. Practically useful configurations differ not only in F1 and resource cost, but also in the degree of supportedness, so the choice of working point depends on what exactly is considered the priority in the applied scenario: maximum agreement with the reference, stricter groundedness, or a trade-off between them.

G.5 ABLATION EXPERIMENTS ON RETRIEVAL AND PROMPTING

To check the robustness of the conclusions about LoRA configurations, additional ablation experiments were conducted in which not only the adapter parameters but also other parts of the pipeline were varied: the retrieval pipeline and the prompt-formation mode. We considered ten regimes obtained by combining five retrieval settings (`base`, `reranker_off`, `dense_only`, `sparse_only`, `hybrid_bm25`) and two prompting modes (`neutral`, `explicit_grounded`). For each regime two reference points were extracted from the 22 configurations: the configuration with the maximum F1 and the configuration with the maximum `groundedness_pass@4`.

The base regime (`base`) used the full retrieval pipeline, including dense retrieval, native sparse retrieval, their fusion via reciprocal rank fusion, and subsequent reranking of the candidates by the pretrained reranker. The `reranker_off` regime excludes only the final reranking step while keeping hybrid retrieval. The `dense_only` regime disables the sparse branch and uses only dense retrieval, while `sparse_only`, conversely, excludes the dense component and uses only sparse retrieval. The `hybrid_bm25` regime preserves the hybrid scheme but replaces native sparse retrieval

with classical BM25, which makes it possible to compare two variants of the sparse component inside the same retrieval pipeline. On top of the retrieval ablations, two prompting modes were considered: `neutral`, corresponding to a neutral generation mode without explicitly requiring the answer to rely on the context, and `explicit_grounded`, in which the prompt explicitly emphasizes the need to answer strictly based on the retrieved material.

The summary results are given in Table 15. The table allows us to see whether the main conclusions about LoRA are preserved when retrieval/prompting is varied, how the optimal working point shifts within a regime, and whether the points optimal in task quality and in groundedness coincide. An aggregated view by adaptation scheme, around which the optimal points concentrate, is additionally shown in Figure 13. The full per-regime plots and the detailed tables with all configurations are moved to the appendices in order not to overload the main exposition.

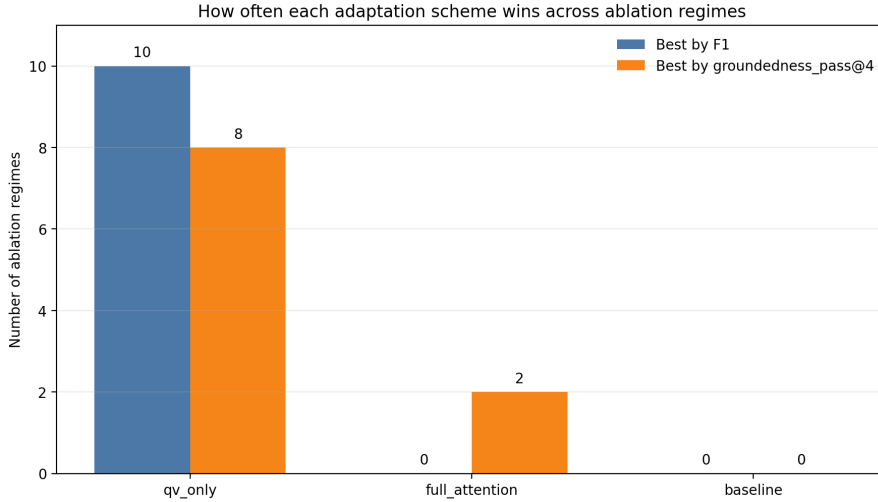


Figure 13: Distribution of optimal configurations by adaptation scheme (`qv_only`, `full_attention`, `baseline`) across the ten ablation regimes: number of regimes in which the scheme gives the best point on F1 and on `groundedness_pass@4`.

retrieval	prompt	best F1 config	F1 [95% CI]	grnd@4	corr@4	lat. (s)	inf. VRAM (GB)	best grnd config	F1 [95% CI]	grnd@4	corr@4	lat. (s)	inf. VRAM (GB)	same point
base	neutral	8B r64 qv_only	0.617 [0.593, 0.639]	0.818	0.827	0.655	21.926	8B r16 qv_only	0.615 [0.592, 0.635]	0.825	0.836	0.690	21.824	no
base	explicit	8B r64 qv_only	0.623 [0.599, 0.645]	0.822	0.824	0.664	21.953	8B r16 qv_only	0.610 [0.589, 0.632]	0.823	0.834	0.662	21.852	no
no_rerank	neutral	8B r64 qv_only	0.617 [0.596, 0.638]	0.819	0.824	0.658	21.926	8B r16 qv_only	0.615 [0.592, 0.637]	0.836	0.842	0.685	21.824	no
no_rerank	explicit	8B r64 qv_only	0.623 [0.601, 0.645]	0.817	0.824	0.649	21.953	8B r16 qv_only	0.610 [0.589, 0.632]	0.829	0.834	0.675	21.852	no
dense	neutral	8B r64 qv_only	0.617 [0.595, 0.640]	0.818	0.828	0.650	21.926	8B r8 qv_only	0.606 [0.585, 0.628]	0.824	0.831	0.673	21.836	no
dense	explicit	8B r64 qv_only	0.623 [0.600, 0.645]	0.824	0.827	0.661	21.953	8B r16 qv_only	0.610 [0.588, 0.633]	0.827	0.832	0.679	21.852	no
sparse	neutral	8B r64 qv_only	0.617 [0.595, 0.640]	0.820	0.823	0.661	21.926	8B r4 full_attention	0.603 [0.580, 0.626]	0.827	0.832	0.801	21.871	no
sparse	explicit	8B r64 qv_only	0.623 [0.600, 0.645]	0.828	0.832	0.646	21.953	8B r16 full_attention	0.601 [0.580, 0.623]	0.829	0.834	0.766	21.877	no
bm25_hybrid	neutral	8B r64 qv_only	0.617 [0.597, 0.639]	0.815	0.824	0.659	21.926	8B r8 qv_only	0.606 [0.586, 0.627]	0.827	0.836	0.646	21.836	no
bm25_hybrid	explicit	8B r64 qv_only	0.623 [0.603, 0.645]	0.823	0.829	0.664	21.953	8B r16 qv_only	0.610 [0.590, 0.631]	0.834	0.838	0.691	21.852	no

Table 15: Ablation summary results by F1 and `groundedness_pass@4`

Table 15 shows that the main conclusions about LoRA do not disappear when retrieval and prompting are changed. At the level of the entire ablation series the same structural pattern is consistently preserved: the points with the maximum point F1 and the points optimal in groundedness in most regimes concentrate around `qv_only` adapters, while `full_attention` only occasionally turns out to be optimal in groundedness. At the same time, the interval estimates show that within individual regimes some of the best-F1 configurations are statistically close to their nearest alternatives. Under moderate changes of the retrieval pipeline and the prompting policy what is therefore reproduced is not so much the advantage of a particular backbone, but the advantage of the `qv_only` adaptation scheme itself.

At the same time, the optimal working point within a regime shifts depending on the chosen quality criterion. In all ten regimes the points with the maximum F1 do not coincide with the points with the maximum `groundedness_pass@4` (`same_point` = no). As a result, retrieval and

prompting affect not only the absolute level of quality, but also the position of the trade-off between task performance and groundedness. The ablation results therefore confirm the methodological necessity of considering LoRA configurations not as a single source of variation, but as part of a more general retrieval-augmented system with conflicting criteria of quality and cost.

G.6 STATISTICAL ROBUSTNESS OF F1 DIFFERENCES

To separate stable F1 differences from narrow gaps, for the key comparisons we computed non-parametric 95% bootstrap CIs on the test set ($n = 785$, 1000 resamples). For individual configuration pairs we additionally used the paired bootstrap for the difference $\Delta F1$, since it correctly assesses whether the observed gap crosses the boundary of statistical noise.

Comparison	$\Delta F1$	95% CI on $\Delta F1$	Significant?
3B r64 qv_only - 3B baseline	+0.056	[+0.033, +0.078]	yes
3B r64 qv_only - 8B baseline	+0.003	[-0.021, +0.026]	no
8B r64 qv_only - 3B r64 qv_only	+0.020	[+0.0005, +0.0410]	yes
8B r64 qv_only - 8B r16 qv_only	+0.003	[-0.011, +0.016]	no
3B r64 qv_only - 3B r64 full_attention	+0.020	[+0.004, +0.036]	yes
8B r64 qv_only - 8B r64 full_attention	+0.011	[-0.003, +0.025]	no
qv_only - full_attention*	+0.0067	[+0.0010, +0.0124]	yes

* mean $\Delta F1$ over 8 param-matched pairs from Table 17.

Table 16: Paired bootstrap estimates of key F1 differences

Table 16 shows that the statistically stable effects on the current test set are primarily three: the improvement of 3B r64 qv_only over 3B baseline, the superiority of 3B r64 qv_only over 3B r64 full_attention, and the positive average difference of qv_only over full_attention across matched rank pairs. On the contrary, the difference between 3B r64 qv_only and 8B baseline, as well as between 8B r64 qv_only and 8B r16 qv_only, does not allow us to claim strict statistical superiority. The main stable conclusion of the work is therefore not connected to any local maximum on F1, but to the fact that LoRA adaptation in the successful qv_only scheme systematically forms stronger working points and gives a confirmed gain in at least some of the key comparisons.

H DISCUSSION

H.1 WHY QV_ONLY ADAPTERS DOMINATE

The obtained results show that the strongest response-time fronts are formed not by the wider full_attention adapters, but by the narrower qv_only solutions. This is confirmed by the bootstrap analysis: the average difference qv_only - full_attention over matched rank pairs is positive and statistically significant ($\Delta F1 = +0.0067$, 95% CI [+0.0010, +0.0124]), with the effect being most pronounced in the 8B family. The most plausible explanation is that, for documentation-oriented question answering inside a fixed retrieval pipeline, the main task of the adapter is not a deep reorganization of the entire attention block, but a more accurate tuning of how the model selects and uses the context already given to it. In this setting, selective adaptation of the q_proj and v_proj projections turns out to be sufficient, while extending LoRA to k_proj and o_proj increases the adapter size and training cost faster than it brings a stable benefit on the Pareto fronts.

The comparison of 3B r64 qv_only and 3B r64 full_attention is particularly telling. In the current set of results the broader module coverage not only fails to improve quality, but also loses in F1; for $\Delta F1$ between these configurations the 95% CI is [+0.004, +0.036]. This means that in the current set of experiments full_attention acts not as a universally better strategy, but as a more expensive way to obtain a less stable result.

H.1.1 PARAM-MATCHED COMPARISON OF QV_ONLY VS FULL_ATTENTION

An additional control check is the param-matched analysis, in which pairs of configurations with the same total number of LoRA parameters are compared. Since `full_attention` adapts four attention projections while `qv_only` only two, the same parameter budget is reached at half the rank for `full_attention`. For every such pair on the final test split ($n = 785$) we computed $\Delta F1 = F1(qv_only) - F1(full_attention)$ and the paired bootstrap 95% CI. The summary is given in Table 17.

Family	Param budget	qv_only	full_attention	$\Delta F1$	95% CI	Significant?
3B	256d	$r = 64$	$r = 32$	+0.0207	[+0.0052, +0.0373]	yes
3B	128d	$r = 32$	$r = 16$	+0.0021	[-0.0133, +0.0174]	no
3B	64d	$r = 16$	$r = 8$	+0.0054	[-0.0083, +0.0203]	no
3B	32d	$r = 8$	$r = 4$	-0.0016	[-0.0137, +0.0109]	no
8B	256d	$r = 64$	$r = 32$	+0.0150	[-0.0013, +0.0301]	no
8B	128d	$r = 32$	$r = 16$	+0.0083	[-0.0056, +0.0225]	no
8B	64d	$r = 16$	$r = 8$	+0.0158	[+0.0034, +0.0265]	yes
8B	32d	$r = 8$	$r = 4$	+0.0032	[-0.0093, +0.0170]	no

Table 17: Param-matched comparison of `qv_only` and `full_attention` by paired bootstrap F1 differences

Table 17 shows that at the same parameter budget `qv_only` is significantly better in 2 of 8 pairs, is statistically comparable in the remaining 6, and in no pair is significantly worse than `full_attention`. It follows that the claim of a structural advantage of `qv_only` does not reduce to the fact that this scheme simply “gets more parameters per projection” at a fixed rank: even in the param-matched setting it is at least no worse and in some comparisons yields a confirmed gain in F1.

H.2 WHY THE BACKBONE SIZE SETS THE OPERATING REGIME BUT DOES NOT CANCEL THE LORA EFFECT

The split between 3B and 8B configurations looks structural, but it should not be interpreted as the main result of the work. The larger 8B model does possess a greater parametric capacity and therefore more often sets the upper bound on F1, but it almost automatically moves the system into a more expensive regime in terms of inference and training memory. The 3B family, on the contrary, forms an area of efficient solutions: with a noticeably smaller resource profile it retains quality high enough to remain a practical choice for constrained hardware. It is particularly telling that the strong adapted configuration 3B `r64 qv_only` turns out to be statistically comparable to the unadapted 8B `baseline` model: the point difference in F1 is only +0.003, while the 95% CI for $\Delta F1$ is [-0.021, +0.026]. The difference between 3B and 8B therefore cannot be reduced to a simple rule of “more parameters means better”: domain-specific adaptation can compensate for the advantage of a larger LoRA-free backbone even where a strict conclusion about superiority in F1 can no longer be drawn.

Thus the backbone scale primarily sets the operating regime of the system, but does not answer the question of which adaptation scheme is successful. This question is decided inside each family separately, and this is where the main effect of the work appears: in both the 3B and the 8B family the `qv_only` adapters turn out to be more competitive in the quality-cost ratio than `full_attention`. The difference between 3B and 8B should therefore be understood as a background against which a more important regularity, related to the structure of LoRA adaptation itself, becomes visible.

H.3 WHY THE EFFECT OF RANK GROWTH IS NON-LINEAR

Increasing the rank does not produce the same effect for all configurations, however in both families an important regularity is observed: increasing r improves quality more strongly than it raises the runtime cost. For 3B `qv_only` adapters the move from $r = 4$ to $r = 64$ raises F1 from 0.572 to 0.597, while the latency of these two extreme points changes only from 0.633 to 0.598 s, and the inference memory from 12.668 to 12.760 GB. This means that in the current pipeline

the main inference cost is determined not so much by the adapter size as by the base model and the retrieval pipeline, and the additional adaptation capacity coming with rank goes mainly into quality improvements.

The same logic is partially reproduced in the larger family as well: inside `qv_only` the move from `8B_r4` to `8B_r64` raises F1 from 0.610 to 0.617, while latency stays in the approximate range of 0.66–0.69 s and inference memory changes very little inside the 8B regime. However, between `8B_r16_qv_only` and `8B_r64_qv_only` the paired bootstrap gives a 95% CI of $[-0.011, +0.016]$, so inside the upper part of the 8B family rank growth is more accurately interpreted as a weak positive trend rather than a strictly established advantage of the higher rank. In other words, a high rank brings the greatest benefit precisely where a structurally successful LoRA adaptation scheme has already been chosen, but inside the 8B family the choice between the top ranks requires accounting for additional criteria.

H.4 WHY RETRIEVAL AND PROMPTING SHIFT THE OPTIMUM POINT BUT DO NOT CANCEL THE CONCLUSIONS ABOUT LORA

The ablation experiments show that the retrieval and prompting components affect not only the absolute values of the metrics, but also the position of the optimal working point inside the same set of adapters. Switching off the reranker, moving to dense-only or sparse-only retrieval, and explicit changes to the prompting policy can shift the local optimum in F1 or in groundedness, since they change both the quality of the supplied context and the freedom of the generator in producing the answer.

However, these changes do not destroy the main conclusion about LoRA configurations; they only modify the conditions in which it shows itself. In other words, retrieval and prompting determine how favourable the environment for the generator turns out to be, but inside this environment the advantage more often stays with `qv_only` adapters. The ablation results should therefore be read not as a refutation of the main LoRA conclusions, but as a confirmation that the adapter, retrieval, and prompting form a single pipeline, inside which a structurally successful adaptation scheme remains a stable source of advantage.

H.5 GENERALIZATION ANALYSIS BY `TOP_K`

As a separate generalization analysis we checked the robustness of the main conclusions with respect to the number of chunks passed to the generator at inference time. In addition to the main regime `top_k = 2`, additional experiments were performed for `top_k = 1` and `top_k = 4` in the `01_base_neutral` regime for all 22 configurations without any further adapter training. This cross-section makes it possible to check that the obtained conclusions do not reduce to one particular value of the retrieval-context budget.

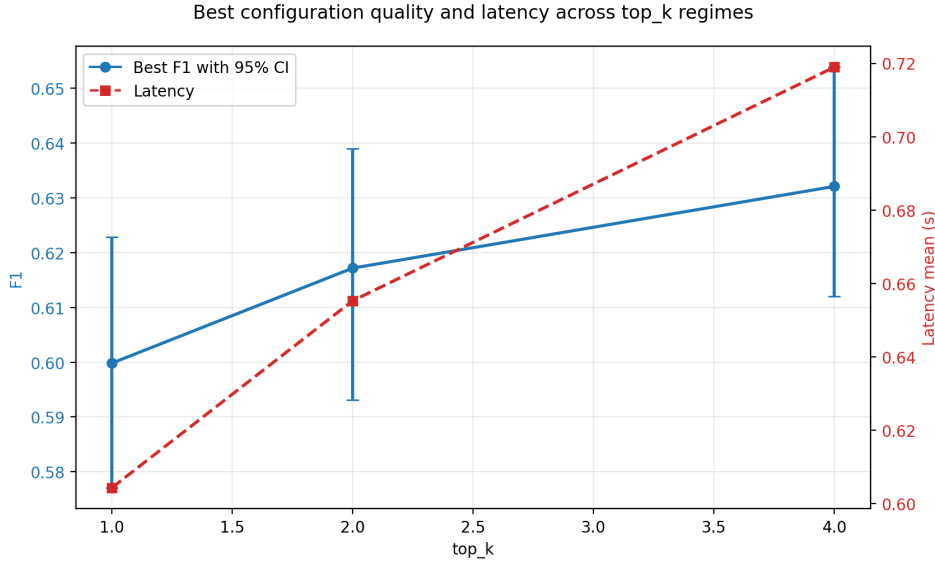


Figure 14: Change of the best quality and latency for different values of top_k

The plot for $\text{top}_k = 1, 2, 4$ shows that increasing the retrieval-context budget consistently raises the maximum of F1 (0.600 \rightarrow 0.617 \rightarrow 0.632), but at the same time raises latency (0.604 \rightarrow 0.655 \rightarrow 0.719 s). This means that increasing top_k does not reduce to a free improvement in quality: a wider context does help the best configuration, but it requires a more expensive inference-time regime.

A comparison of the concrete best points is given in Table 18.

top_k	best F1 config	F1 [95% CI]	lat. (s)	inf. VRAM (GB)	runtime Pareto front
1	8B r64 qv_only	0.600 [0.577, 0.623]	0.604	21.820	8B r64 qv_only
2	8B r64 qv_only	0.617 [0.593, 0.639]	0.655	21.926	3B r64 qv_only, 8B r64 qv_only
4	8B r64 qv_only	0.632 [0.612, 0.654]	0.719	22.078	3B r64 qv_only, 8B r64 qv_only

Table 18: Comparison of the best configurations for different values of top_k

Table 18 shows that for all three values of top_k the best configuration in F1 remains the same: 8B r64 qv_only. At the same time, the structure of the runtime trade-off changes only mildly: for $\text{top}_k = 1$ the quality-latency front collapses to the single point 8B r64 qv_only, while for $\text{top}_k = 2$ and $\text{top}_k = 4$ it simultaneously contains the lightweight point 3B r64 qv_only and the highest-quality point 8B r64 qv_only. The generalization analysis therefore shows that varying top_k affects primarily the absolute values of quality and cost, but does not cancel the main conclusion about the advantage of LoRA adapters that adapt the q- and v-projections of attention.

H.6 PRACTICAL RECOMMENDATIONS

From the obtained results, several explicit recommendations on the choice of configuration can be drawn.

- If the priority is a lightweight inference regime with high quality preserved, the preferred configuration is 3B r64 qv_only.
- If minimizing training cost while keeping acceptable quality is important, a reasonable starting point is 3B r4 qv_only, since it is the cheapest non-dominated configuration in training time and memory.

- If one needs the best quality-cost compromise inside the light family, the most practical intermediate configuration is 3B r32 qv_only: it already lies on the training Pareto front and is noticeably close to the upper points in quality without moving to the 8B regime.
- If it is important to obtain quality statistically comparable to 8B baseline but with a lighter resource profile, a reasonable working point is 3B r64 qv_only.
- If inside the 8B family it is more important to keep higher groundedness at statistically comparable quality, 8B r16 qv_only is preferable, since exactly this configuration yields the maximum groundedness_pass@4 in the base regime.
- If the priority is the maximum point-quality estimate and a substantially larger resource budget is available, 8B r64 qv_only is preferable; however its advantage in F1 over 8B r16 qv_only on the current test set is not statistically confirmed.
- full_attention configurations are reasonable to consider as a niche option: in the current set of runs they rarely give a stable advantage in F1 and more often lose in cost.

H.7 ERROR ANALYSIS

Alongside the aggregate metrics it is useful to consider the typical error classes that recur across different RAG-system configurations. In the present work it is convenient to group these errors not by individual failing examples, but by the failure mechanism inside the retrieval-augmented pipeline. This allows us to separate errors caused by low-quality context from errors that arise already at the answer-generation stage given relevant context.

To make this section quantitative, we built a reproducible sample of 100 failing answers on the final test split: 50 randomly chosen cases with F1 < 1 for 3B r64 qv_only and 8B r64 qv_only each (seed = 42). Each example was then assigned to one of four operational error classes: retrieval miss (the relevant source chunk did not enter the final context), overclaiming (the answer adds extra unsupported statements), incomplete answer (the answer extracts only part of the required information), and exact/precision failure (an error of exact reproduction of a command, field, version, name, or other literal value). The summary is given in Table 19.

Table 19: Quantitative cross-section of error types on a sample of 100 failing answers

Error type	3B r64 qv_only	8B r64 qv_only	Total
retrieval miss	11 (22%)	8 (16%)	19 (19%)
overclaiming	2 (4%)	2 (4%)	4 (4%)
incomplete answer	17 (34%)	7 (14%)	24 (24%)
exact/precision failure	20 (40%)	33 (66%)	53 (53%)

Table 19 shows that in this sample exact-reproduction errors dominate (53%), and this is especially pronounced for 8B r64 qv_only (66% against 40% for 3B r64 qv_only). This indicates that a noticeable share of the remaining errors is connected not with the full absence of relevant context, but with inaccurate reproduction of short commands, field names, versions, and other local facts. The second place is occupied by incomplete answers (24%), followed by retrieval miss (19%), while overclaiming is noticeably rarer in this sample (4%).

Below are some illustrative examples from the same sample.

- retrieval miss: for the question What does kube-proxy provide for Services? the reference answer is formulated as provides load balancing, while the model answers A virtual IP mechanism.; for the question What protocol does kube-proxy not understand? the reference is does not understand HTTP, while the model returns TCP, UDP, AND SCTP STREAM FORWARDING..
- overclaiming: for the question What does the term storage version describe in Kubernetes? the reference is limited to the formula how an object is stored in your cluster, but the model adds an extra part about the ob-

ject’s representation in the API; for the question Why might a Windows Pod show ErrImgPull or ImagePullBackOff? the reference ties the error to running on an incompatible Windows node, while the model substitutes more general reasons such as a wrong image name or a missing imagePullSecret.

- incomplete answer: for the question Which method is easier to use for adding custom resources: CRDs or aggregated APIs? the reference answer is two-part: CRDs are easier to use. Aggregated APIs are more flexible., while the model keeps only the first part; for the question Does Kubernetes have a User object for storing usernames in its API? the reference simultaneously states the absence of a User object and the absence of storing usernames in the API, while the model answers only No..
- exact/precision failure: for the question What is the default API server bind port for kubeadm init phase kubeconfig all? the reference value is 6443, while the model returns 6444; for the question Which flag forces Windows line endings in kubectl edit? the reference form is -windows-line-endings, while the model returns the string windows-line-endings.

First, a noticeable but non-dominant share is made up of retrieval miss-type errors, in which the relevant documentation fragment does not enter the final context. In this case the generator is forced to answer from incomplete or indirectly related material, and therefore even strong adapters cannot stably recover the correct answer. Practically such cases show up either as a factual error or as a partially correct but overly general answer.

Second, we observe unsupported-addition (overclaiming) errors. In the current sample there are few of them, but they remain methodologically important: the answer looks plausible and often gets an acceptable F_1 , but it adds statements that do not directly follow from the retrieved context. This error type is especially sensitive to the judge-based groundedness evaluation and explains why configurations optimal in F_1 do not coincide with configurations optimal in `groundedness_pass@4`.

Third, we see incomplete answers in the presence of relevant context. On the quantitative sample this is the second most frequent error type. Here retrieval has already worked well enough, but the generator extracts from the found material only part of the required information: it omits a caveat, a constraint, a condition, or one element of a multi-part answer. Such errors are especially important for technical documentation, where even a brief omission may change the practical meaning of the answer.

Fourth, for the class of exact questions, format and precision-of-reproduction errors are typical, and exactly this type turns out to be the largest in the quantitative sample. Even with the correct context, the model can give an answer that is close in meaning but not literally correct: it rephrases the field name, inaccurately reproduces a flag, a path, an API version, or a specific value. Such failures show that some of the errors in documentation-oriented question answering are related not to the absence of knowledge as such, but to the difficulty of accurately reproducing local facts.

Finally, a separate class is made up of prompt-sensitive failures. The ablation experiments show that changing the retrieval/prompting policy can shift the optimal working point even for the same LoRA configurations. This effect was not encoded as a separate row in Table 19, since it shows up primarily at the level of between-regime comparison rather than inside a single fixed sample of answers. It follows that a proper error analysis for a RAG system should treat the generator, retrieval, and prompting as interrelated components of one pipeline, not as independent sources of quality.

I PER-REGIME DETAILED TABLES

This appendix contains the detailed metric tables for each of the 10 ablation regimes referenced in Section 7. For every regime we report, for each of the 12 LoRA configurations and the two non-adapted baselines (3B/8B), the point estimates of F_1 , judge `groundedness_pass@4`, judge `correctness_pass@4` together with their 95% bootstrap confidence intervals (1,000 resamples on the test split, $n = 785$), as well as the corresponding latency and inference VRAM. The same numbers underpin all per-regime plots in Appendix J and the aggregate ablation summary in Section 7.

01_BASE__NEUTRAL

config	F1 [95% CI]	grmd@4 [95% CI]	corr@4 [95% CI]	lat. (s)	inf. VRAM (GB)
3B baseline	0.542 [0.517, 0.565]	0.716 [0.684, 0.745]	0.717 [0.684, 0.748]	0.628	12.664
3B r4 full_attention	0.577 [0.554, 0.600]	0.795 [0.767, 0.823]	0.808 [0.781, 0.834]	0.975	12.674
3B r4 qv_only	0.572 [0.550, 0.592]	0.800 [0.772, 0.827]	0.806 [0.777, 0.833]	0.633	12.668
3B r8 full_attention	0.578 [0.558, 0.599]	0.789 [0.761, 0.819]	0.808 [0.782, 0.834]	0.734	12.701
3B r8 qv_only	0.575 [0.553, 0.597]	0.803 [0.772, 0.831]	0.813 [0.787, 0.842]	0.731	12.676
3B r16 full_attention	0.590 [0.568, 0.614]	0.801 [0.774, 0.829]	0.810 [0.782, 0.838]	0.753	12.719
3B r16 qv_only	0.583 [0.562, 0.605]	0.783 [0.755, 0.811]	0.790 [0.758, 0.818]	0.649	12.701
3B r32 full_attention	0.577 [0.554, 0.600]	0.789 [0.759, 0.817]	0.803 [0.775, 0.831]	0.776	12.732
3B r32 qv_only	0.592 [0.569, 0.614]	0.796 [0.764, 0.824]	0.808 [0.781, 0.834]	0.621	12.719
3B r64 full_attention	0.578 [0.554, 0.601]	0.799 [0.772, 0.827]	0.818 [0.792, 0.845]	0.783	12.924
3B r64 qv_only	0.597 [0.574, 0.622]	0.782 [0.752, 0.811]	0.791 [0.762, 0.817]	0.598	12.760
8B baseline	0.595 [0.572, 0.620]	0.772 [0.739, 0.800]	0.775 [0.746, 0.804]	0.755	21.836
8B r4 full_attention	0.603 [0.583, 0.625]	0.819 [0.794, 0.846]	0.828 [0.801, 0.855]	0.792	21.871
8B r4 qv_only	0.610 [0.589, 0.631]	0.822 [0.795, 0.847]	0.832 [0.806, 0.859]	0.686	21.828
8B r8 full_attention	0.599 [0.578, 0.620]	0.809 [0.782, 0.837]	0.815 [0.789, 0.841]	0.772	21.859
8B r8 qv_only	0.606 [0.584, 0.628]	0.822 [0.795, 0.847]	0.833 [0.806, 0.860]	0.706	21.836
8B r16 full_attention	0.604 [0.583, 0.625]	0.805 [0.777, 0.832]	0.810 [0.783, 0.836]	0.807	21.885
8B r16 qv_only	0.615 [0.592, 0.635]	0.825 [0.797, 0.854]	0.836 [0.811, 0.862]	0.690	21.824
8B r32 full_attention	0.602 [0.581, 0.624]	0.800 [0.772, 0.827]	0.808 [0.780, 0.838]	0.844	21.961
8B r32 qv_only	0.612 [0.590, 0.634]	0.811 [0.783, 0.837]	0.814 [0.786, 0.841]	0.665	21.850
8B r64 full_attention	0.606 [0.583, 0.628]	0.814 [0.789, 0.839]	0.815 [0.789, 0.842]	0.899	22.164
8B r64 qv_only	0.617 [0.593, 0.639]	0.818 [0.791, 0.842]	0.827 [0.797, 0.855]	0.655	21.926

Table 20: Per-configuration metrics for the 01_base__neutral regime: F1, groundedness, and correctness (pass@4) with 95% bootstrap CI (1000 resamples on the final test split), inference latency, and peak inference VRAM.

02_BASE__EXPLICIT_GROUNDED

config	F1 [95% CI]	grmd@4 [95% CI]	corr@4 [95% CI]	lat. (s)	inf. VRAM (GB)
3B baseline	0.536 [0.512, 0.562]	0.729 [0.698, 0.761]	0.724 [0.693, 0.754]	0.610	12.686
3B r4 full_attention	0.559 [0.536, 0.583]	0.778 [0.749, 0.806]	0.796 [0.768, 0.824]	0.736	12.695
3B r4 qv_only	0.566 [0.545, 0.587]	0.806 [0.777, 0.836]	0.813 [0.783, 0.839]	0.653	12.689
3B r8 full_attention	0.569 [0.546, 0.591]	0.787 [0.760, 0.817]	0.803 [0.776, 0.829]	0.768	12.723
3B r8 qv_only	0.571 [0.549, 0.593]	0.778 [0.750, 0.806]	0.792 [0.762, 0.820]	0.668	12.697
3B r16 full_attention	0.577 [0.556, 0.598]	0.789 [0.759, 0.815]	0.805 [0.778, 0.832]	0.777	12.740
3B r16 qv_only	0.574 [0.551, 0.597]	0.795 [0.764, 0.822]	0.805 [0.776, 0.832]	0.651	12.723
3B r32 full_attention	0.567 [0.544, 0.591]	0.786 [0.759, 0.814]	0.803 [0.773, 0.831]	0.814	12.754
3B r32 qv_only	0.576 [0.551, 0.600]	0.775 [0.744, 0.801]	0.783 [0.755, 0.811]	0.669	12.740
3B r64 full_attention	0.573 [0.549, 0.597]	0.787 [0.759, 0.815]	0.808 [0.781, 0.834]	0.897	12.945
3B r64 qv_only	0.598 [0.575, 0.619]	0.776 [0.749, 0.805]	0.790 [0.759, 0.818]	0.596	12.781
8B baseline	0.603 [0.578, 0.627]	0.780 [0.753, 0.806]	0.778 [0.750, 0.805]	0.752	21.795
8B r4 full_attention	0.602 [0.580, 0.623]	0.819 [0.792, 0.846]	0.825 [0.799, 0.852]	0.814	21.863
8B r4 qv_only	0.602 [0.580, 0.623]	0.811 [0.783, 0.838]	0.824 [0.799, 0.851]	0.687	21.855
8B r8 full_attention	0.601 [0.579, 0.623]	0.813 [0.786, 0.837]	0.819 [0.794, 0.846]	0.789	21.852
8B r8 qv_only	0.606 [0.585, 0.627]	0.820 [0.794, 0.846]	0.836 [0.810, 0.860]	0.693	21.863
8B r16 full_attention	0.601 [0.580, 0.622]	0.813 [0.783, 0.838]	0.814 [0.786, 0.842]	0.843	21.877
8B r16 qv_only	0.610 [0.589, 0.632]	0.823 [0.797, 0.848]	0.834 [0.806, 0.859]	0.662	21.852
8B r32 full_attention	0.601 [0.579, 0.622]	0.804 [0.776, 0.831]	0.811 [0.781, 0.838]	0.808	21.953
8B r32 qv_only	0.610 [0.588, 0.632]	0.813 [0.786, 0.838]	0.815 [0.789, 0.841]	0.648	21.877
8B r64 full_attention	0.603 [0.580, 0.623]	0.808 [0.777, 0.833]	0.815 [0.786, 0.845]	0.806	22.156
8B r64 qv_only	0.623 [0.599, 0.645]	0.822 [0.795, 0.848]	0.824 [0.796, 0.850]	0.664	21.953

Table 21: Per-configuration metrics for the 02_base__explicit_grounded regime: F1, groundedness, and correctness (pass@4) with 95% bootstrap CI (1000 resamples on the final test split), inference latency, and peak inference VRAM.

03_RERANKER_OFF__NEUTRAL

config	F1 [95% CI]	grnd@4 [95% CI]	corr@4 [95% CI]	lat. (s)	inf. VRAM (GB)
3B baseline	0.541 [0.516, 0.564]	0.729 [0.699, 0.761]	0.718 [0.685, 0.746]	0.634	12.664
3B r4 full_attention	0.573 [0.552, 0.595]	0.780 [0.753, 0.809]	0.794 [0.767, 0.820]	0.732	12.674
3B r4 qv_only	0.571 [0.548, 0.593]	0.800 [0.772, 0.829]	0.811 [0.783, 0.838]	0.636	12.668
3B r8 full_attention	0.579 [0.557, 0.600]	0.799 [0.772, 0.824]	0.808 [0.780, 0.836]	0.784	12.701
3B r8 qv_only	0.574 [0.554, 0.597]	0.799 [0.769, 0.827]	0.808 [0.778, 0.836]	0.647	12.676
3B r16 full_attention	0.586 [0.564, 0.608]	0.803 [0.775, 0.831]	0.815 [0.786, 0.838]	0.798	12.719
3B r16 qv_only	0.581 [0.558, 0.605]	0.791 [0.762, 0.817]	0.799 [0.772, 0.827]	0.649	12.701
3B r32 full_attention	0.579 [0.557, 0.601]	0.794 [0.766, 0.823]	0.814 [0.785, 0.839]	0.781	12.732
3B r32 qv_only	0.589 [0.568, 0.611]	0.794 [0.766, 0.823]	0.804 [0.778, 0.829]	0.626	12.719
3B r64 full_attention	0.575 [0.549, 0.596]	0.790 [0.762, 0.819]	0.805 [0.776, 0.832]	0.777	12.924
3B r64 qv_only	0.597 [0.572, 0.620]	0.786 [0.758, 0.815]	0.794 [0.766, 0.823]	0.613	12.760
8B baseline	0.592 [0.569, 0.617]	0.771 [0.741, 0.801]	0.766 [0.735, 0.796]	0.779	21.836
8B r4 full_attention	0.603 [0.583, 0.625]	0.823 [0.796, 0.848]	0.831 [0.804, 0.856]	0.788	21.871
8B r4 qv_only	0.610 [0.587, 0.631]	0.822 [0.794, 0.848]	0.829 [0.804, 0.855]	0.656	21.828
8B r8 full_attention	0.599 [0.577, 0.619]	0.808 [0.780, 0.834]	0.815 [0.785, 0.841]	0.742	21.859
8B r8 qv_only	0.606 [0.584, 0.627]	0.828 [0.800, 0.854]	0.832 [0.805, 0.857]	0.656	21.836
8B r16 full_attention	0.604 [0.584, 0.624]	0.809 [0.782, 0.836]	0.811 [0.783, 0.838]	0.809	21.885
8B r16 qv_only	0.615 [0.592, 0.637]	0.836 [0.809, 0.861]	0.842 [0.815, 0.868]	0.685	21.824
8B r32 full_attention	0.602 [0.580, 0.622]	0.797 [0.767, 0.824]	0.806 [0.778, 0.833]	0.817	21.961
8B r32 qv_only	0.612 [0.590, 0.636]	0.817 [0.791, 0.843]	0.820 [0.794, 0.848]	0.641	21.850
8B r64 full_attention	0.606 [0.585, 0.627]	0.815 [0.787, 0.842]	0.817 [0.786, 0.841]	0.843	22.164
8B r64 qv_only	0.617 [0.596, 0.638]	0.819 [0.792, 0.846]	0.824 [0.796, 0.851]	0.658	21.926

Table 22: Per-configuration metrics for the 03_reranker_off__neutral regime: F1, ground-edness, and correctness (pass@4) with 95% bootstrap CI (1000 resamples on the final test split), inference latency, and peak inference VRAM.

04_RERANKER_OFF__EXPLICIT_GROUNDED

config	F1 [95% CI]	grmd@4 [95% CI]	corr@4 [95% CI]	lat. (s)	inf. VRAM (GB)
3B baseline	0.537 [0.514, 0.561]	0.740 [0.710, 0.769]	0.740 [0.707, 0.772]	0.665	12.686
3B r4 full_attention	0.559 [0.537, 0.583]	0.780 [0.749, 0.810]	0.786 [0.761, 0.813]	0.783	12.695
3B r4 qv_only	0.566 [0.544, 0.587]	0.800 [0.772, 0.827]	0.809 [0.781, 0.836]	0.624	12.689
3B r8 full_attention	0.569 [0.545, 0.592]	0.800 [0.775, 0.829]	0.810 [0.783, 0.837]	0.760	12.723
3B r8 qv_only	0.571 [0.547, 0.593]	0.789 [0.761, 0.817]	0.803 [0.773, 0.831]	0.670	12.697
3B r16 full_attention	0.577 [0.554, 0.598]	0.794 [0.762, 0.822]	0.805 [0.778, 0.832]	0.788	12.740
3B r16 qv_only	0.574 [0.551, 0.597]	0.790 [0.763, 0.818]	0.804 [0.776, 0.832]	0.631	12.723
3B r32 full_attention	0.567 [0.544, 0.589]	0.794 [0.767, 0.822]	0.804 [0.776, 0.831]	0.782	12.754
3B r32 qv_only	0.576 [0.552, 0.597]	0.785 [0.757, 0.814]	0.797 [0.769, 0.824]	0.633	12.740
3B r64 full_attention	0.573 [0.550, 0.595]	0.799 [0.772, 0.827]	0.808 [0.780, 0.834]	0.881	12.945
3B r64 qv_only	0.598 [0.575, 0.621]	0.777 [0.745, 0.805]	0.785 [0.757, 0.815]	0.602	12.781
8B baseline	0.599 [0.575, 0.620]	0.773 [0.744, 0.803]	0.775 [0.743, 0.805]	0.780	21.795
8B r4 full_attention	0.602 [0.581, 0.624]	0.817 [0.789, 0.842]	0.827 [0.800, 0.854]	0.785	21.863
8B r4 qv_only	0.602 [0.579, 0.624]	0.815 [0.787, 0.845]	0.824 [0.796, 0.851]	0.714	21.855
8B r8 full_attention	0.601 [0.579, 0.624]	0.819 [0.791, 0.845]	0.823 [0.794, 0.851]	0.786	21.852
8B r8 qv_only	0.606 [0.584, 0.626]	0.819 [0.790, 0.846]	0.827 [0.800, 0.854]	0.683	21.863
8B r16 full_attention	0.601 [0.580, 0.624]	0.823 [0.796, 0.851]	0.828 [0.804, 0.855]	0.816	21.877
8B r16 qv_only	0.610 [0.589, 0.632]	0.829 [0.801, 0.856]	0.834 [0.806, 0.860]	0.675	21.852
8B r32 full_attention	0.601 [0.581, 0.622]	0.804 [0.776, 0.831]	0.810 [0.783, 0.836]	0.832	21.953
8B r32 qv_only	0.610 [0.589, 0.631]	0.810 [0.783, 0.837]	0.820 [0.792, 0.847]	0.647	21.877
8B r64 full_attention	0.603 [0.580, 0.625]	0.808 [0.777, 0.834]	0.811 [0.783, 0.837]	0.829	22.156
8B r64 qv_only	0.623 [0.601, 0.645]	0.817 [0.791, 0.843]	0.824 [0.795, 0.851]	0.649	21.953

Table 23: Per-configuration metrics for the 04_reranker_off__explicit_grounded regime: F1, groundedness, and correctness (pass@4) with 95% bootstrap CI (1000 resamples on the final test split), inference latency, and peak inference VRAM.

05_DENSE_ONLY__NEUTRAL

config	F1 [95% CI]	grmd@4 [95% CI]	corr@4 [95% CI]	lat. (s)	inf. VRAM (GB)
3B baseline	0.536 [0.512, 0.559]	0.724 [0.693, 0.757]	0.724 [0.694, 0.754]	0.598	11.676
3B r4 full_attention	0.573 [0.552, 0.594]	0.786 [0.757, 0.814]	0.806 [0.781, 0.833]	0.725	12.674
3B r4 qv_only	0.571 [0.546, 0.593]	0.810 [0.783, 0.838]	0.814 [0.787, 0.841]	0.616	12.668
3B r8 full_attention	0.579 [0.558, 0.601]	0.797 [0.767, 0.824]	0.811 [0.785, 0.837]	0.762	12.701
3B r8 qv_only	0.574 [0.551, 0.597]	0.796 [0.769, 0.823]	0.805 [0.777, 0.833]	0.660	12.676
3B r16 full_attention	0.586 [0.563, 0.606]	0.803 [0.775, 0.828]	0.813 [0.786, 0.841]	0.807	12.719
3B r16 qv_only	0.581 [0.557, 0.604]	0.787 [0.759, 0.817]	0.792 [0.763, 0.819]	0.633	12.701
3B r32 full_attention	0.579 [0.556, 0.602]	0.800 [0.772, 0.827]	0.809 [0.780, 0.833]	0.759	12.732
3B r32 qv_only	0.589 [0.566, 0.609]	0.796 [0.767, 0.825]	0.806 [0.777, 0.832]	0.630	12.719
3B r64 full_attention	0.575 [0.554, 0.598]	0.782 [0.754, 0.810]	0.800 [0.773, 0.829]	0.782	12.924
3B r64 qv_only	0.597 [0.573, 0.621]	0.787 [0.760, 0.814]	0.800 [0.773, 0.827]	0.620	12.760
8B baseline	0.581 [0.556, 0.605]	0.764 [0.735, 0.794]	0.768 [0.740, 0.796]	0.810	20.795
8B r4 full_attention	0.603 [0.582, 0.623]	0.817 [0.791, 0.843]	0.825 [0.799, 0.850]	0.787	21.871
8B r4 qv_only	0.610 [0.588, 0.631]	0.818 [0.791, 0.843]	0.827 [0.796, 0.851]	0.676	21.828
8B r8 full_attention	0.599 [0.575, 0.621]	0.817 [0.790, 0.842]	0.822 [0.795, 0.850]	0.769	21.859
8B r8 qv_only	0.606 [0.585, 0.628]	0.824 [0.796, 0.851]	0.831 [0.805, 0.855]	0.673	21.836
8B r16 full_attention	0.604 [0.582, 0.626]	0.809 [0.782, 0.834]	0.813 [0.785, 0.839]	0.801	21.885
8B r16 qv_only	0.615 [0.592, 0.635]	0.817 [0.789, 0.841]	0.831 [0.805, 0.856]	0.655	21.824
8B r32 full_attention	0.602 [0.581, 0.624]	0.799 [0.769, 0.825]	0.806 [0.778, 0.832]	0.812	21.961
8B r32 qv_only	0.612 [0.591, 0.635]	0.813 [0.785, 0.841]	0.818 [0.789, 0.843]	0.667	21.850
8B r64 full_attention	0.606 [0.582, 0.627]	0.815 [0.789, 0.841]	0.817 [0.790, 0.843]	0.835	22.164
8B r64 qv_only	0.617 [0.595, 0.640]	0.818 [0.791, 0.845]	0.828 [0.801, 0.854]	0.650	21.926

Table 24: Per-configuration metrics for the 05_dense_only__neutral regime: F1, ground-
edness, and correctness (pass@4) with 95% bootstrap CI (1000 resamples on the final test split),
inference latency, and peak inference VRAM.

06_DENSE_ONLY__EXPLICIT_GROUNDED

config	F1 [95% CI]	grnd@4 [95% CI]	corr@4 [95% CI]	lat. (s)	inf. VRAM (GB)
3B baseline	0.532 [0.508, 0.555]	0.734 [0.702, 0.766]	0.727 [0.697, 0.757]	0.579	11.676
3B r4 full_attention	0.559 [0.537, 0.583]	0.783 [0.754, 0.811]	0.799 [0.772, 0.825]	0.778	12.695
3B r4 qv_only	0.566 [0.544, 0.587]	0.804 [0.776, 0.831]	0.810 [0.782, 0.837]	0.636	12.689
3B r8 full_attention	0.569 [0.546, 0.590]	0.792 [0.764, 0.819]	0.804 [0.776, 0.831]	0.792	12.723
3B r8 qv_only	0.571 [0.548, 0.593]	0.783 [0.755, 0.809]	0.799 [0.772, 0.827]	0.660	12.697
3B r16 full_attention	0.577 [0.556, 0.598]	0.790 [0.762, 0.818]	0.803 [0.776, 0.829]	0.827	12.740
3B r16 qv_only	0.574 [0.551, 0.597]	0.790 [0.761, 0.819]	0.795 [0.768, 0.822]	0.628	12.723
3B r32 full_attention	0.567 [0.544, 0.590]	0.790 [0.759, 0.818]	0.803 [0.776, 0.829]	0.789	12.754
3B r32 qv_only	0.576 [0.552, 0.598]	0.782 [0.752, 0.811]	0.792 [0.764, 0.820]	0.659	12.740
3B r64 full_attention	0.573 [0.550, 0.595]	0.795 [0.769, 0.822]	0.809 [0.781, 0.836]	0.804	12.945
3B r64 qv_only	0.598 [0.574, 0.621]	0.783 [0.755, 0.814]	0.792 [0.762, 0.820]	0.668	12.781
8B baseline	0.586 [0.560, 0.611]	0.769 [0.740, 0.800]	0.767 [0.739, 0.795]	0.732	20.797
8B r4 full_attention	0.602 [0.581, 0.625]	0.823 [0.794, 0.850]	0.828 [0.803, 0.855]	0.810	21.863
8B r4 qv_only	0.602 [0.580, 0.623]	0.813 [0.783, 0.839]	0.823 [0.799, 0.847]	0.700	21.855
8B r8 full_attention	0.601 [0.581, 0.624]	0.820 [0.792, 0.848]	0.827 [0.800, 0.851]	0.786	21.852
8B r8 qv_only	0.606 [0.582, 0.627]	0.823 [0.796, 0.850]	0.832 [0.806, 0.856]	0.688	21.863
8B r16 full_attention	0.601 [0.579, 0.625]	0.815 [0.790, 0.841]	0.819 [0.792, 0.847]	0.821	21.877
8B r16 qv_only	0.610 [0.588, 0.633]	0.827 [0.799, 0.854]	0.832 [0.805, 0.856]	0.679	21.852
8B r32 full_attention	0.601 [0.579, 0.622]	0.801 [0.773, 0.829]	0.808 [0.778, 0.836]	0.871	21.953
8B r32 qv_only	0.610 [0.588, 0.632]	0.814 [0.785, 0.841]	0.820 [0.792, 0.846]	0.680	21.877
8B r64 full_attention	0.603 [0.580, 0.624]	0.809 [0.781, 0.838]	0.818 [0.790, 0.843]	0.825	22.156
8B r64 qv_only	0.623 [0.600, 0.645]	0.824 [0.797, 0.850]	0.827 [0.800, 0.851]	0.661	21.953

Table 25: Per-configuration metrics for the 06_dense_only__explicit_grounded regime: F1, groundedness, and correctness (pass@4) with 95% bootstrap CI (1000 resamples on the final test split), inference latency, and peak inference VRAM.

07_SPARSE_ONLY__NEUTRAL

config	F1 [95% CI]	grnd@4 [95% CI]	corr@4 [95% CI]	lat. (s)	inf. VRAM (GB)
3B baseline	0.532 [0.507, 0.555]	0.713 [0.680, 0.744]	0.716 [0.683, 0.746]	0.523	11.643
3B r4 full_attention	0.573 [0.552, 0.594]	0.790 [0.762, 0.819]	0.803 [0.776, 0.828]	0.746	12.674
3B r4 qv_only	0.571 [0.549, 0.592]	0.804 [0.775, 0.831]	0.809 [0.781, 0.839]	0.613	12.668
3B r8 full_attention	0.579 [0.557, 0.601]	0.796 [0.766, 0.824]	0.809 [0.780, 0.836]	0.731	12.701
3B r8 qv_only	0.574 [0.552, 0.596]	0.795 [0.766, 0.823]	0.809 [0.781, 0.836]	0.671	12.676
3B r16 full_attention	0.586 [0.564, 0.608]	0.809 [0.781, 0.836]	0.815 [0.789, 0.842]	0.756	12.719
3B r16 qv_only	0.581 [0.559, 0.604]	0.796 [0.768, 0.822]	0.803 [0.776, 0.828]	0.619	12.701
3B r32 full_attention	0.579 [0.556, 0.601]	0.794 [0.767, 0.822]	0.813 [0.785, 0.839]	0.897	12.732
3B r32 qv_only	0.589 [0.567, 0.612]	0.791 [0.763, 0.819]	0.800 [0.771, 0.827]	0.641	12.719
3B r64 full_attention	0.575 [0.552, 0.600]	0.796 [0.769, 0.824]	0.809 [0.781, 0.834]	0.791	12.924
3B r64 qv_only	0.597 [0.573, 0.621]	0.791 [0.764, 0.819]	0.797 [0.769, 0.824]	0.595	12.760
8B baseline	0.588 [0.564, 0.613]	0.763 [0.734, 0.794]	0.757 [0.725, 0.786]	0.666	20.396
8B r4 full_attention	0.603 [0.580, 0.626]	0.827 [0.800, 0.854]	0.832 [0.805, 0.857]	0.801	21.871
8B r4 qv_only	0.610 [0.588, 0.630]	0.820 [0.791, 0.847]	0.825 [0.799, 0.850]	0.694	21.828
8B r8 full_attention	0.599 [0.576, 0.620]	0.817 [0.787, 0.843]	0.820 [0.794, 0.846]	0.758	21.859
8B r8 qv_only	0.606 [0.584, 0.627]	0.823 [0.795, 0.850]	0.829 [0.804, 0.854]	0.641	21.836
8B r16 full_attention	0.604 [0.583, 0.627]	0.808 [0.778, 0.834]	0.818 [0.791, 0.845]	0.794	21.885
8B r16 qv_only	0.615 [0.593, 0.636]	0.825 [0.800, 0.851]	0.831 [0.804, 0.856]	0.654	21.824
8B r32 full_attention	0.602 [0.580, 0.622]	0.797 [0.768, 0.826]	0.804 [0.773, 0.832]	0.842	21.961
8B r32 qv_only	0.612 [0.590, 0.635]	0.811 [0.785, 0.837]	0.824 [0.800, 0.851]	0.637	21.850
8B r64 full_attention	0.606 [0.582, 0.627]	0.815 [0.786, 0.842]	0.818 [0.790, 0.845]	0.827	22.164
8B r64 qv_only	0.617 [0.595, 0.640]	0.820 [0.792, 0.848]	0.823 [0.799, 0.847]	0.661	21.926

Table 26: Per-configuration metrics for the 07_sparse_only__neutral regime: F1, ground-
edness, and correctness (pass@4) with 95% bootstrap CI (1000 resamples on the final test split),
inference latency, and peak inference VRAM.

08_sparse_only__explicit_grounded

config	F1 [95% CI]	grmd@4 [95% CI]	corr@4 [95% CI]	lat. (s)	inf. VRAM (GB)
3B baseline	0.533 [0.508, 0.559]	0.721 [0.689, 0.752]	0.717 [0.687, 0.750]	0.513	11.643
3B r4 full_attention	0.561 [0.539, 0.584]	0.781 [0.750, 0.810]	0.790 [0.762, 0.817]	0.749	12.695
3B r4 qv_only	0.561 [0.540, 0.582]	0.800 [0.771, 0.827]	0.808 [0.778, 0.837]	0.623	12.689
3B r8 full_attention	0.569 [0.546, 0.591]	0.791 [0.763, 0.818]	0.804 [0.777, 0.829]	0.751	12.723
3B r8 qv_only	0.569 [0.549, 0.591]	0.777 [0.746, 0.806]	0.796 [0.768, 0.823]	0.669	12.697
3B r16 full_attention	0.575 [0.552, 0.598]	0.787 [0.757, 0.814]	0.797 [0.769, 0.827]	0.779	12.740
3B r16 qv_only	0.571 [0.550, 0.593]	0.780 [0.749, 0.806]	0.791 [0.761, 0.818]	0.624	12.723
3B r32 full_attention	0.572 [0.550, 0.593]	0.797 [0.771, 0.825]	0.805 [0.778, 0.831]	0.806	12.754
3B r32 qv_only	0.582 [0.558, 0.604]	0.782 [0.754, 0.810]	0.791 [0.763, 0.818]	0.733	12.740
3B r64 full_attention	0.576 [0.553, 0.599]	0.795 [0.766, 0.822]	0.806 [0.777, 0.833]	0.768	12.945
3B r64 qv_only	0.593 [0.568, 0.614]	0.776 [0.744, 0.804]	0.785 [0.757, 0.813]	0.605	12.781
8B baseline	0.596 [0.573, 0.618]	0.771 [0.743, 0.800]	0.768 [0.739, 0.799]	0.670	20.396
8B r4 full_attention	0.602 [0.578, 0.625]	0.824 [0.797, 0.848]	0.836 [0.808, 0.861]	0.809	21.863
8B r4 qv_only	0.602 [0.579, 0.623]	0.819 [0.791, 0.843]	0.831 [0.804, 0.856]	0.706	21.855
8B r8 full_attention	0.601 [0.581, 0.623]	0.822 [0.792, 0.847]	0.827 [0.800, 0.854]	0.802	21.852
8B r8 qv_only	0.606 [0.585, 0.627]	0.822 [0.794, 0.848]	0.831 [0.801, 0.860]	0.653	21.863
8B r16 full_attention	0.601 [0.580, 0.623]	0.829 [0.803, 0.855]	0.834 [0.808, 0.860]	0.766	21.877
8B r16 qv_only	0.610 [0.588, 0.633]	0.823 [0.795, 0.850]	0.831 [0.804, 0.856]	0.665	21.852
8B r32 full_attention	0.601 [0.578, 0.622]	0.806 [0.777, 0.833]	0.806 [0.780, 0.833]	0.842	21.953
8B r32 qv_only	0.610 [0.587, 0.631]	0.813 [0.785, 0.841]	0.818 [0.789, 0.846]	0.654	21.877
8B r64 full_attention	0.603 [0.578, 0.624]	0.813 [0.782, 0.838]	0.817 [0.791, 0.845]	0.821	22.156
8B r64 qv_only	0.623 [0.600, 0.645]	0.828 [0.800, 0.854]	0.832 [0.805, 0.856]	0.646	21.953

Table 27: Per-configuration metrics for the 08_sparse_only__explicit_grounded regime: F1, groundedness, and correctness (pass@4) with 95% bootstrap CI (1000 resamples on the final test split), inference latency, and peak inference VRAM.

09_HYBRID_BM25__NEUTRAL

config	F1 [95% CI]	grnd@4 [95% CI]	corr@4 [95% CI]	lat. (s)	inf. VRAM (GB)
3B baseline	0.543 [0.519, 0.568]	0.729 [0.697, 0.759]	0.721 [0.690, 0.752]	0.617	11.789
3B r4 full_attention	0.572 [0.550, 0.595]	0.790 [0.762, 0.815]	0.801 [0.772, 0.829]	0.753	12.674
3B r4 qv_only	0.569 [0.547, 0.592]	0.797 [0.768, 0.824]	0.803 [0.776, 0.829]	0.635	12.668
3B r8 full_attention	0.579 [0.557, 0.601]	0.801 [0.772, 0.831]	0.814 [0.785, 0.839]	0.752	12.701
3B r8 qv_only	0.571 [0.549, 0.591]	0.797 [0.768, 0.824]	0.804 [0.776, 0.831]	0.628	12.676
3B r16 full_attention	0.587 [0.564, 0.610]	0.801 [0.773, 0.829]	0.811 [0.783, 0.837]	0.774	12.719
3B r16 qv_only	0.577 [0.553, 0.601]	0.785 [0.757, 0.813]	0.797 [0.771, 0.827]	0.624	12.701
3B r32 full_attention	0.578 [0.556, 0.600]	0.801 [0.773, 0.828]	0.817 [0.787, 0.845]	0.751	12.732
3B r32 qv_only	0.593 [0.570, 0.617]	0.792 [0.763, 0.822]	0.803 [0.775, 0.833]	0.652	12.719
3B r64 full_attention	0.576 [0.553, 0.598]	0.797 [0.771, 0.825]	0.810 [0.781, 0.837]	0.767	12.924
3B r64 qv_only	0.597 [0.573, 0.621]	0.786 [0.755, 0.815]	0.792 [0.764, 0.820]	0.673	12.760
8B baseline	0.596 [0.574, 0.620]	0.778 [0.748, 0.806]	0.778 [0.748, 0.806]	0.769	20.768
8B r4 full_attention	0.603 [0.581, 0.623]	0.824 [0.797, 0.850]	0.834 [0.808, 0.859]	0.811	21.871
8B r4 qv_only	0.610 [0.588, 0.633]	0.819 [0.791, 0.847]	0.829 [0.804, 0.856]	0.675	21.828
8B r8 full_attention	0.599 [0.576, 0.621]	0.811 [0.785, 0.838]	0.817 [0.790, 0.845]	0.766	21.859
8B r8 qv_only	0.606 [0.586, 0.627]	0.827 [0.801, 0.852]	0.836 [0.808, 0.861]	0.646	21.836
8B r16 full_attention	0.604 [0.581, 0.625]	0.810 [0.782, 0.836]	0.808 [0.780, 0.836]	0.806	21.885
8B r16 qv_only	0.615 [0.592, 0.636]	0.818 [0.791, 0.845]	0.824 [0.797, 0.848]	0.660	21.824
8B r32 full_attention	0.602 [0.581, 0.623]	0.797 [0.768, 0.824]	0.806 [0.777, 0.833]	0.829	21.961
8B r32 qv_only	0.612 [0.591, 0.635]	0.819 [0.792, 0.846]	0.825 [0.797, 0.852]	0.649	21.850
8B r64 full_attention	0.606 [0.583, 0.627]	0.814 [0.787, 0.841]	0.822 [0.796, 0.848]	0.866	22.164
8B r64 qv_only	0.617 [0.597, 0.639]	0.815 [0.787, 0.842]	0.824 [0.797, 0.851]	0.659	21.926

Table 28: Per-configuration metrics for the 09_hybrid_bm25__neutral regime: F1, ground-
edness, and correctness (pass@4) with 95% bootstrap CI (1000 resamples on the final test split),
inference latency, and peak inference VRAM.

10_HYBRID_BM25__EXPLICIT_GROUNDED

config	F1 [95% CI]	grmd@4 [95% CI]	corr@4 [95% CI]	lat. (s)	inf. VRAM (GB)
3B baseline	0.543 [0.520, 0.567]	0.735 [0.704, 0.766]	0.729 [0.696, 0.758]	0.615	11.789
3B r4 full_attention	0.561 [0.538, 0.584]	0.778 [0.752, 0.809]	0.796 [0.769, 0.824]	0.775	12.695
3B r4 qv_only	0.561 [0.540, 0.585]	0.799 [0.771, 0.825]	0.806 [0.778, 0.833]	0.656	12.689
3B r8 full_attention	0.569 [0.547, 0.591]	0.796 [0.768, 0.824]	0.810 [0.782, 0.837]	0.805	12.723
3B r8 qv_only	0.569 [0.548, 0.590]	0.778 [0.748, 0.806]	0.791 [0.762, 0.819]	0.667	12.697
3B r16 full_attention	0.575 [0.554, 0.598]	0.781 [0.753, 0.809]	0.794 [0.762, 0.822]	0.776	12.740
3B r16 qv_only	0.571 [0.548, 0.596]	0.786 [0.754, 0.814]	0.794 [0.764, 0.820]	0.642	12.723
3B r32 full_attention	0.572 [0.549, 0.593]	0.800 [0.771, 0.829]	0.811 [0.783, 0.838]	0.841	12.754
3B r32 qv_only	0.582 [0.559, 0.604]	0.780 [0.750, 0.808]	0.791 [0.763, 0.818]	0.737	12.740
3B r64 full_attention	0.576 [0.551, 0.598]	0.795 [0.767, 0.824]	0.809 [0.782, 0.837]	0.783	12.945
3B r64 qv_only	0.593 [0.570, 0.615]	0.780 [0.750, 0.809]	0.792 [0.766, 0.822]	0.593	12.781
8B baseline	0.603 [0.580, 0.625]	0.781 [0.755, 0.808]	0.781 [0.753, 0.810]	0.734	20.768
8B r4 full_attention	0.602 [0.580, 0.625]	0.820 [0.795, 0.846]	0.829 [0.804, 0.856]	0.804	21.863
8B r4 qv_only	0.602 [0.579, 0.623]	0.808 [0.781, 0.834]	0.818 [0.791, 0.843]	0.714	21.855
8B r8 full_attention	0.601 [0.580, 0.623]	0.820 [0.792, 0.846]	0.822 [0.792, 0.848]	0.795	21.852
8B r8 qv_only	0.606 [0.585, 0.627]	0.832 [0.808, 0.857]	0.842 [0.815, 0.869]	0.675	21.863
8B r16 full_attention	0.601 [0.581, 0.624]	0.827 [0.800, 0.850]	0.832 [0.806, 0.857]	0.842	21.877
8B r16 qv_only	0.610 [0.590, 0.631]	0.834 [0.808, 0.860]	0.838 [0.811, 0.861]	0.691	21.852
8B r32 full_attention	0.601 [0.579, 0.621]	0.804 [0.776, 0.829]	0.808 [0.780, 0.834]	0.850	21.953
8B r32 qv_only	0.610 [0.589, 0.633]	0.808 [0.782, 0.836]	0.813 [0.783, 0.838]	0.672	21.877
8B r64 full_attention	0.603 [0.580, 0.624]	0.810 [0.785, 0.838]	0.817 [0.790, 0.842]	0.820	22.156
8B r64 qv_only	0.623 [0.603, 0.645]	0.823 [0.795, 0.847]	0.829 [0.803, 0.855]	0.664	21.953

Table 29: Per-configuration metrics for the 10_hybrid_bm25__explicit_grounded regime: F1, groundedness, and correctness (pass@4) with 95% bootstrap CI (1000 resamples on the final test split), inference latency, and peak inference VRAM.

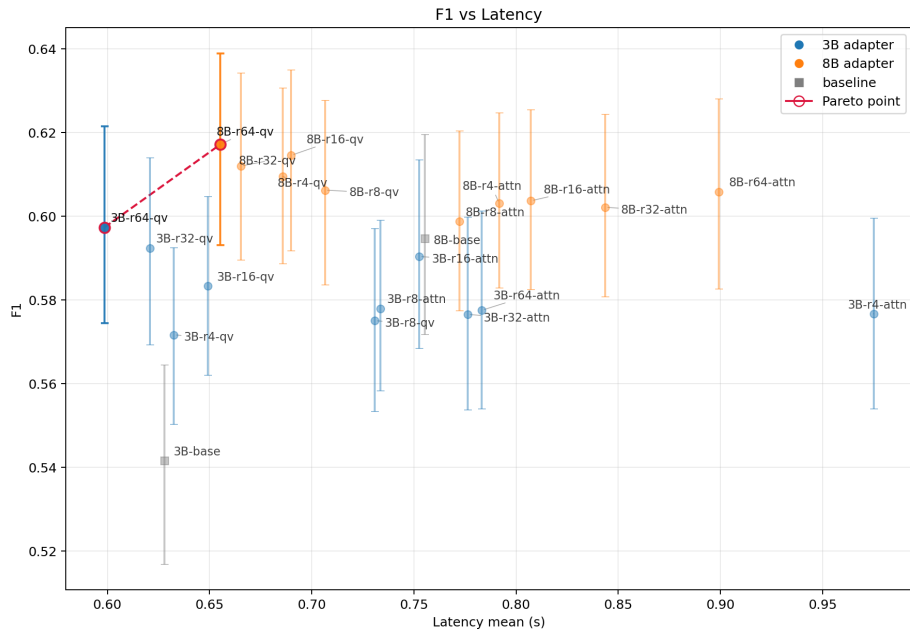
J PER-REGIME PLOTS

This appendix contains the detailed plots for each of the 10 ablation regimes referenced in Section 7. For every regime we show the main two-dimensional projections used in the trade-off analysis. Plots with an F_1 axis (f1_vs_latency, f1_vs_inference_vram, f1_vs_groundedness_pass4) are drawn with vertical error bars corresponding to 95% bootstrap confidence intervals on the final test split ($n = 785, 1,000$ resamples). Analogously, for the judge metrics groundedness_pass4 and correctness_pass4 (per-example binomial indicators of passing the Likert-score threshold ≥ 4) we compute 95% bootstrap CIs; the groundedness_pass4_vs_latency plot has vertical error bars on the groundedness axis, while f1_vs_groundedness_pass4 has two-sided error bars (on both axes). The point CI values are mirrored in the corresponding tables of Appendix I. The f1_vs_inference_vram plot is drawn as two adjacent panels (separate zoom on the 3B and 8B families), because under a single axis the configuration points cluster into two narrow bands of about 0.3 GB and overlap with each other; separate panels allow the within-cluster structure to be distinguished. The groundedness_pass4_vs_inference_vram projection is not included in the appendix: in it the spread along the VRAM axis within each family does not exceed 0.3–0.4 GB, while the corresponding groundedness spread fully lies inside the 95% CI band, so the plot carries no information beyond f1_vs_inference_vram.

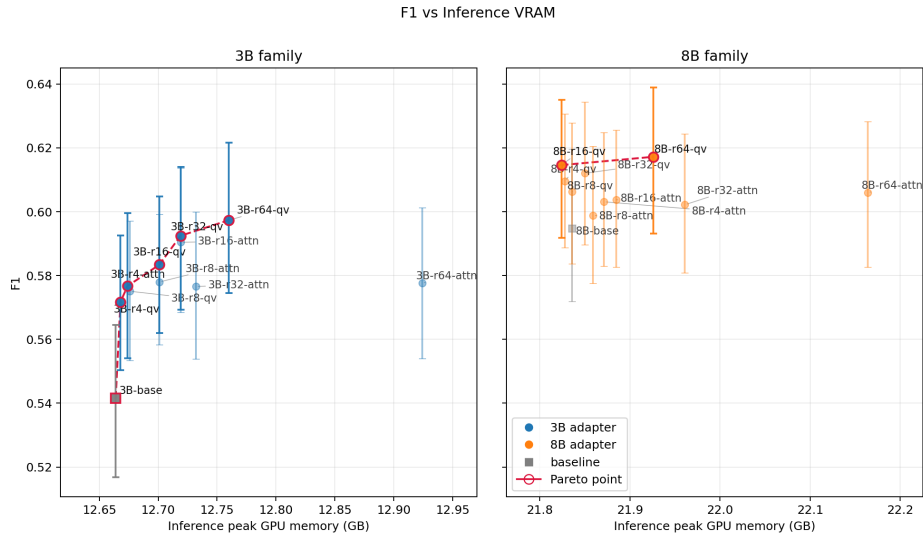
01_BASE__NEUTRAL

Regime: base + neutral.

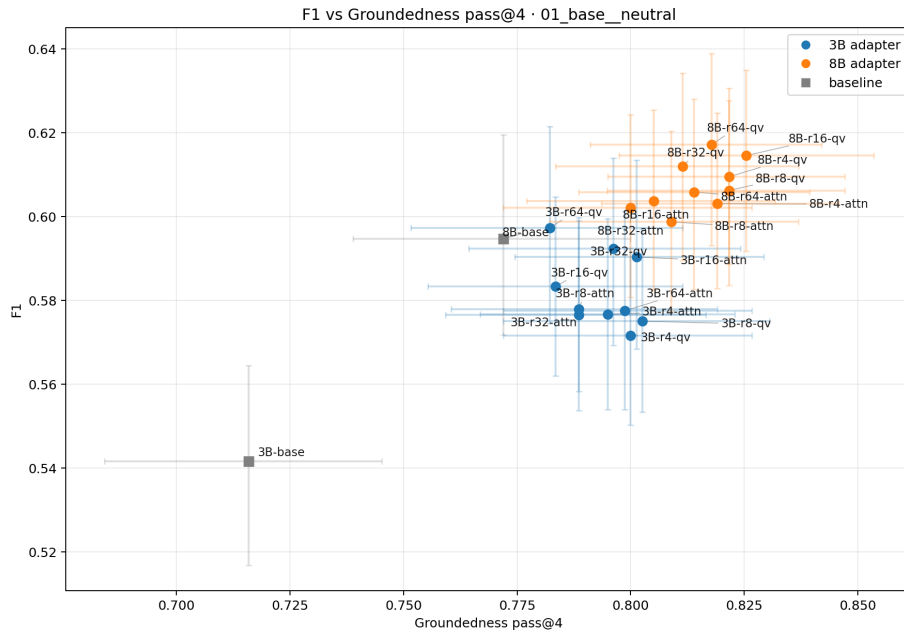
F1 vs Latency



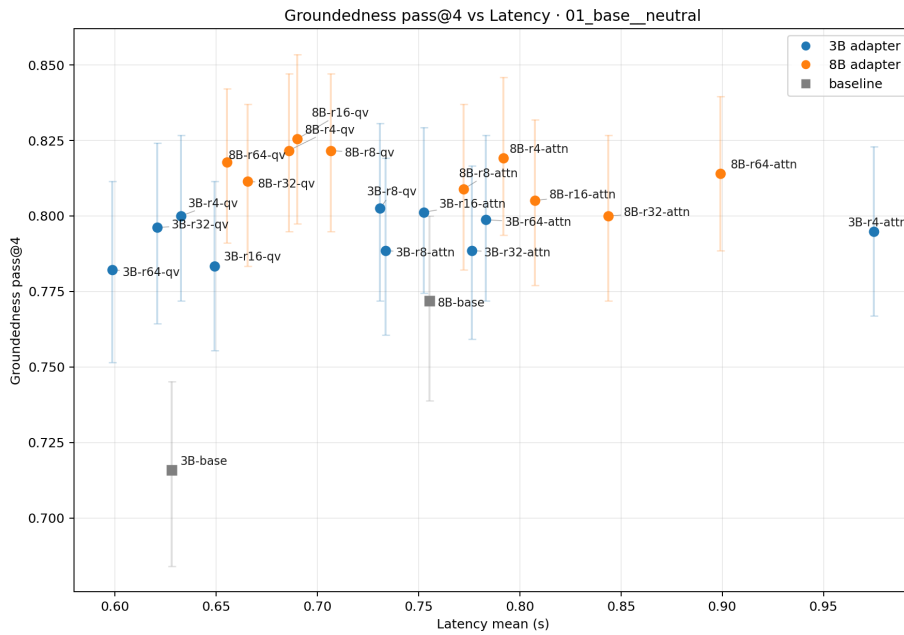
F1 vs Inference VRAM



F1 vs Groundedness pass@4



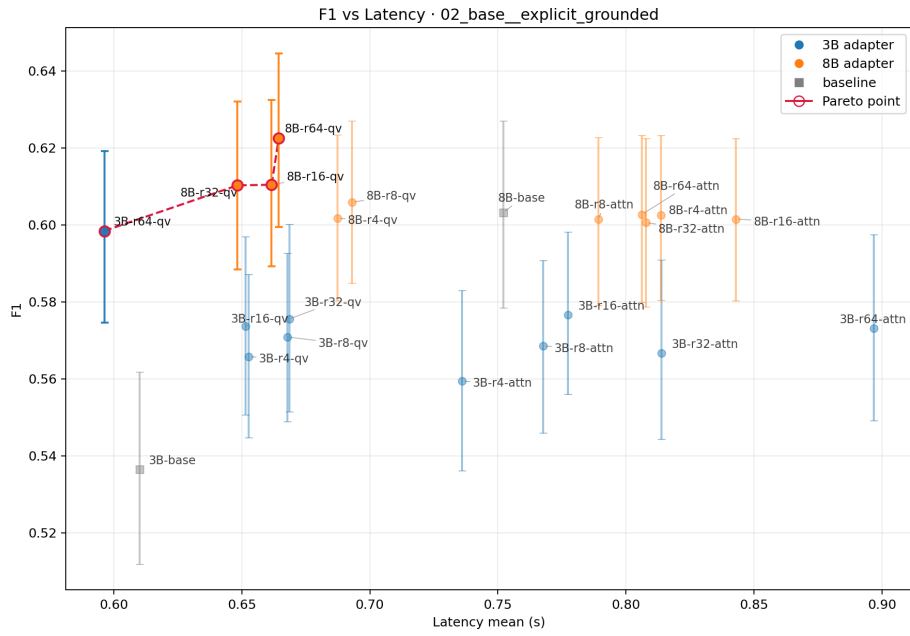
Groundedness pass@4 vs Latency



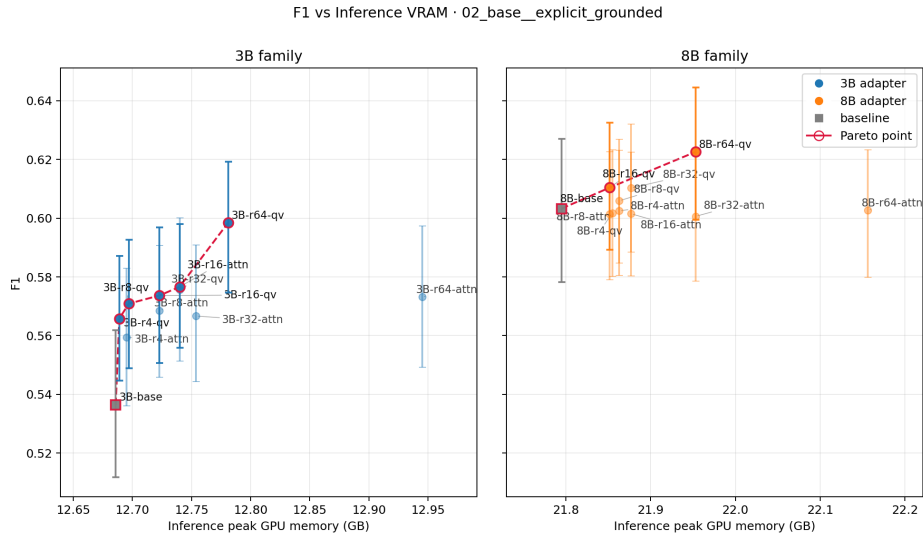
O2_BASE__EXPLICIT_GROUNDED

Regime: base + explicit_grounded.

F1 vs Latency



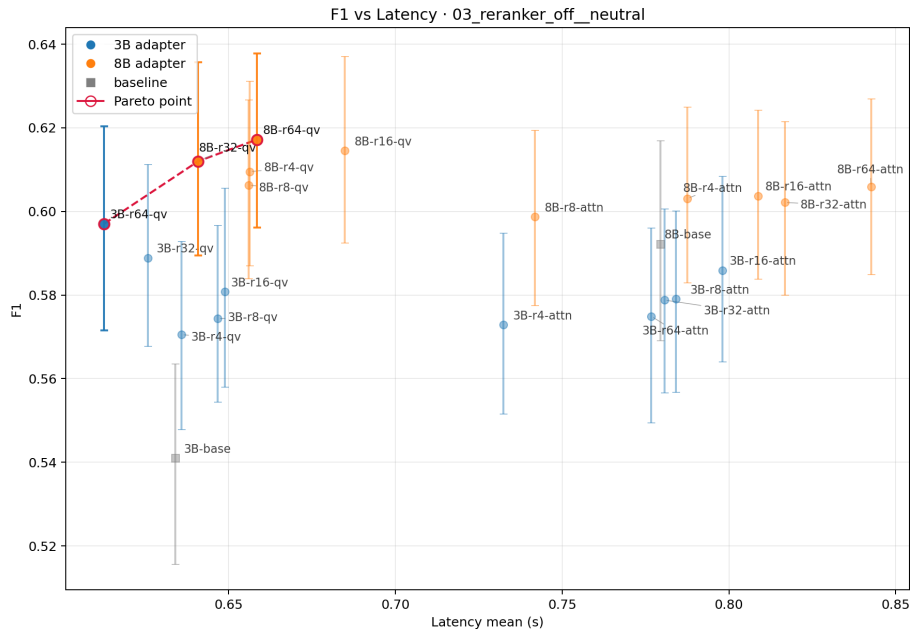
F1 vs Inference VRAM



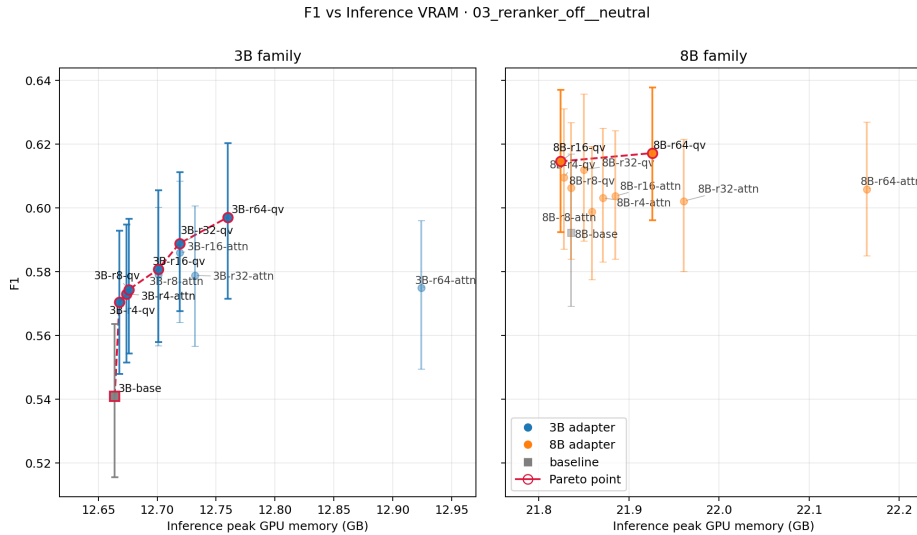
03_RERANKER_OFF__NEUTRAL

Regime: reranker_off + neutral.

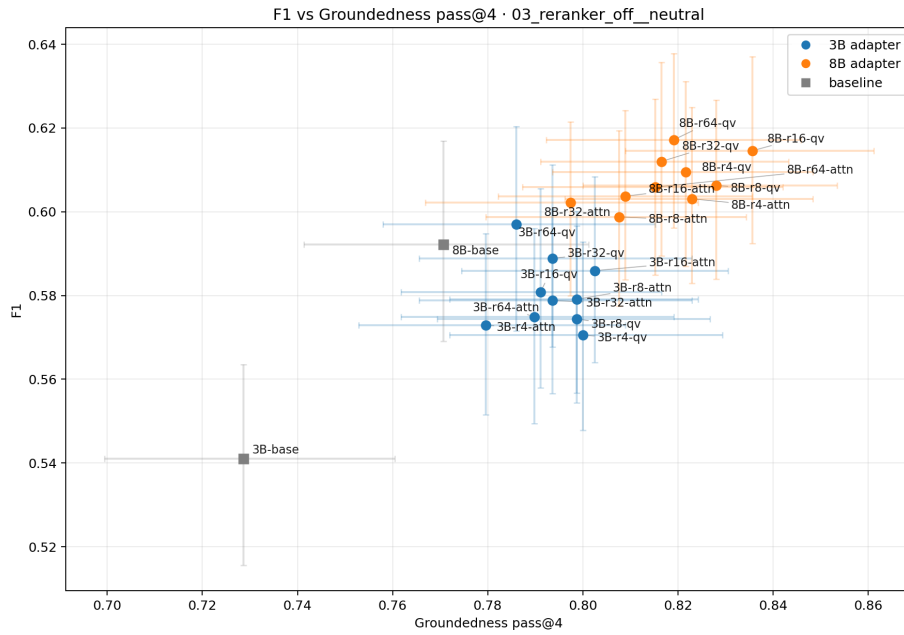
F1 vs Latency



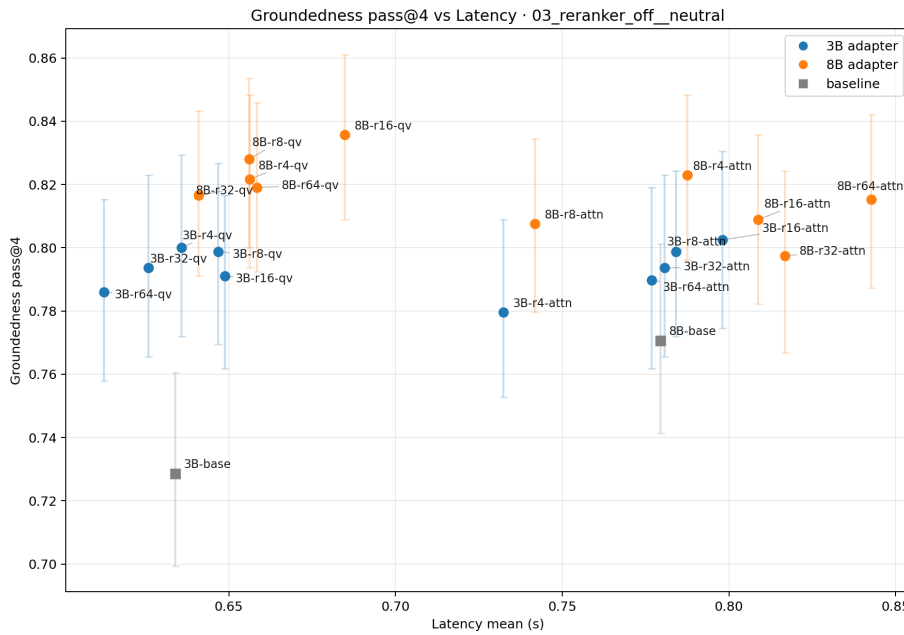
F1 vs Inference VRAM



F1 vs Groundedness pass@4



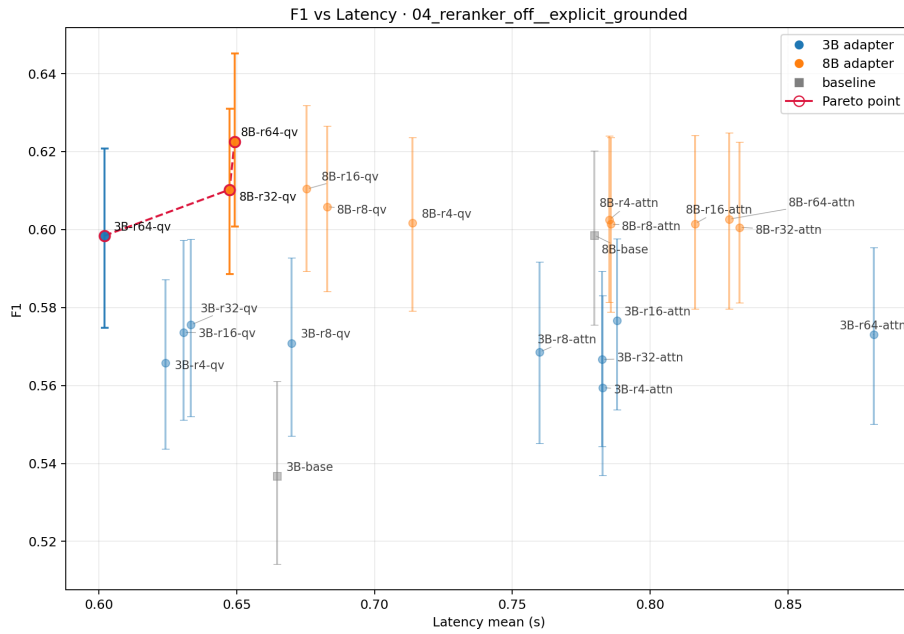
Groundedness pass@4 vs Latency



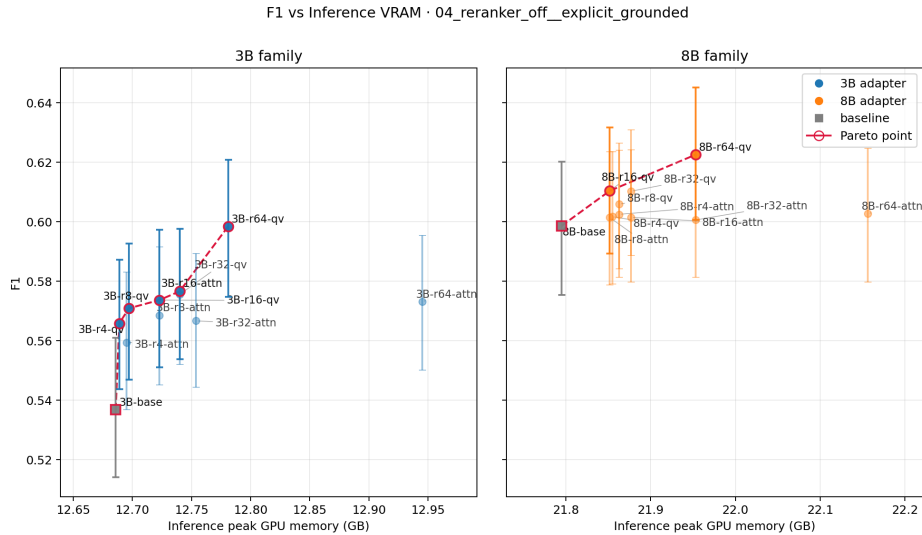
04_RERANKER_OFF_EXPLICIT_GROUNDED

Regime: reranker_off + explicit_grounded.

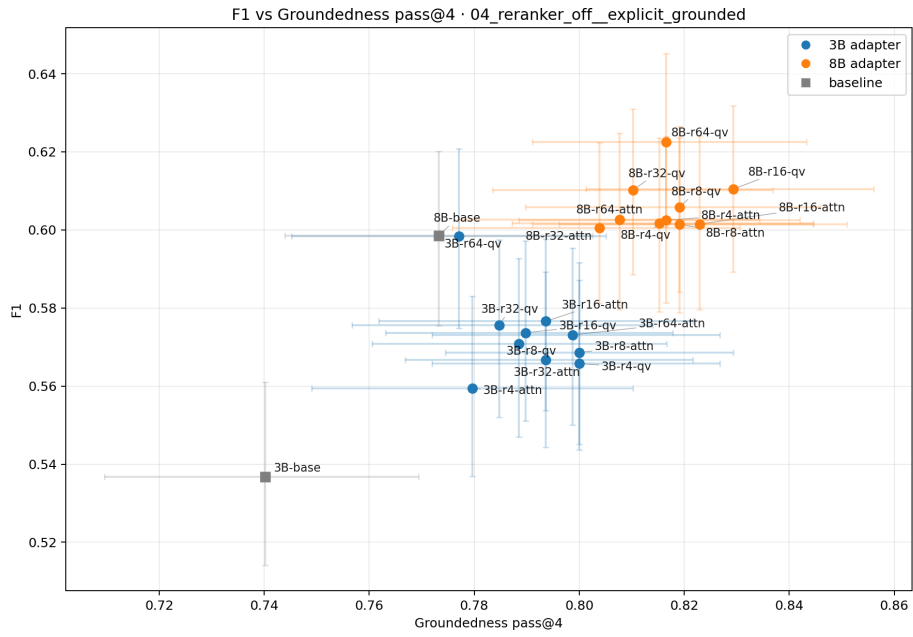
F1 vs Latency



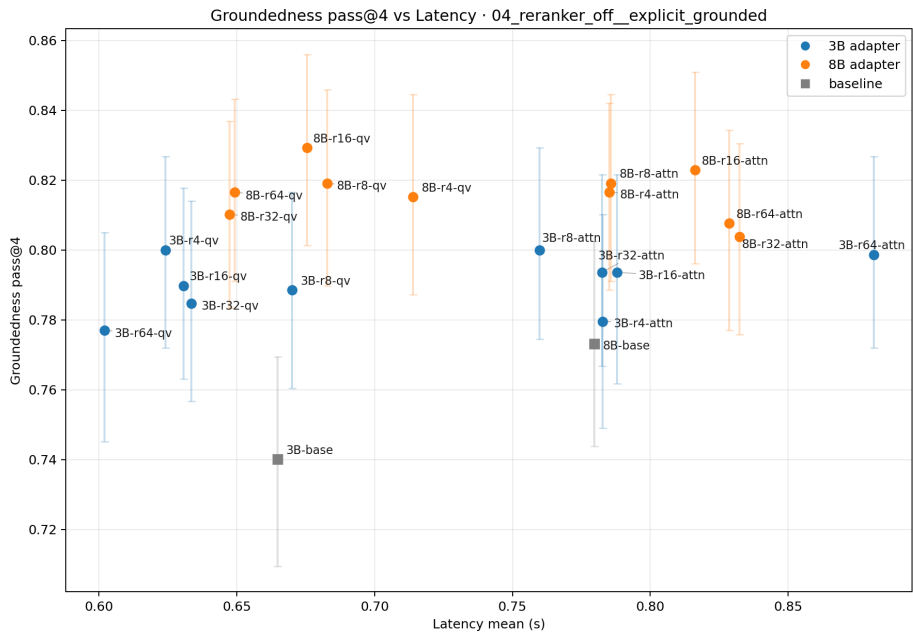
F1 vs Inference VRAM



F1 vs Groundedness pass@4



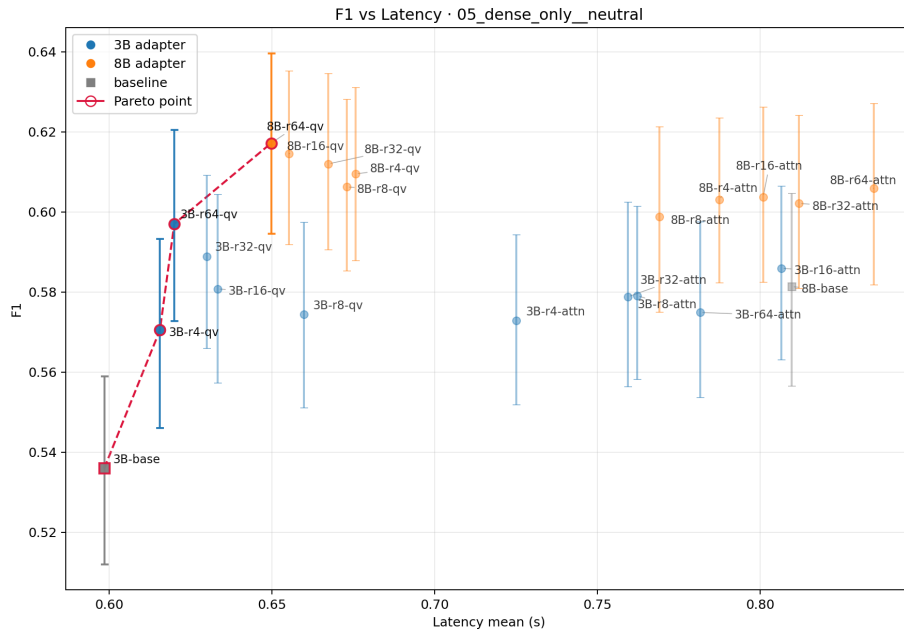
Groundedness pass@4 vs Latency



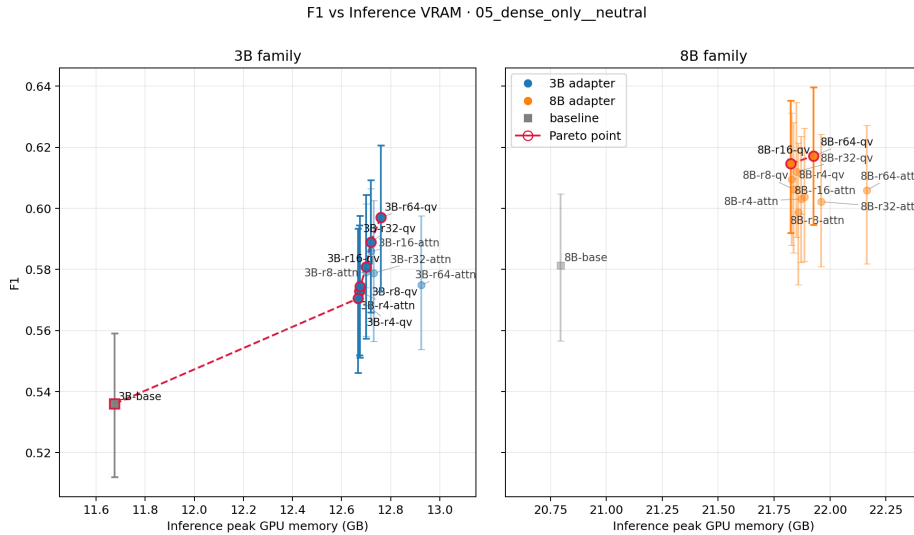
05_DENSE_ONLY__NEUTRAL

Regime: dense_only + neutral.

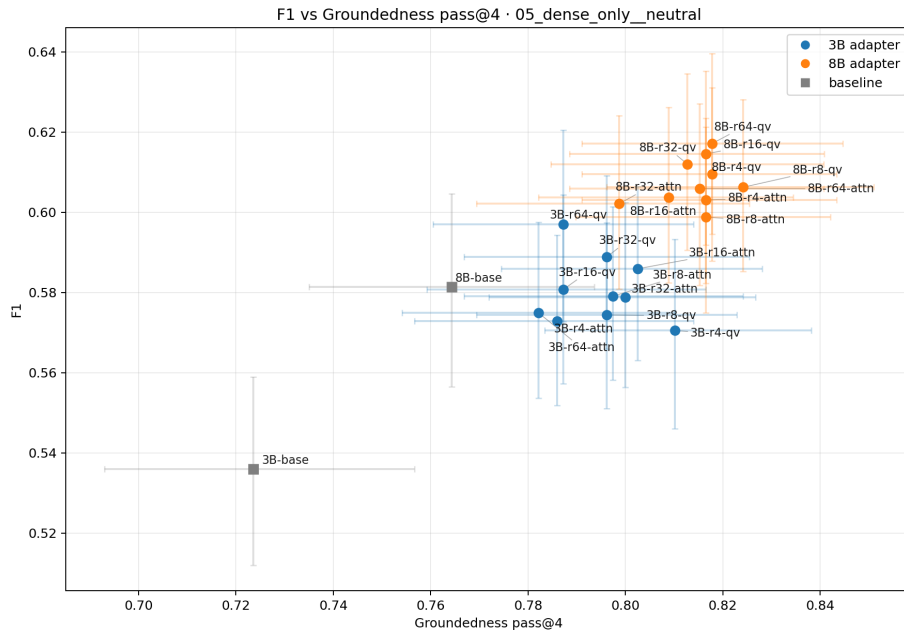
F1 vs Latency



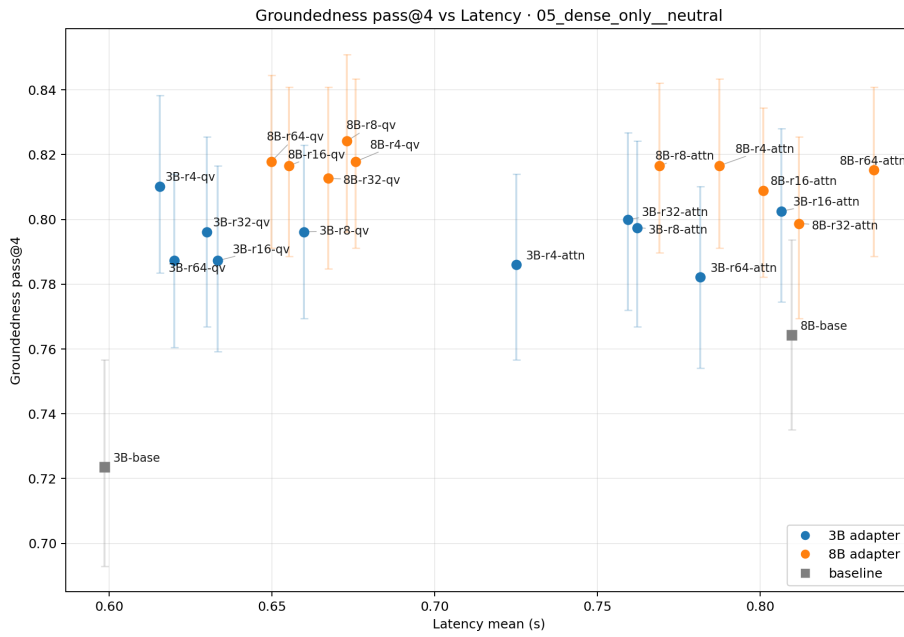
F1 vs Inference VRAM



F1 vs Groundedness pass@4



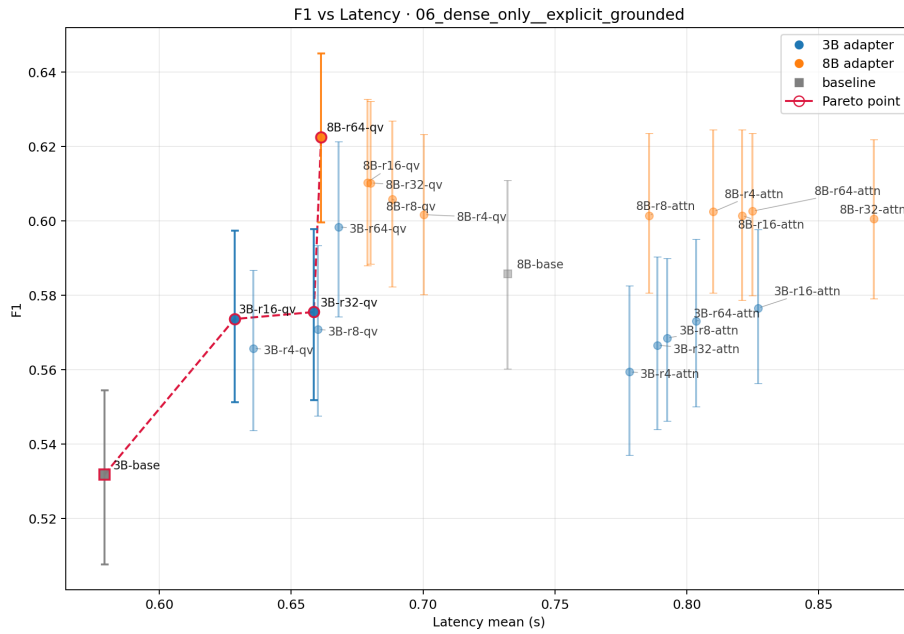
Groundedness pass@4 vs Latency



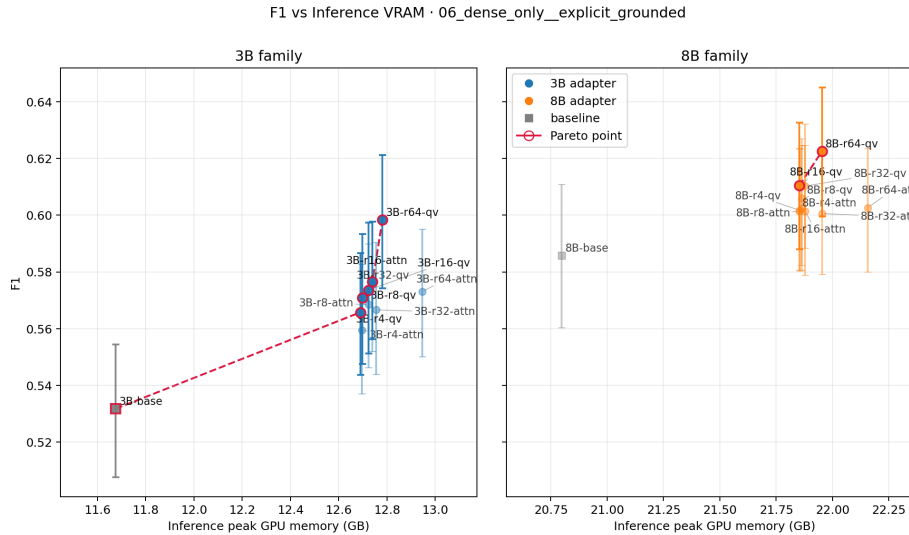
06_DENSE_ONLY_EXPLICIT_GROUNDED

Regime: dense_only + explicit_grounded.

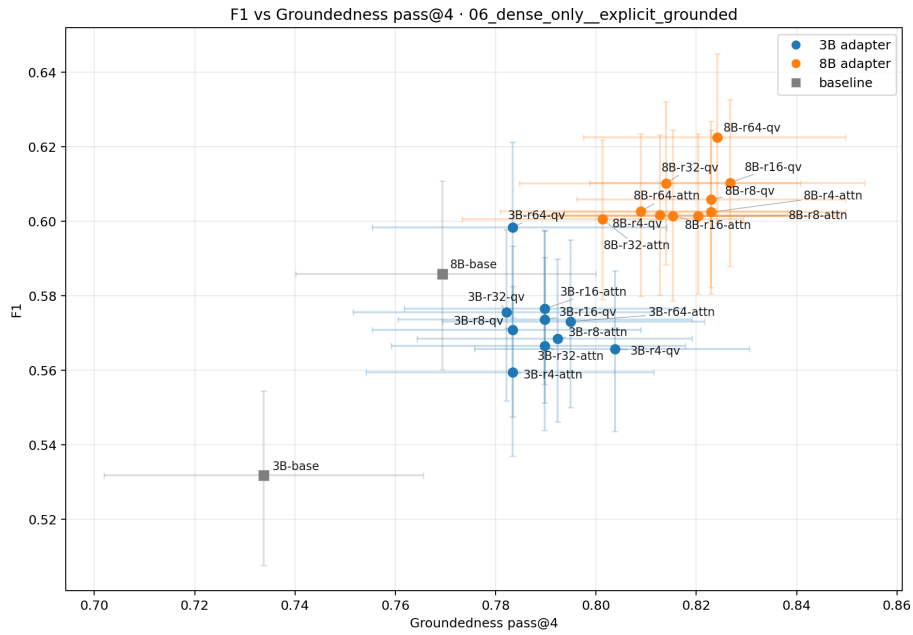
F1 vs Latency



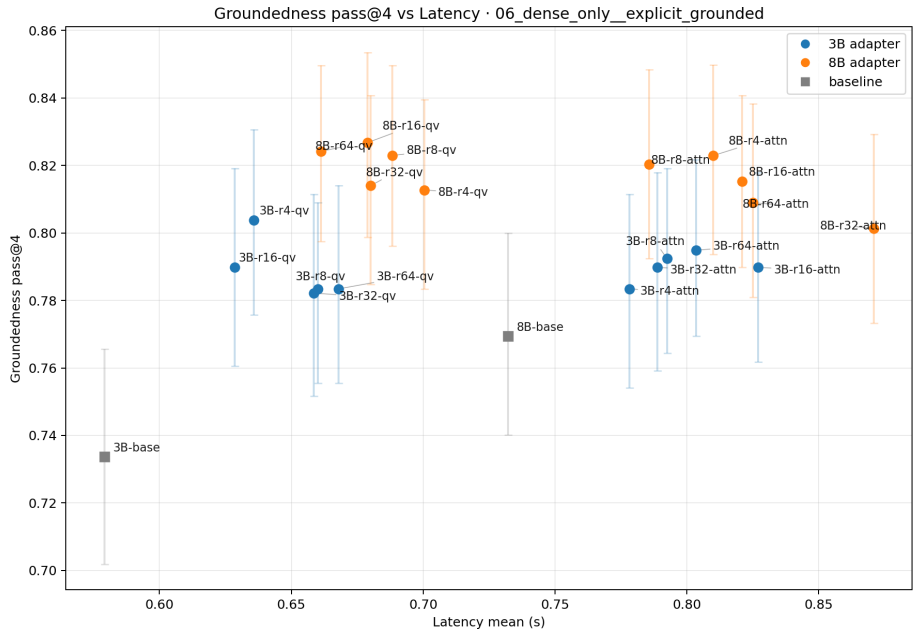
F1 vs Inference VRAM



F1 vs Groundedness pass@4



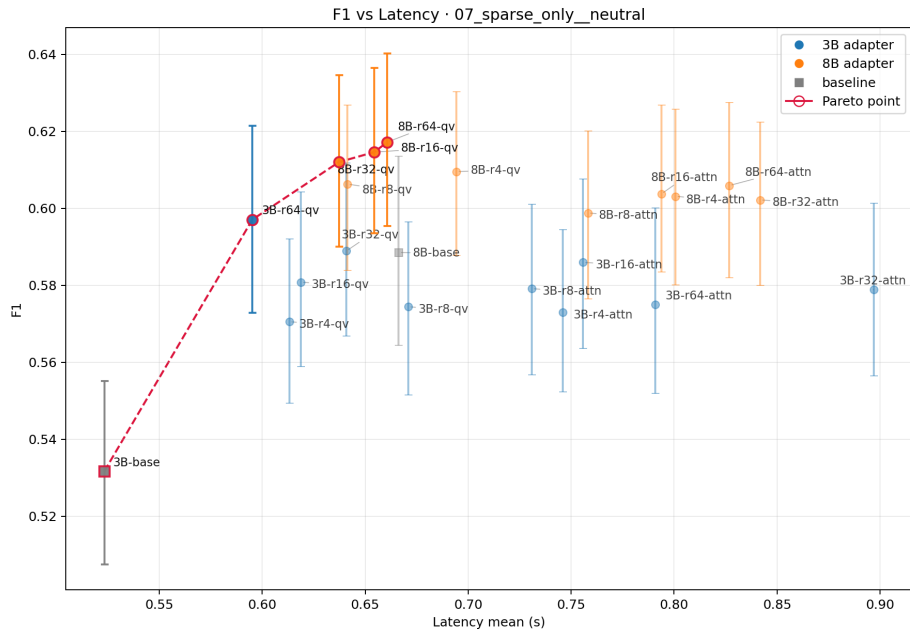
Groundedness pass@4 vs Latency



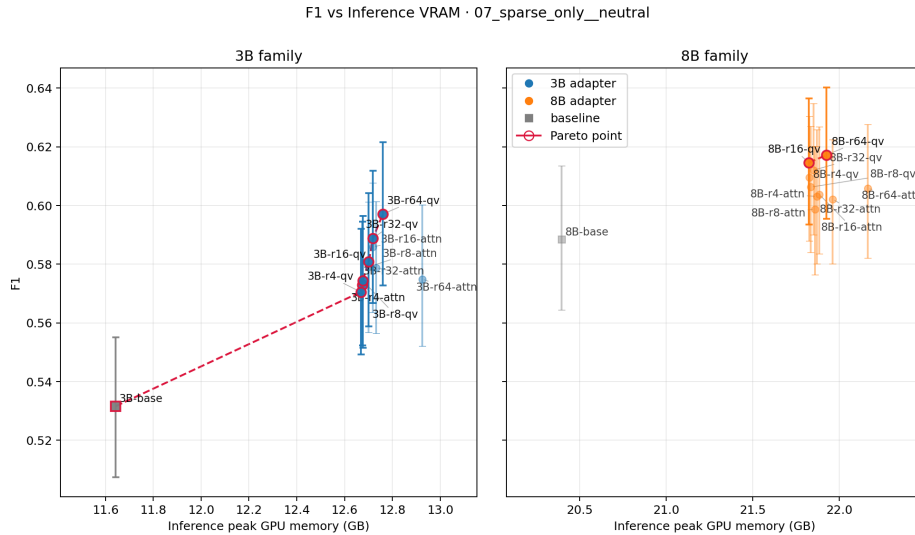
07_SPARSE_ONLY__NEUTRAL

Regime: sparse_only + neutral.

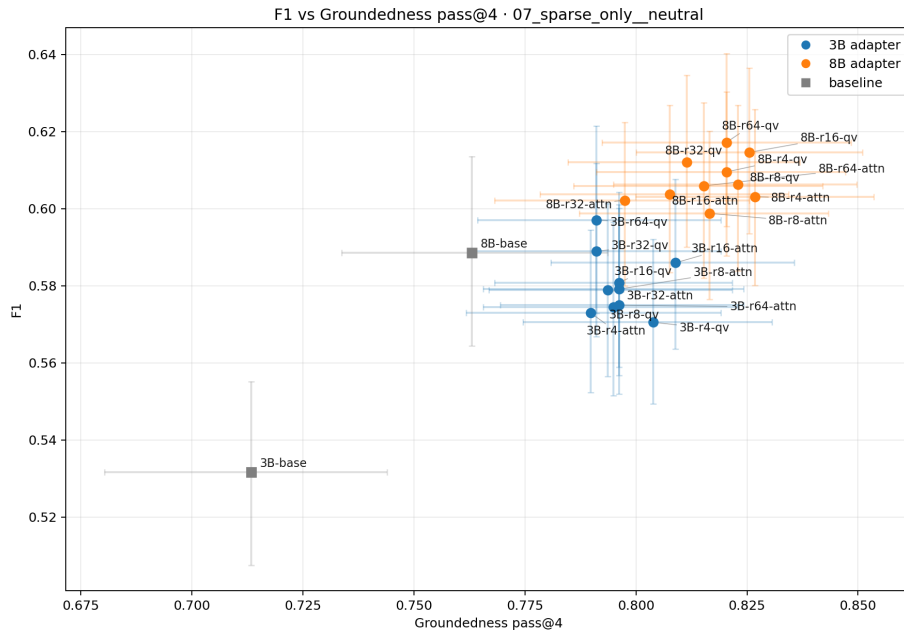
F1 vs Latency



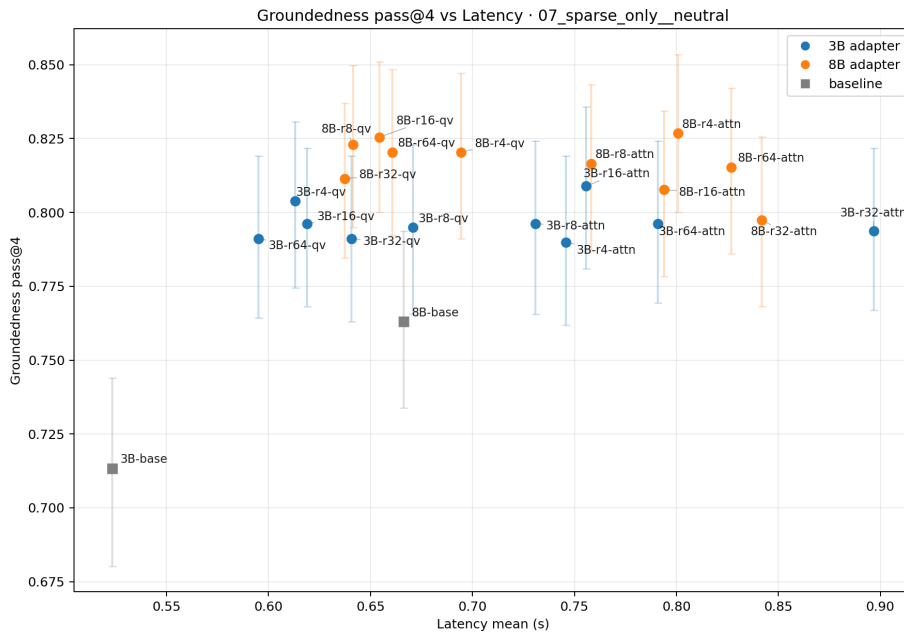
F1 vs Inference VRAM



F1 vs Groundedness pass@4



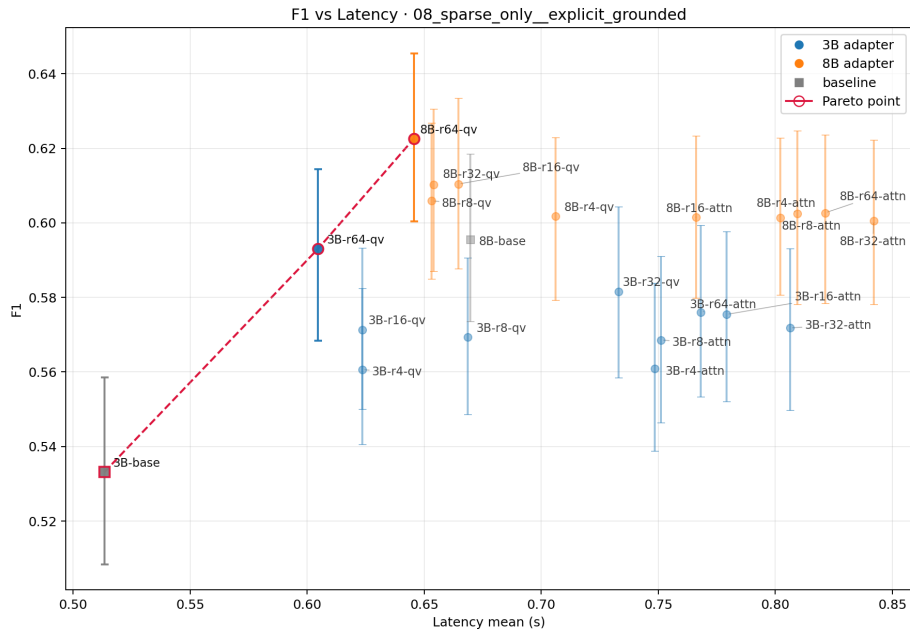
Groundedness pass@4 vs Latency



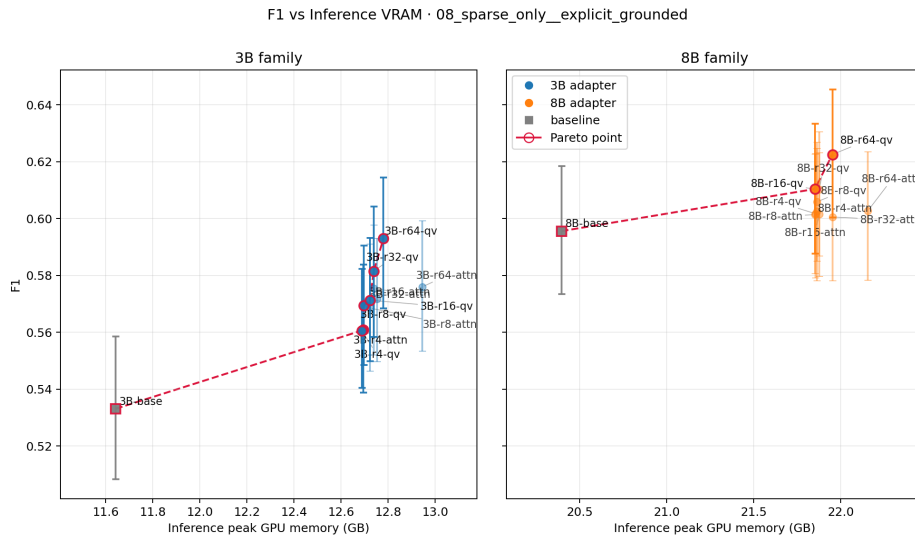
08_sparse_only__explicit_grounded

Regime: sparse_only + explicit_grounded.

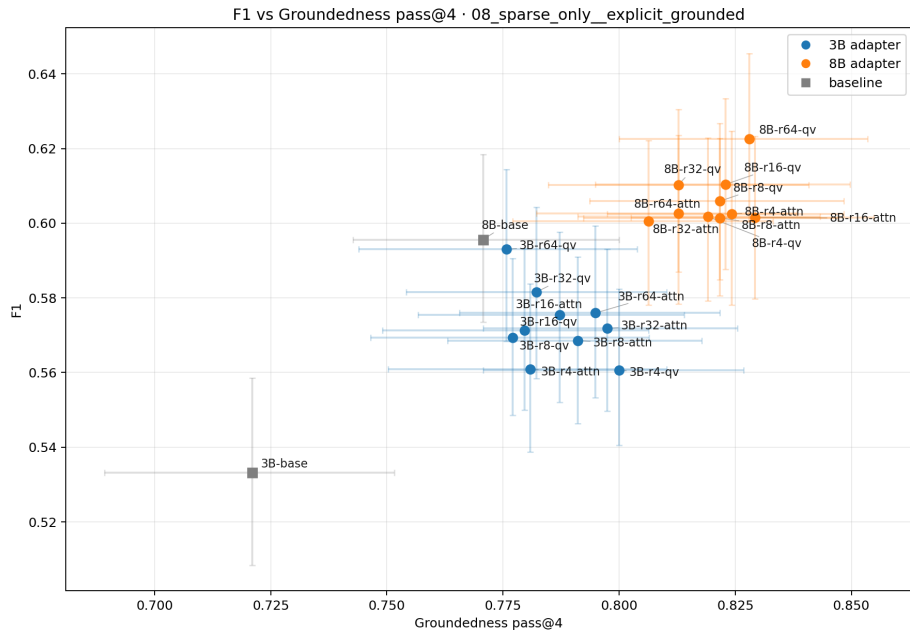
F1 vs Latency



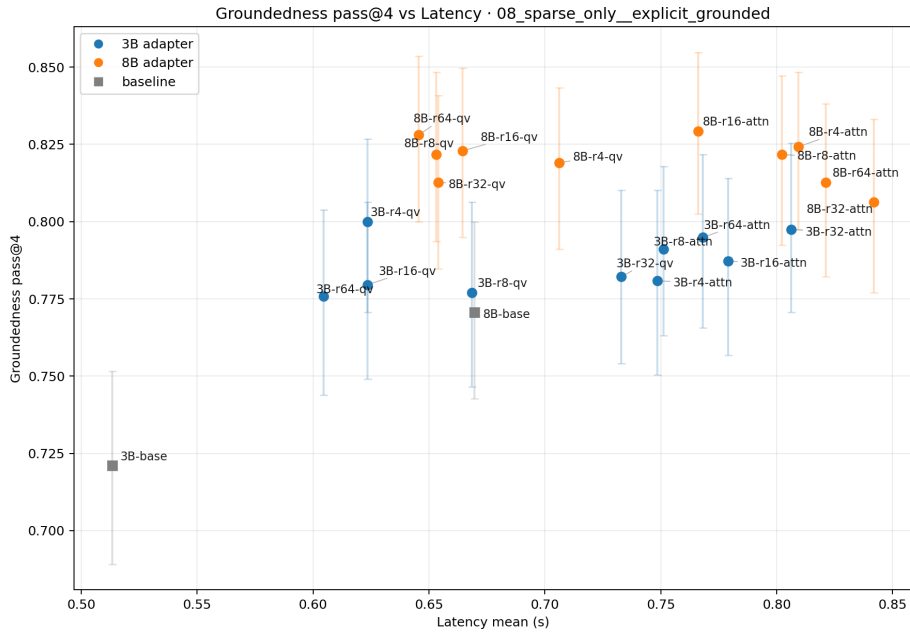
F1 vs Inference VRAM



F1 vs Groundedness pass@4



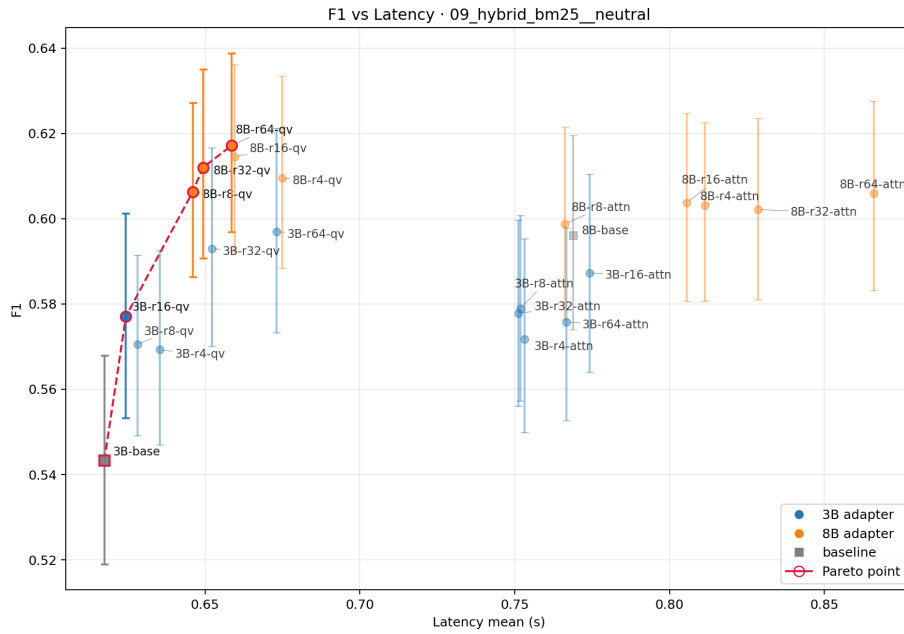
Groundedness pass@4 vs Latency



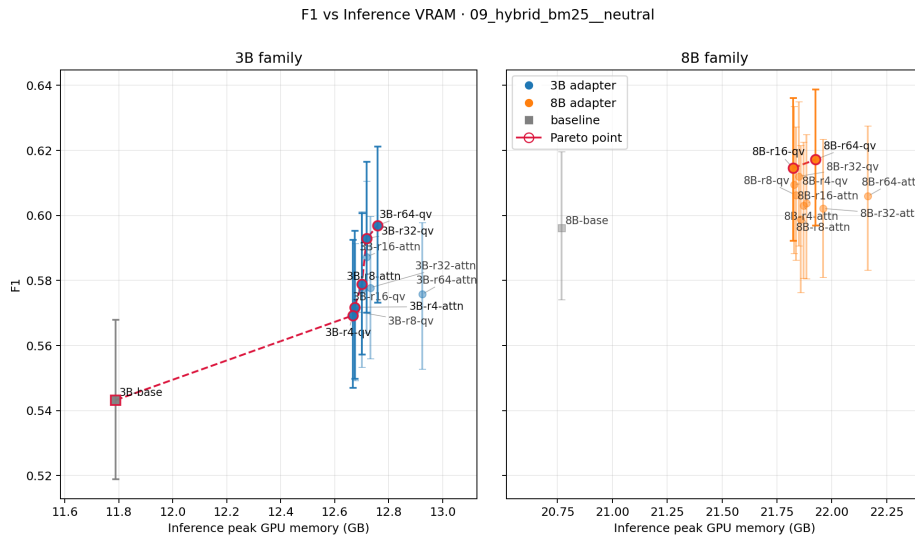
09_HYBRID_BM25__NEUTRAL

Regime: hybrid_bm25 + neutral.

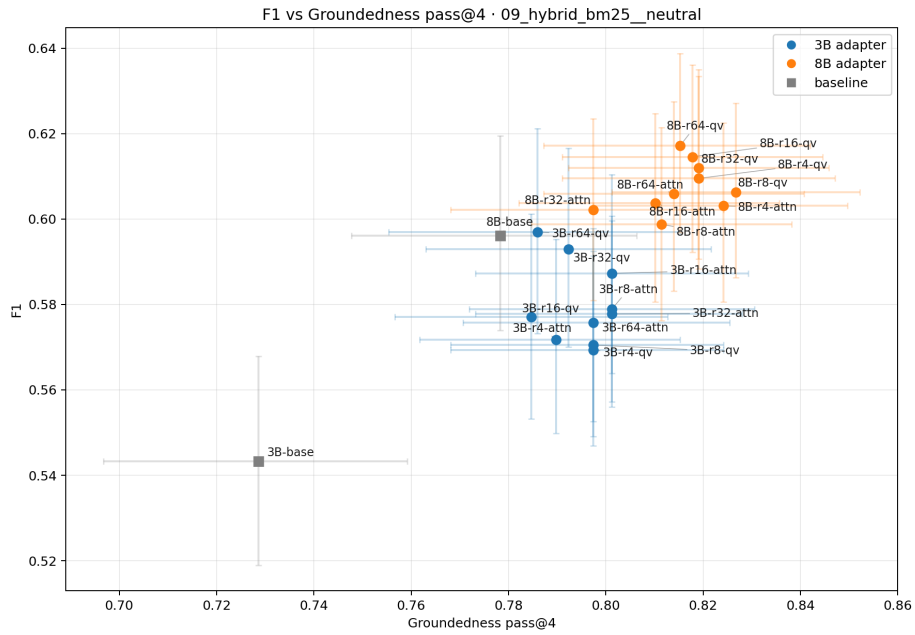
F1 vs Latency



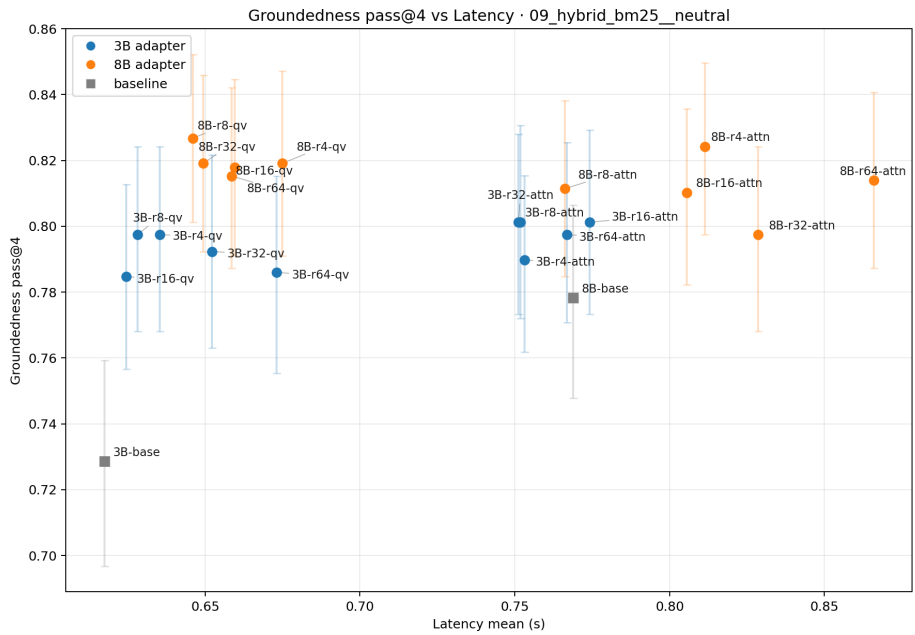
F1 vs Inference VRAM



F1 vs Groundedness pass@4



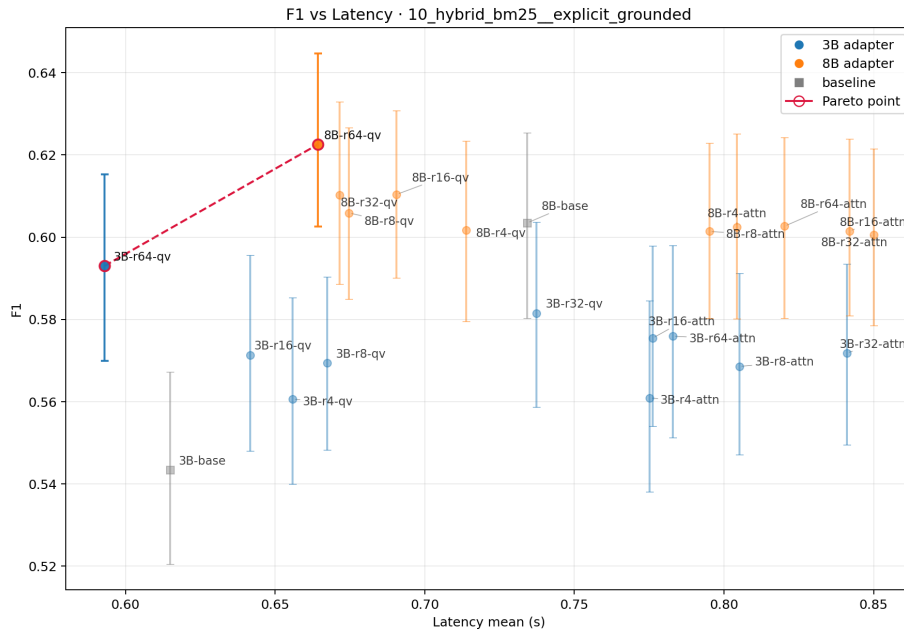
Groundedness pass@4 vs Latency



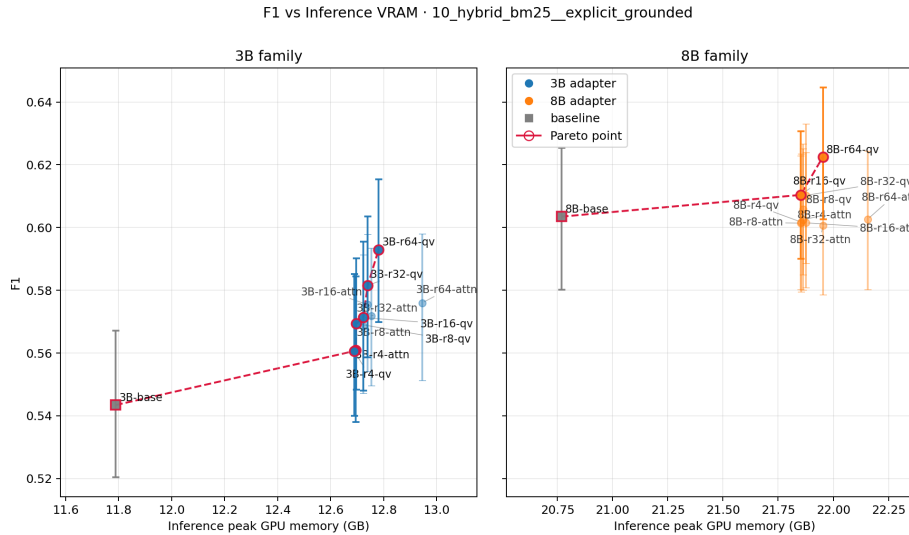
10_HYBRID_BM25__EXPLICIT_GROUNDED

Regime: hybrid_bm25 + explicit_grounded.

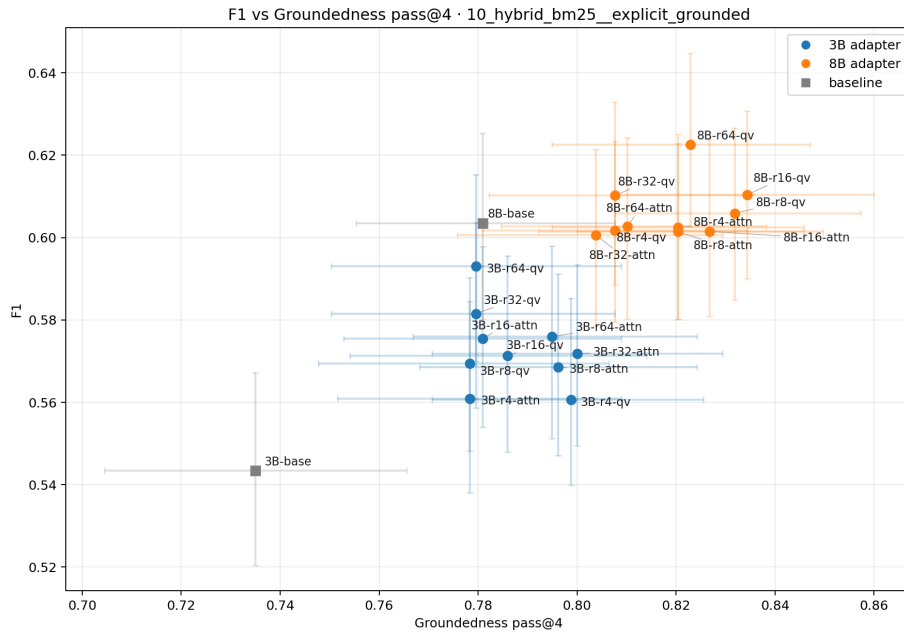
F1 vs Latency



F1 vs Inference VRAM



F1 vs Groundedness pass@4



Groundedness pass@4 vs Latency

